FEDERAL UNIVERSITY OF CEARA
TECHNOLOGY CENTER
DEPARTMENT OF ELECTRICAL ENGINEERING
GRADUATE PROGRAM IN ELECTRICAL ENGINEERING

RENÉ DESCARTES OLIMPIO PEREIRA

SMITH PREDICTOR-BASED CONTROLLERS FOR HIGH-ORDER DEAD-TIME PROCESSES

FORTALEZA

2023

RENÉ DESCARTES OLIMPIO PEREIRA

SMITH PREDICTOR-BASED CONTROLLERS FOR HIGH-ORDER DEAD-TIME PROCESSES

Thesis presented to the Graduate Program in Electrical Engineering of Federal University of Ceara as a partial requirement to obtain the title of Doctor in Electrical Engineering. Concentration field: Electric Power Systems.

Supervisor: Prof. Dr. Bismark Claure Torrico
Co-supervisor: Prof. Dr. Fabrício Gonzalez Nogueira

FORTALEZA

2023

Dados Internacionais de Catalogação na Publicação
Universidade Federal do Ceará
Sistema de Bibliotecas
Gerada automaticamente pelo módulo Catalog, mediante os dados fornecidos pelo(a) autor(a)

P495s Pereira, René Descartes Olimpio.
Smith predictor-based controllers for high-order dead-time processes / René Descartes Olimpio Pereira. – 2023.
104 f. : il. color.

Tese (doutorado) – Universidade Federal do Ceará, Centro de Tecnologia, Programa de Pós-Graduação em Engenharia Elétrica, Fortaleza, 2023.
Orientação: Prof. Dr. Bismark Claure Torrico.
Coorientação: Prof. Dr. Fabricio Gonzalez Nogueira.

1. Smith predictor. 2. Dead-time processes. 3. High-order models. 4. Measurable disturbances. 5. Newborn intensive care unit. I. Título.

CDD 621.3

RENÉ DESCARTES OLIMPIO PEREIRA

SMITH PREDICTOR-BASED CONTROLLERS FOR HIGH-ORDER DEAD-TIME PROCESSES

Thesis presented to the Graduate Program in Electrical Engineering of Federal University of Ceara as a partial requirement to obtain the title of Doctor in Electrical Engineering. Concentration field: Electric Power Systems.

Approved at Fortaleza, April 25, 2023.

EXAMINATION BOARD

Prof. Dr. Bismark Claure Torrico (Supervisor)
Federal University of Ceara

Prof. Dr. Fabrício Gonzalez Nogueira (Co-supervisor)
Federal University of Ceara

Prof. Dr. Julio Elias Normey-Rico
Federal University of Santa Catarina

Prof. Dr. Tito Luís Maia Santos
Federal University of Bahia

Prof. Dr. Diego de Sousa Madeira
Federal University of Ceara

This work is dedicated to my parents, Gabriel and Mércia.

ACKNOWLEDGEMENTS

To my Supervisor, Prof. Dr. Bismark Claure Torrico and my Co-supervisor, Prof. Dr. Fabrício Gonzalez Nogueira, for sharing their knowledge in process control theory and practice, and for their guidance and suggestions to make this work possible.

To all members of the examination board, for their time spent, attention, and important contributions to improve this work.

To my family and friends, for their comprehension and support, manifested in different ways, that helped me to accomplish this work.

To my colleagues at the laboratory of the Research Group in Automation, Control, and Robotics (GPAR), for all the knowledge shared between us and for the mutual help in our research. In this case, a special acknowledgment to my friend José Nogueira do Nascimento Junior, for his incentive and help with this thesis.

To the Coordenação de Aperfeiçoamento de Pessoal de Nível Superior (CAPES), for the financial support, by providing a scholarship, and to the Fundação Cearense de Apoio ao Desenvolvimento Científico e Tecnológico (FUNCAP), Edital FUNCAP No 06/2021 - Energias Renováveis (Processo 09779122/2021).

Heaven and earth are ruthless, and treat the myriad creatures as straw dogs.
Lao Tzu

ABSTRACT

This work studies and proposes controllers based on the Smith predictor (SP) for both high-order dead-time processes and processes with measurable disturbances. Relevant SP-based controllers from the literature are studied, and their main characteristics are highlighted. A control structure suitable for high-order dead-time processes with non-minimum phase (NMP) zeros is proposed, namely, the simplified filtered SP (SFSP). The proposed strategy uses a state-space formulation and can be applied in a unified manner to stable, unstable, and integrating linear dead-time processes of any order. In general, dead-time compensators (DTCs) first predict the process output with zero error at a steady state, and then a primary controller with an integrator is designed based on the delay-free model. The main advantage of the proposed structure is that the primary controller is only a state-feedback gain with no explicit integrators. This leads to fewer parameters to tune and lower-order filters, while a robustness filter is used to reject disturbances and guarantee zero error at a steady state. Simulation results show better or equivalent performance than other recently published works, even by keeping controller design simple. The basic fundamentals of feedforward control for measurable disturbances are presented, and important SP-based controllers for dead-time processes with measurable disturbances are studied. A feedforward extension for the SFSP for high-order dead-time processes to deal with measurable disturbances is also proposed. Compared to other control strategies, the main advantage of using the predictor approach is the ability to deal with processes with large dead time. The structure improves the disturbance rejection performance by feedforwarding the disturbance while maintaining the good robustness and noise attenuation properties of the SFSP. Simulation results also show better performance indices compared with other strategies from the recent literature. In addition, to show their effectiveness in a real process, the proposed strategies are applied to control the temperature in a newborn intensive care unit (NICU).

Keywords: Smith predictor. Dead-time processes. High-order models. Non-minimum phase zeros. Feedforward control. Measurable disturbances. Newborn intensive care unit.

RESUMO

Este trabalho estuda e propõe controladores baseados no preditor de Smith (SP, do inglês *Smith predictor*) para processos com atraso de transporte de ordem elevada e para processos com perturbações mensuráveis. Relevantes controladores da literatura baseados no SP são estudados e suas principais características destacadas. Uma estrutura de controle adequada para processos com atraso de transporte, de ordem elevada e com zeros de fase não-mínima (NMP, do inglês *non-minimum phase*) é proposta, a saber, o SP filtrado simplificado (SFSP, do inglês *simplified filtered Smith predictor*). A estratégia proposta usa uma formulação de espaço de estados e pode ser aplicada de maneira unificada a processos lineares com atraso, sendo eles estáveis, instáveis e integradores e de qualquer ordem. Em geral, os compensadores de atraso de transporte (DTCs, do inglês *dead-time compensators*) primeiro preveem a saída do processo com erro zero em um estado estacionário e, em seguida, um controlador primário com um integrador é projetado com base no modelo sem atraso. A principal vantagem da estrutura proposta é que o controlador primário é apenas um ganho de realimentação de estados sem integradores explícitos. Isso leva a menos parâmetros para sintonizar e filtros de ordem inferior, enquanto um filtro de robustez é usado para rejeitar distúrbios e garantir erro zero em regime permanente. Os resultados de simulações mostram um desempenho melhor ou equivalente em comparação com outros trabalhos publicados recentemente, mesmo mantendo o projeto de controlador simples. Os fundamentos básicos do controle feedforward para distúrbios mensuráveis são apresentados e importantes controladores baseados no SP para processos com atraso de transporte e com perturbações mensuráveis são estudados. Uma extensão feedforward para o SFSP para processos com atraso de transporte de ordem elevada para lidar com perturbações mensuráveis também é proposta. Em comparação com outras estratégias de controle, a principal vantagem de usar a abordagem do preditor é a capacidade de lidar com processos com atraso longo. A estrutura melhora o desempenho de rejeição de perturbação ao alimentar à frente a perturbação enquanto mantém as boas propriedades de robustez e atenuação de ruído do SFSP. Os resultados de simulações também mostram melhores índices de desempenho em comparação com outras estratégias da literatura recente. Além disso, para mostrar sua eficácia em um processo real, as estratégias propostas são aplicadas no controle de temperatura de uma incubadora neonatal.

Palavras-chave: Preditor de Smith. Processos com atraso de transporte. Modelos de ordem elevada. Zeros de fase não-miníma. Controle *feedforward*. Perturbações mensuráveis. Incubadora neonatal.

LIST OF FIGURES

LIST OF TABLES

LIST OF ABBREVIATIONS AND ACRONYMS

SISO	single input single output
2DOF	two degree of freedom
NMP	non-minimum phase
PI	proportional integral
PID	proportional integral derivative
DTC	dead-time compensator
SP	Smith predictor
GP	Generalized Predictor
PDRC	predictor-based disturbance rejection control
ESO	extended state observer
ADRC	active disturbance rejection control
MESO	model-based extended state observer
FSP	filtered Smith predictor
SFSP	simplified filtered Smith predictor
SDTC	simplified dead-time compensator
FOPDT	first order plus dead time
UFOPDT	unstable first order plus dead time
IPDT	integrator plus dead time
FIR	finite impulse response
ZOH	zero-order hold
IAE	integrated absolute error
TV	total variation
CV	control variance
IMC	internal model control

PSD	power spectral density
MSP	modified Smith predictor
MPC	model predictive control
GPC	generalized predictive control
DTC-GPC	dead time compensator based on generalized predictive control
FSP-FF	filtered Smith predictor with feedforward action
SDTC-FF	simplified dead-time compensator with feedforward action
SFSP-FF	simplified filtered Smith predictor with feedforward action
CSTR	continuously stirred-tank reactor
NICU	newborn intensive care unit
PWM	pulse width modulation
TITO	two input two output

LIST OF SYMBOLS

t	time
r	set point
e	error
e_f	filtered error
u	control signal
q	input disturbance
w	measurement noise
y	process variable
s	frequency
L	continuous-time delay
d	discrete-time delay
$F_{eq}(s)$	Laplace transform of the equivalent reference filter
$C_{eq}(s)$	Laplace transform of the equivalent controller
$F_{eq}(z)$	z-transform of the equivalent reference filter
$C_{eq}(z)$	z-transform of the equivalent controller
$P(s)$	Laplace transform of the process model
$P_r(s)$	Laplace transform of the process
$P_i(s)$	Laplace transform of the process for a certain operating point within a desired region
$\delta P_i(s)$	Laplace transform of the multiplicative uncertainty for a certain operating point
$\overline{\delta P_i}(s)$	Laplace transform of the upper bound of the norm of the multiplicative uncertainty
$G(s)$	Laplace transform of the delay-free process
$Y(s)$	Laplace transform of the process variable

$U(s)$	Laplace transform of the control signal
$W(s)$	Laplace transform of the measurement noise
$R(s)$	Laplace transform of the set-point
$Q(s)$	Laplace transform of the input disturbance
$P_r(z)$	z-transform of the process
$G_r(z)$	z-transform of the delay-free process
d_r	discrete-time dead time of the process
$P(z)$	z-transform of the nominal process model
$G(z)$	z-transform of the nominal delay-free process model
d	discrete-time dead time of the nominal process model
b	discrete-time numerator parameter of the nominal delay-free first-order process model
a	discrete-time denominator parameter of the nominal delay-free first-order process model
$V(z)$	z-transform of the robustness filter of the SFSP and of the SDTC
$N_v(z)$	numerator of the robustness filter of the SFSP
$D_v(z)$	denominator of the robustness filter of the SFSP
v_i	numerator parameters of the robustness filter
$H_{yr}(s)$	transfer function from the set-point to the process variable
$H_{yq}(s)$	transfer function from the disturbance input to the process variable
$H_{yr}(z)$	discrete-time transfer function from the set-point to the process variable
$H_{yq}(z)$	discrete-time transfer function from the disturbance input to the process variable
$H_{uw}(z)$	discrete-time transfer function from the measurement noise to the control signal
$F_1(z)$	FIR filter of the SDTC
$F_2(z)$	FIR filter of the SDTC

ω	frequency
$I_r(\omega)$	robustness index
$\delta\bar{P}(\omega)$	norm-bound multiplicative uncertainty
T_s	sampling period
z_c	discrete-time closed-loop pole
k	controller gain of the SFSP
k_r	reference gain of the SFSP and of the SDTC
v_i	discrete-time numerator parameters of the robustness filter of the SFSP
β_i	tuning parameters of the robustness filter of the SFSP
b_i	discrete-time numerator parameter of the nominal delay-free process model
a_i	discrete-time denominator parameter of the nominal delay-free process model
A	state matrix of the nominal state-space process model
B	input matrix of the nominal state-space process model
C	output matrix of the nominal state-space process model
I	identity matrix
$F(s)$	Laplace transform of the reference filter
$F(z)$	z-transform of the reference filter
$C(s)$	Laplace transform of the primary controller
$S(s)$	implementation structure transfer function of the FSP, SFSP and SDTC
$S(z)$	z-transform of the implementation structure transfer function of the FSP, SFSP and SDTC
K	gain vector of the SFSP
$F_r(s)$	Laplace transform of the robustness filter of the FSP
β_f	tuning parameter of the reference filter of the SFSP for high-order process
α_f	tuning parameter of the reference filter of the SFSP for high-order process
$P_Q(z)$	z-transform of the quotient of the polynomial long division

$P_R(z)$	z-transform of the remainder of the polynomial long division
p_k	discrete-time desired closed-loop poles
E_c	desired closed-loop characteristic equation
n_p	parameter that determines the reference filter order
n_z	parameter that determines the reference filter order
p_i	poles of the process model
m_1	number of poles of the model
m_2	disturbance order
n_v	number of poles of $V(z)$
n_s	number of equations from the set used in the design of $V(z)$
$N_g(z)$	numerator of the delay-free process model
$D_g(z)$	denominator of the delay-free process model
v	variables vector
A_s	coefficients matrix
B_s	vector of independent terms
N_v^*	numerator of the partial fraction decomposition of $G(z)V(z)$ related to $V(z)$
$M_Q(z)$	z-transform of the right quotient matrix of the right division of polynomial matrices
$M_R(z)$	z-transform of the right remainder matrix of the right division of polynomial matrices
L_r	real process dead time
ΔL	difference between the real process dead time and process model dead time
p_c	continuous-time desired closed-loop pole
t_q	time at which the disturbance is applied
t_w	time at which the noise is applied
μ	mean of the control signal
N_q	number of samples of the disturbance rejection response

N_w	number of samples of the noise attenuation response
ω_n	natural frequency
ξ	damping factor
$P_q(s)$	Laplace transform of the transfer function related to $Q(s)$
$G_q(s)$	Laplace transform of the delay-free transfer function related to $Q(s)$
$P_q(z)$	z-transform of the transfer function related to $Q(s)$
$G_q(z)$	z-transform of the delay-free transfer function related to $Q(s)$
L_q	continuous-time delay
d_q	discrete-time delay
$C_{ff}(s)$	Laplace transform of the equivalent feedforward control
$F_{ff}(s)$	Laplace transform of the feedforward filter of the FSP-FF
$V_{ff}(s)$	Laplace transform of the feedforward filter of the SDTC-FF
$S_q(s)$	implementation structure feedforward transfer function
$S_q(z)$	z-transform of the implementation structure feedforward transfer function
$\tilde{S}(z)$	z-transform of the stable implementation transfer function
$\tilde{S}_q(z)$	z-transform of the stable implementation feedforward transfer function
$\tilde{x}$	discrete-time states
$\tilde{A}$	discrete-time state matrix of the nominal state-space process
$\tilde{B}$	discrete-time input matrix of the nominal state-space process
$\tilde{C}$	discrete-time output matrix of the nominal state-space process
A_q	discrete-time state matrix of the nominal state-space process related to $q(t)$
B_q	discrete-time input matrix of the nominal state-space process related to $q(t)$
C_q	discrete-time output matrix of the nominal state-space process related to $q(t)$
$\mathbb{M}$	minimal realization operator
A^*	continuous-time state matrix of the nominal state-space process related to $u(t)$

B^*	continuous-time input matrix of the nominal state-space process related to $u(t)$
C^*	continuous-time output matrix of the nominal state-space process related to $u(t)$
A_q^*	continuous-time state matrix of the nominal state-space process related to $q(t)$
B_q^*	continuous-time input matrix of the nominal state-space process related to $q(t)$
C_q^*	continuous-time output matrix of the nominal state-space process related to $q(t)$
$\bar{x}$	continuous-time augmented states
$\bar{A}$	continuous-time augmented state matrix of the nominal state-space process
$\bar{B}$	continuous-time augmented input matrix of the nominal state-space process
$\bar{C}$	continuous-time augmented output matrix of the nominal state-space process
$\check{x}$	continuous-time minimal realization states
$\check{A}$	continuous-time minimal realization state matrix of the nominal state-space process
$\check{B}$	continuous-time minimal realization input matrix of the nominal state-space process
$\check{C}$	continuous-time minimal realization output matrix of the nominal state-space process
k_f	feedforward gain
K_q	state feedforward gain
u_{fb}	control signal due to the feedback action
u_{ff}	control signal due to the feedforward action
$U_{fb}(z)$	z-transform of the control signal due to the feedback action
$U_{ff}(z)$	z-transform of the control signal due to the feedforward action
$M(z)$	z-transform of the set-point tracking closed-loop transfer function
α	desired close-loop poles of the SFSP-FF

β	tuning parameters of the robustness filter of the SFSP-FF
N_{S_q}	numerator of $S_q(z)$
D_{S_q}	denominator of $S_q(z)$
m_{q1}	number of poles of $G_q(z)$
m_{q2}	disturbance order
p_{qi}	non-integrating poles of $G_q(z)$
$N^*_{Vq}(z)$	numerator of the partial fraction decomposition of $G_q(z)V(z)$ related to $V(z)$
$N^*_{G_q}(z)$	numerator of the partial fraction decomposition of $G_q(z)V(z)$ related to $G_q(z)$
$D_{G_q}(z)$	denominator of $G_q(z)$
τ_{rt}	desired closed-loop time constant of the FSP-FF
τ_{sp}	tuning parameter of the robustness filter of the FSP-FF
τ_{dr}	tuning parameter of the feedforward filter of the FSP-FF
$\beta_{SDTC-FF}$	tuning parameter of the robustness filter of the SDTC-FF
$\alpha_{SDTC-FF}$	tuning parameter of the feedforward filter of the SDTC-FF
$C_i(t)$	input concentration of a reactor
$C(t)$	output concentration of a reactor
$F(t)$	reactor inflow
V	reactor volume
$T(t)$	temperature of the CSTR
$T_c(t)$	temperature of the external cooling in the CSTR
$V_0(t)$	measurable disturbance in the CSTR
$F_0(t)$	measurable inlet flow rate of the CSTR

CONTENTS

1 INTRODUCTION

In process control, a dead time exists when there is a time interval between when a signal is applied to the process input and when this signal starts to affect the process output. Compared to when there is no dead time, the control of the process with dead time is more challenging because its presence affects the robustness and performance of the control system, turns more complex the analysis and synthesis of the controller (NORMEY-RICO; CAMACHO, 2007).

Another theme of great relevance in process control is the rejection of disturbances (ALBERTOS; SANZ; GARCIA, 2015). In the literature, different strategies are proposed to attenuate the effects of disturbances and reject them faster. Among them is the feedforward control of processes with measurable disturbances, where the disturbance is measured and then used to achieve faster rejection responses. This control problem turns more complex when the process has dead time.

1.1 State of the art

1.1.1 Smith predictor-based control for high-order dead-time processes

Processes with dead time are found in many industrial application fields, such as biomedical, chemical, aerospace, among others. In most cases, they can be represented by unstable, integrating, and stable models with dead time. Dead times decrease the phase of the system and cannot be expressed as a rational transfer function, increasing the complexity of controller design and analysis (NORMEY-RICO; CAMACHO, 2007). The control problem can become more challenging if the models have non-minimum phase (NMP) zeros, because the inverse of the delay-free model is unstable (WANG; SU, 2015).

The first closed-loop control scheme to compensate dead time was the Smith predictor (SP), proposed in 1957 (SMITH, 1957). However, the SP was not able to handle integrating and unstable open-loop systems and presented some drawback regarding robustness (MICHIELS; NICULESCU, 2003; MORARI; ZAFIRIOU, 1989). Later, in (WATANABE; ITO, 1981) and (ARTSTEIN, 1982), the SP was extended for unstable processes using a state-space representation. However, the aforementioned works (SMITH, 1957; WATANABE; ITO, 1981; ARTSTEIN, 1982) were neither concerned with robustness nor with disturbance rejection performance. These problems have been motivated several researchers to an extensive study of the dead time over the past two decades.

In the context of single-input single-output (SISO) systems, most approaches first predict the process output explicitly and then design a controller considering the delay-free model. In (NORMEY-RICO; CAMACHO, 2009; SANTOS; BOTURA; N.-R., 2010), a robustness filter is included in the SP and designed to stabilize the predictor, known as filtered Smith predictor (FSP).

Many other controllers based on predictors and extended observers for time-delay systems can be found in the literature (CASTILLO et al., 2019; SANZ et al., 2020; CASTILLO; GARCÍA, 2021). In (GARCÍA; ALBERTOS, 2008; ALBERTOS; GARCÍA, 2009; GARCÍA; ALBERTOS, 2013) a stable predictor is proposed, namely Generalized Predictor (GP), the robustness and disturbance rejection are improved based on estimation error. In (LIU et al., 2018; LIU et al., 2018), a predictor based on the GP and a two-degree-of-freedom (2DOF) control scheme were introduced.

Recently, in (SANZ; GARCÍA; ALBERTOS, 2018), a generalized SP was presented with enhanced results for unstable processes with long delay. To guarantee the predictor stability, the delay-free plant model is decomposed in two in order to separate the non-minimum phase zeros and unstable poles.

In (LIU et al., 2019), a predictor-based disturbance rejection control (PDRC) technique was presented. This work used the FSP to predict the process output and, to estimate the disturbances, an extended state observer (ESO) was implemented.

Active disturbance rejection controllers (ADRCs) have also been developed with the purpose of enhancing disturbance rejection response (WANG; SU, 2015; ZHAO; GAO, 2014; FU; TAN, 2017). The main idea consists of estimating the disturbances using an ESO and then canceling out its effect using the control signal. More recently, in (GENG et al., 2019), a model-based ESO (MESO) and a generalized predictor were designed to estimate the disturbance and the delay-free system output, respectively. The key point of the work was handling NMP systems. Many works have also recently emerged to compensate dead times using structures based on ADRC (LIU et al., 2019; ZHANG; TAN; LI, 2020).

The aforementioned recent works have increased the number of filters or gains to improve the overall closed-loop response. Focusing on industrial applications, the simplicity of the control structure and tuning could be essential. In (TORRICO et al., 2013), a tuning procedure for the FSP was proposed to simplify its design, regarding disturbance rejection, robustness, and noise attenuation by using a simpler control structure called simplified FSP (SFSP). The key idea was that the robustness filter could deal with disturbance rejection. Thus, a simpler primary controller could be tuned for set-point tracking without including integral action. Nevertheless, the SFSP is only suitable for first-order-plus-dead-time (FOPDT) models. In (TORRICO; CORREIA; NOGUEIRA, 2016; TORRICO et al., 2018), finite impulse response (FIR) filters were included to the SFSP to handle higher-order plants. However, the case of NMP zeros is not studied.

Recently, focusing on industrial applications, the works in (TORRICO et al., 2021; SÁ RODRIGUES et al., 2021) have presented simple tuning rules for the SFSP by using a similar structure of the FSP but with fewer parameters to tune. As a result, the SFSP allowed obtaining better or equivalent results than other structures based on predictors with respect to disturbance rejection and noise attenuation.

1.1.2 Smith predictor-based feedforward control for dead-time processes with measurable disturbances

In process control, disturbance rejection is a theme of great relevance (ALBERTOS; SANZ; GARCIA, 2015). In the industry, a control system with good disturbance rejection leads to improvements in several aspects, ranging from process operation safety to economical advantages. Moreover, it is directly related to the quality of final products, decrease in production costs, energy saving, etc.

In the case of measurable disturbances, its rejection can be significantly improved by feedforwarding its values in the control signal before the disturbance affects the process output. Most of the aforementioned works presented in the previous Section do not deal with measurable disturbances for dead-time processes. Many works in the past years have studied this control problem (DAVISON, 1973; GUZMÁN; HÄGGLUND, 2011; HAST; HÄGGLUND, 2014; SILVA et al., 2018), but only a few deal with the presence of dead time in the process (RODRÍGUEZ et al., 2016b; RODRÍGUEZ et al., 2016a; ALVES LIMA et al., 2019; SANZ et al., 2021; RODRÍGUEZ et al., 2020; GARCÍA-MAÑAS et al., 2021).

For measurable disturbances, feedforward control structures allow attenuating the disturbance effect before it is felt in the process output. This phenomenon also occurs if dead-time compensators are used in the case of time-delay processes. In these kinds of processes, feedforward control structures allow improving the disturbance attenuation even more because the effect of the disturbance is felt in the output only after the disturbance model delay. The work in (RODRÍGUEZ et al., 2016a) proposes a feedforward compensator for the FSP with measurable disturbances. The structure adds a feedforward path, including the disturbance model and a filter used as a tuning parameter. In (ALVES LIMA et al., 2019), the same feedforward structure from (RODRÍGUEZ et al., 2016a) was applied to the SFSP for first-order dead-time processes, obtaining better disturbance rejection with a lower-order robustness filter. The work in (RODRÍGUEZ et al., 2020) proposes tuning rules for a feedforward control methodology that uses low-order process models. In (GARCÍA-MAÑAS et al., 2021), a comparison of recently published tuning rules for feedforward compensation is made by simulations and experiments.

1.2 Motivation

In process control, the more complex the process model, the greater the difficult in designing and tuning the controller. In this context, there is always a need to turn more simple the controller design and tuning for high-order process with dead-time.

Furthermore, there is also a need to improve the disturbance rejection responses of control systems. Hence, feedforward control of dead-time process with measurable disturbances presents itself as one of the more suitable alternatives to obtain improvements for disturbance rejection.

1.3 Objectives

The main objectives of this work is to propose SP-based controllers that can deal with high-order dead-time processes and that can obtain faster disturbance rejection responses by using a feedforward action for measurable disturbances. In order to achieve this purpose, this text aims at:

- to extend the formulation of the SFSP for higher-order models with NMP zeros, keeping the simplicity of the original structure (TORRICO et al., 2013);
- to show that the proposed SFSP is suitable for open-loop stable, unstable, and integrating high-order models with dead time;
- to show that, because of its state-space model representation, the proposed SFSP can deal with NMP zeros without increasing the control complexity;
- to further improve the disturbance rejection in processes with measurable disturbances, this work proposes a new feedforward structure for the SFSP for high-order dead-time processes;
- to present that the main novelty comes from the idea of including a static gain in the feedforward path, so that the control action can deal in advance with the disturbance prior to its effects on the measured plant output;
- to show that the proposed controller has the same tuning degrees of freedom as the original SFSP, since there are no free tuning parameters to design the feedforward controller;
- to show the better performance of the SFSP and the SFSP with feedforward action, even with a simpler control schemes, when compared with others SP-based controllers from the literature;
- to validate and show that both proposed controllers have great potential for industrial applications by presenting experimental results obtained in the temperature control in a newborn intensive care unit (NICU).

1.4 Published works related to this thesis

This doctorate thesis is based on two articles published during the candidate's doctorate program:

- TORRICO, B. C.; PEREIRA, R. D. O.; SOMBRA, A. K. R.; NOGUEIRA, F. G., Simplified filtered Smith predictor for high-order dead-time processes. ISA Transactions, v. 109, p. 11–21, 2021;

- PEREIRA, R. D. O.; TORRICO, B. C.; DO NASCIMENTO JR., J. N.; ALVES LIMA, T.; DE ALMEIDA FILHO, M. P.; NOGUEIRA, F. G., Smith predictor-based feedforward controller for measurable disturbances, Control Engineering Practice, Volume 133, 105439, 2023.

1.5 Organization of the work

The work is organized as follows: Chapter 2 presents relevant controllers based on the SP, the SFSP for high-order dead-time processes is presented in Chapter 3, in Chapter 4 fundamentals of feedforward control for measurable disturbances and SP-based controllers with feedforward action are presented, the SFSP with feedforward action for measurable disturbances is presented in Chapter 5, and in Chapter 6 are the conclusions of this work.

2 SMITH PREDICTOR-BASED CONTROLLERS

Since the SP was presented in (SMITH, 1957), several controllers based on its control structure were proposed. These controllers improved the performance and robustness of the original SP and overcame some of its limitations. This chapter presents the SP itself and other controllers that are relevant to the contributions of this work.

2.1 Important definitions and concepts

2.1.1 Process model

Throughout this text, the nominal process model used by the controller and the real process are represented by P and P_r, respectively. The continuous-time process model in the s-domain is defined as

$$P(s) = G(s)e^{-Ls}, \tag{2.1}$$

where $G(s)$ is the delay-free model and L is the time delay. The discrete-time process model in the z-domain, by using the zero-order hold (ZOH) discretization method, is also defined as

$$P(z) = G(z)z^{-d}, \tag{2.2}$$

where d is the time delay. Furthermore, control input, process output, input and output disturbances are represented by u, y, q and w, respectively.

2.1.2 Equivalent two-degree-of-freedom control structure

Very often, to turn the control analysis easier or even for implementation purposes, a controller structure can be reduced to an equivalent two-degree-of-freedom (2DOF) control structure. A commonly used 2DOF control structure is shown in Fig. 1, where r is the set-point input, F_{eq} is the equivalent reference filter and C_{eq} is the equivalent controller. Note that the condition $F_{eq}(s=0) = F_{eq}(z=1) = 1$ must be satisfied to guarantee null steady-state error.

2.1.3 Closed-loop robust stability analysis

Consider a dead-time process in the s-domain that can be modeled by unstructured multiplicative uncertainty (MORARI; ZAFIRIOU, 1989):

$$P_i(s) = P(s)(1 + \delta P_i(s)), \tag{2.3}$$

where $P_i(s)$ represents the process for a certain operating point within a desired region and $\delta P_i(s)$ is the multiplicative uncertainty for a certain operating point.

Figure 1 – 2DOF control structure.

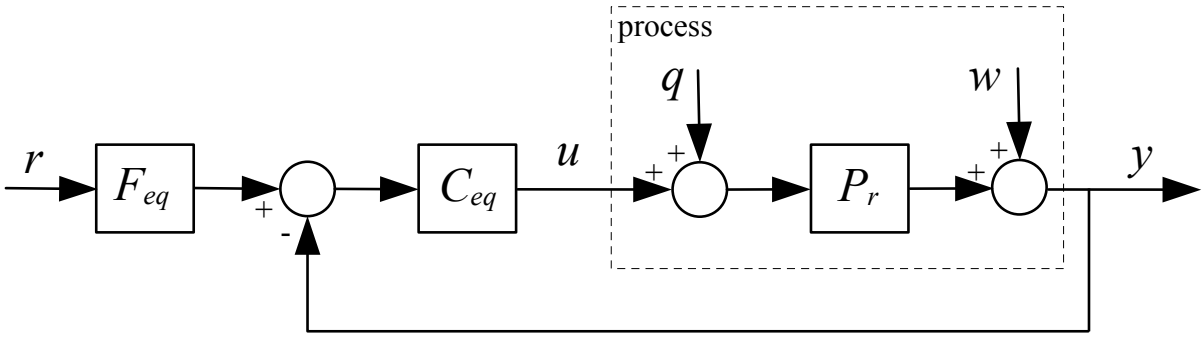

Source: The author.

Considering $s = j\omega$, the upper bound of the norm of the multiplicative uncertainty is computed by

$$\overline{\delta P}(\omega) \geq |\delta P_i(j\omega)| = \left| \frac{P_i(j\omega) - P(j\omega)}{P(j\omega)} \right|, \forall i, \tag{2.4}$$

Following the general robust stability theorem (MORARI; ZAFIRIOU, 1989), derived from Nyquist's stability criterion, the robust stability condition can be obtained from

$$I_r(\omega) = \frac{|1 + C_{eq}(j\omega)P(j\omega)|}{|C_{eq}(j\omega)P(j\omega)|} > \overline{\delta P}(\omega), \ \forall \omega > 0. \tag{2.5}$$

where $I_r(\omega)$ is the robustness index.

A similar analysis can be made in the z-domain, considering $z = e^{j\Omega}$, where $\Omega = \omega T_s$, T_s is the sampling time, and ω is the frequency in the range $0 < \omega < \pi/T_s$.

2.2 Smith predictor

The SP continuous-time conceptual control structure is presented in Fig. 2, where $F(s)$ is the reference filter and $C(s)$ is the primary controller.

Reducing the control structure of Fig. 2 to the equivalent 2DOF control structure, it results

$$F_{eq}(s) = F(s), \tag{2.6}$$

$$C_{eq}(s) = \frac{C(s)}{1 + C(s)S(s)}, \tag{2.7}$$

where

$$S(s) = G(s)(1 - e^{-Ls}). \tag{2.8}$$

Figure 2 – SP conceptual control structure.

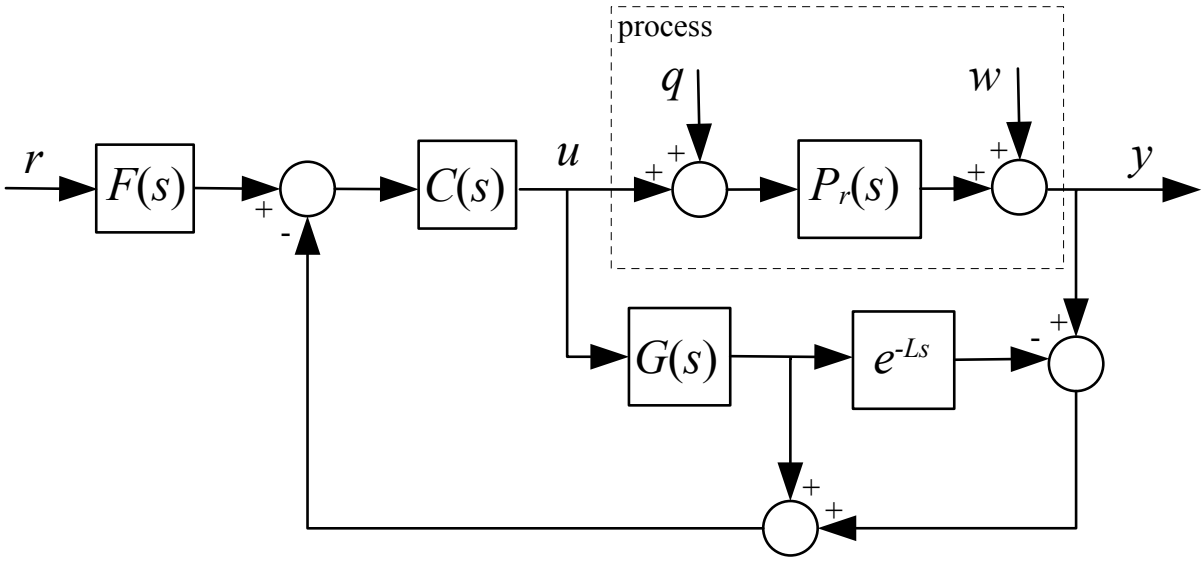

Source: The author.

By using (2.1) and (2.7), one can easily obtain the closed-loop transfer functions that represent the input-output relationships, given by

$$H_{yr}(s) = \frac{Y(s)}{R(s)} = \frac{C(s)G(s)}{1+C(s)G(s)}e^{-Ls}, \tag{2.9}$$

$$H_{yq}(s) = \frac{Y(s)}{Q(s)} = P(s)\left[1 - \frac{C(s)G(s)}{1+C(s)G(s)}e^{-Ls}\right], \tag{2.10}$$

$$H_{uw}(s) = \frac{U(s)}{W(s)} = \frac{-C(s)}{1+C(s)G(s)}. \tag{2.11}$$

With respect to the tuning of the SP, the primary controller $C(s)$ can be designed, for example, by an internal model control (IMC) method, where only $G(s)$ is considered in the design. In the IMC design from (SKOGESTAD, 2003), for first-order stable models, $C(s)$ results a PI controller, and, for second-order stable models, $C(s)$ results a PID controller. Afterwards, the reference filter $F(s)$ can be tuned to obtain a desired set-point tracking performance.

In practice, for stable processes, the SP can be implemented in the conceptual control structure from Fig. 2 after the discretization (with a ZOH, for example) of each controller parameter. However, for unstable processes, this structure is internally unstable due to the unstable poles of $G(z)$ and, for integrating processes, it does not reject disturbances.

2.2.1 Closed-loop robust stability

Considering (2.5), the robust stability condition of the SP results as

$$I_r(\omega) = \left|\frac{1+C(j\omega)G(j\omega)}{C(j\omega)G(j\omega)}\right| > \overline{\delta P}(\omega),\ \forall\omega > 0. \tag{2.12}$$

Figure 3 – FSP conceptual control structure.

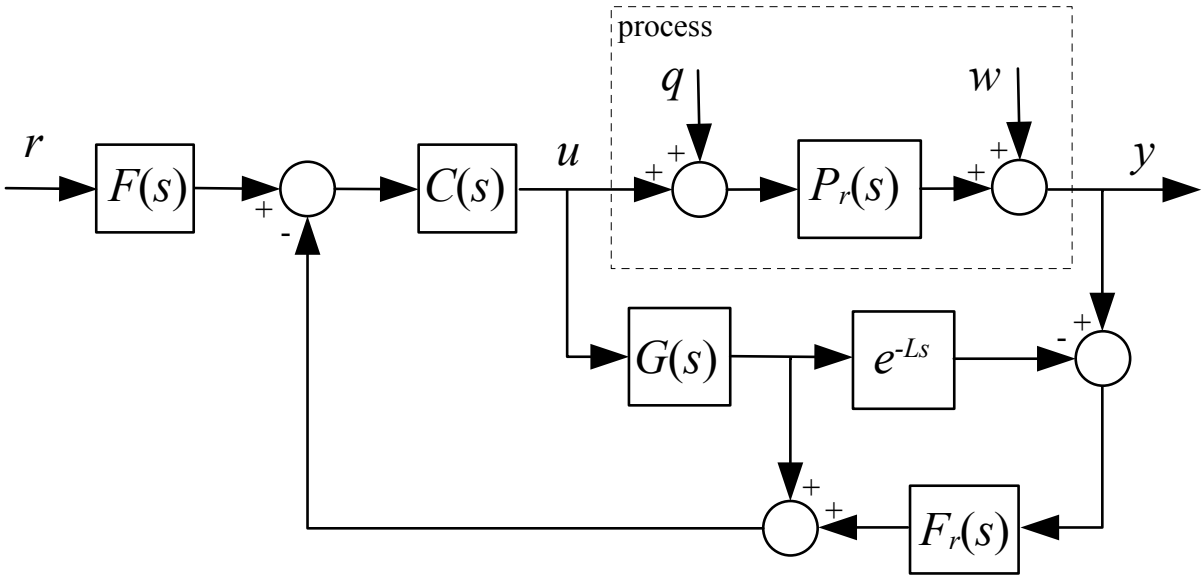

Source: The author.

2.3 Filtered Smith predictor

The filtered SP (FSP) (NORMEY-RICO; CAMACHO, 2009) is an unified controller in the sense that it can deal with stable, unstable and integrating processes by using models of any order.

The continuous-time conceptual control structure of the FSP is shown in Fig. 3, where $F_r(s)$ is the robustness filter.

The structure of Fig. 3 can be reduced to the equivalent 2DOF control structure of Fig. 1. This results in the following equivalent controller parameters:

$$F_{eq}(s) = \frac{F(s)}{F_r(s)}, \tag{2.13}$$

$$C_{eq}(s) = \frac{C(s)F_r(s)}{1+C(s)S(s)}, \tag{2.14}$$

where

$$S(s) = G(s)(1-F_r(s)e^{-Ls}). \tag{2.15}$$

Considering the nominal case, where $P_r(s) = P(s)$, one obtains the closed-loop transfer functions as

$$H_{yr}(s) = \frac{Y(s)}{R(s)} = \frac{F(s)C(s)G(s)}{1+C(s)G(s)}e^{-Ls}, \tag{2.16}$$

Figure 4 – FSP implementation control structure.

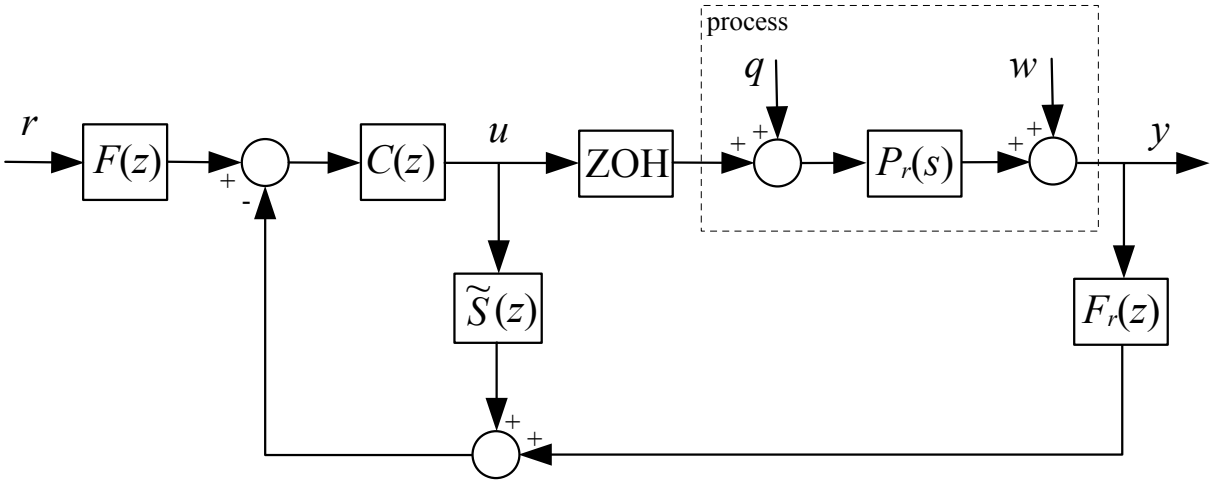

Source: The author.

$$H_{yq}(s) = \frac{Y(s)}{Q(s)} = P(s)\left[1 - \frac{F_r(s)C(s)G(s)}{1+C(s)G(s)}e^{-Ls}\right], \tag{2.17}$$

$$H_{uw}(s) = \frac{U(s)}{W(s)} = \frac{-C(s)F_r(s)}{1+C(s)G(s)}. \tag{2.18}$$

Note that the robustness filter $F_r(s)$ is not present in $H_{yr}(s)$. In other words, it has no influence over the set-point tracking response. However, it has an important influence over disturbance rejection responses and over measurement noise attenuation in the control signal, as seen in the expressions for $H_{yq}(s)$ and $H_{uw}(s)$, respectively.

2.3.1 Stable implementation

For stable processes, the FSP can be implemented in practice by discretization of each controller parameter of the structure from Fig. 3. However, for unstable and integrating processes, the structure from Fig. 3 is internally unstable and only used for analysis. In such cases, the structure from Fig. 4 must be used instead.

Taking in account the design procedure of the robustness filter $F_r(s)$, the condition $S(s)|_{s=p_i} = 0$ (where p_i are the poles of $G(s)$) must be satisfied (NORMEY-RICO; CAMACHO, 2009). Furthermore, analyzing (2.14) and (2.15), the poles of $G(z)$ appear explicitly in the resulting numerator of $C_{eq}(z)$. Therefore, for the stable implementation of the controller and to obtain $\tilde{S}(z)$, the poles of $G(z)$ must be eliminated from $S(z)$. In the z-domain, this is obtained by explicit pole-zero cancellation.

Figure 5 – SFSP conceptual control structure.

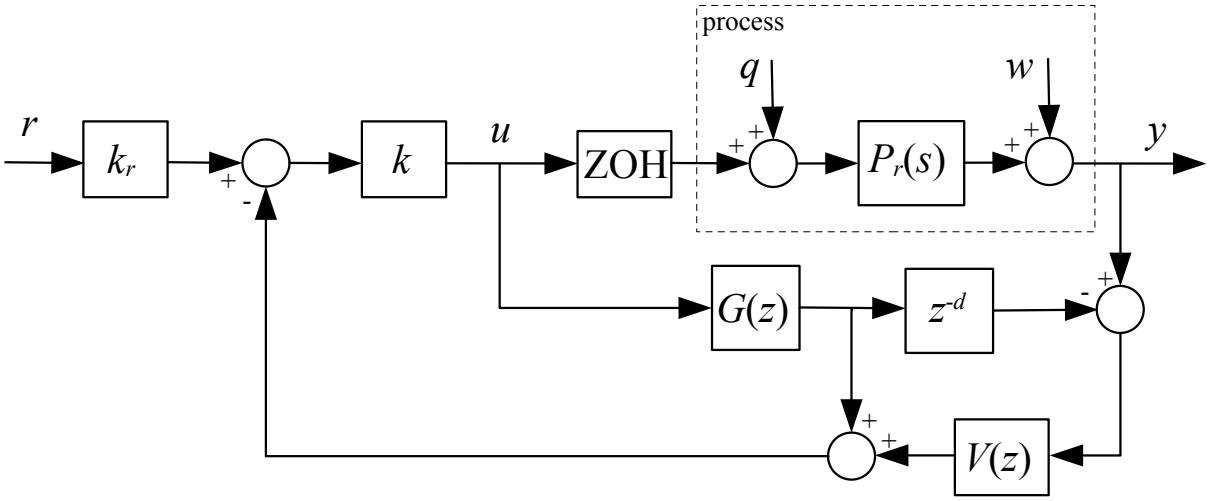

Source: The author.

2.3.2 Closed-loop robust stability

Considering the analysis presented in Section 2.1.3, the closed-loop robust stability condition for the FSP is defined as

$$I_r(\omega) = \left| \frac{1 + C(j\omega)G(j\omega)}{F_r(j\omega)C(j\omega)G(j\omega)} \right| > \overline{\delta P}(\omega), \ \forall \omega > 0. \tag{2.19}$$

2.4 Simplified filtered Smith predictor

The simplified filtered Smith predictor (SFSP), firstly presented in (TORRICO et al., 2013), is a controller for stable, unstable and integrating processes represented by first-order models with dead time. Its conceptual control structure is shown in Fig. 5, where the gain k is the primary controller, k_r is the reference gain, and $V(z)$ is the robustness filter.

By simplifying the conceptual control structure of Fig. 5 to the equivalent 2DOF control structure of Fig. 1, one obtains

$$F_{eq}(z) = \frac{k_r}{V(z)}, \tag{2.20}$$

and

$$C_{eq}(z) = \frac{kV(z)}{1 + kS(z)}, \tag{2.21}$$

where

$$S(z) = G(z)(1 - V(z)z^{-d}). \tag{2.22}$$

It is important to note from (2.20) that, to attain set-point tracking, the condition $V(1) = k_r$ must be satisfied, resulting in $F_{eq}(1) = 1$. Therefore, there is no steady-state error due to model mismatches.

Figure 6 – SFSP implementation control structure.

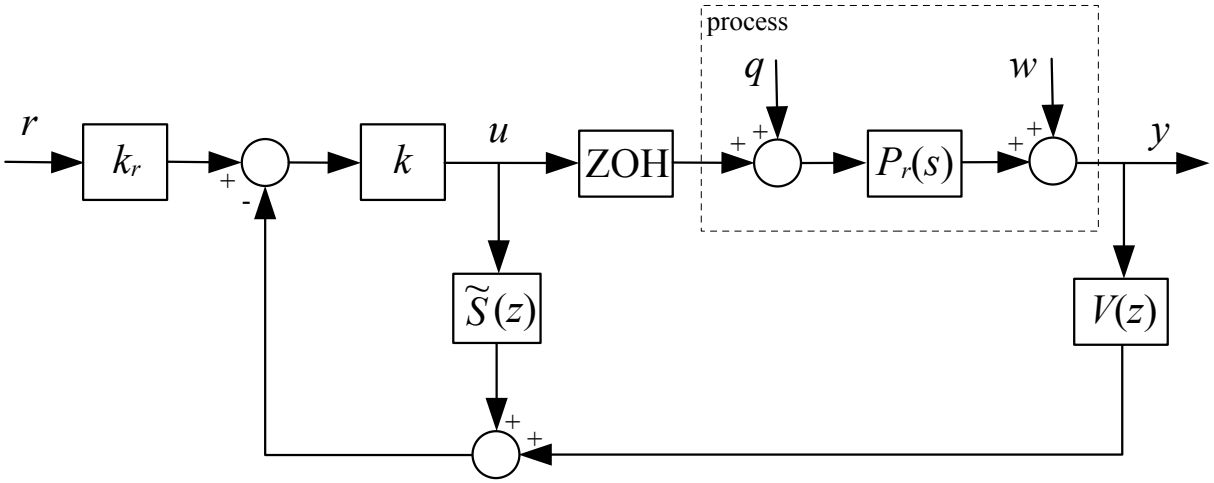

Source: The author.

Consider that the discretization of $P_r(s)$ with a ZOH results in $P_r(z)$. In the nominal case, where $P_r(z) = P(z)$, the following closed-loop transfer functions are obtained:

$$H_{yr}(z) = \frac{Y(z)}{R(z)} = \frac{k_r kG(z)}{1 + kG(z)} z^{-d}, \tag{2.23}$$

$$H_{yq}(z) = \frac{Y(z)}{Q(z)} = P(z)\left[1 - \frac{V(z)kG(z)}{1 + kG(z)} z^{-d}\right], \tag{2.24}$$

$$H_{uw}(z) = \frac{U(z)}{W(z)} = \frac{-kV(z)}{1 + kG(z)}. \tag{2.25}$$

As in the FSP, the robustness filter has no influence over the set-point tracking response, but it has an important influence over the rejection of disturbances, as can be seen by (2.24) and (2.25).

2.4.1 Stable implementation

For stable process, practical implementation is made by using the structure from Fig. 5. However, for unstable and integrating processes, this structure is internally unstable. Thus, the structure from Fig. 6 must be used instead. As in the FSP, taking in account the procedure design of $V(z)$ (TORRICO et al., 2013), $\tilde{S}(z)$ must be obtained by pole-zero cancellation.

2.4.2 Closed-loop robust stability

Considering a similar analysis from Section 2.1.3 in the z-domain, the robust stability condition of the SFSP is obtained as

$$I_r(\omega) = \left| \frac{1 + kG(e^{j\Omega})}{V(e^{j\Omega})kG(e^{j\Omega})} \right| > \overline{\delta P}(\omega), \ \forall \omega > 0, \tag{2.26}$$

Figure 7 – SDTC conceptual control structure.

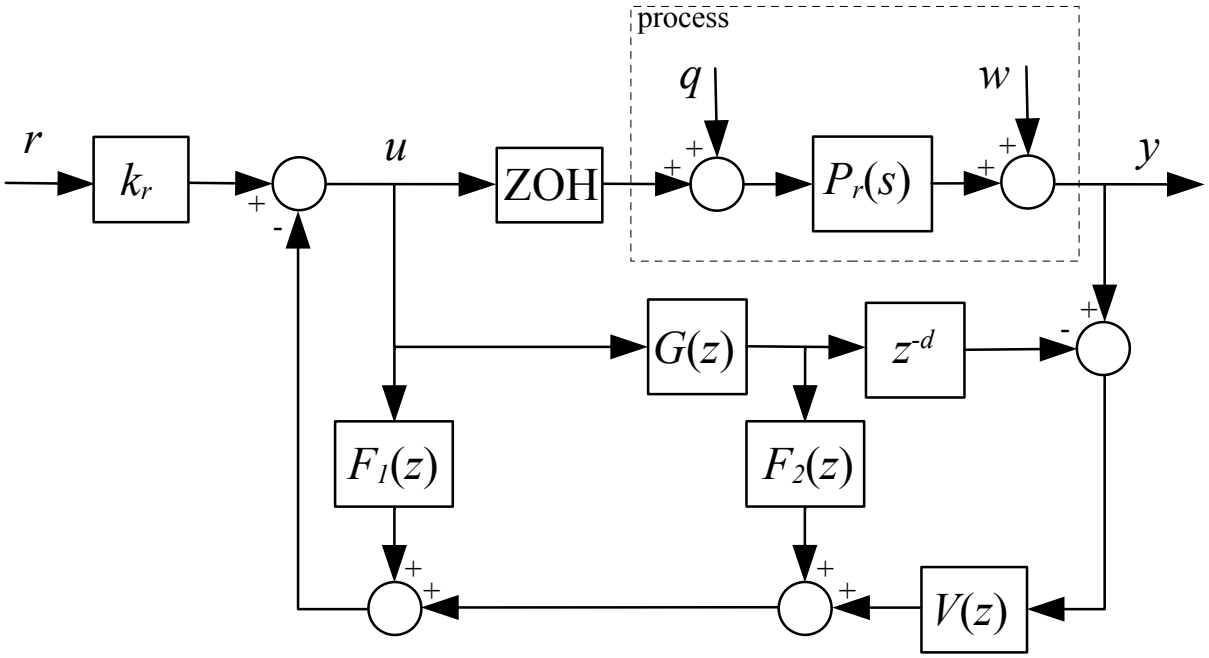

Source: The author.

where $\Omega = \omega T_s$.

2.5 Simplified dead-time compensator

The simplified dead-time compensator (SDTC) is an extension of the SFSP that can use high-order models with dead time and was firstly presented in (TORRICO; CORREIA; NOGUEIRA, 2016). The conceptual control structure of the SDTC is presented in Fig. 7, where $F_1(z)$ and $F_2(z)$ are finite impulse response (FIR) filters.

By reducing the conceptual control structure of Fig. 7 to the equivalent 2DOF control structure of Fig. 1, one obtains

$$F_{eq}(z) = \frac{k_r}{V(z)}, \tag{2.27}$$

$$C_{eq}(z) = \frac{V(z)}{1+S(z)}, \tag{2.28}$$

where

$$S(z) = F_1(z) + G(z)(F_2(z) - V(z)z^{-d}). \tag{2.29}$$

Note that, as in the SFSP, the condition $V(1) = k_r$ must also be satisfied to result $F_eq(1) = 1$ and to guarantee set-point tracking.

By discretizing $P_r(s)$ with a ZOH and making $P_r(z) = P(z)$, the following closed-loop transfer functions are obtained:

$$H_{yr}(z) = \frac{Y(z)}{R(z)} = \frac{F(z)G(z)}{1 + F_1(z) + F_2(z)G(z)} z^{-d}, \tag{2.30}$$

$$H_{yq}(z) = \frac{Y(z)}{Q(z)} = P(z)\left[1 - \frac{V(z)G(z)}{1 + F_1(z) + F_2(z)G(z)} z^{-d}\right], \tag{2.31}$$

$$H_{uw}(z) = \frac{U(z)}{W(z)} = \frac{-V(z)}{1 + F_1(z) + F_2(z)G(z)}. \tag{2.32}$$

As in the FSP and the SFSP, the robustness filter $V(z)$ has no influence over the set-point tracking, but continues to influence the disturbance rejection responses. More details on how to properly tune the robustness filter to improve disturbance rejection responses can be found in (TORRICO et al., 2018).

2.5.1 Stable implementation

Following the ideas presented for the FSP and the SFSP, for stable processes, the conceptual control structure can be used for practical implementation. As this structure is internally unstable for unstable and integrating processes, the structure from Fig. 8 must be used instead in practice for such processes. To obtain $\tilde{S}(z)$, a procedure of pole-zero cancellation is used following the design and tuning of $V(z)$ (TORRICO; CORREIA; NOGUEIRA, 2016; TORRICO et al., 2018).

2.5.2 Closed-loop robust stability

Following the analysis presented in Section 2.1.3 for the discrete-time case, the robust stability condition for the SDTC is obtained as

$$I_r(\omega) = \left| \frac{1 + F_1(e^{j\Omega}) + F_2(e^{j\Omega})G(e^{j\Omega})}{V(e^{j\Omega})G(e^{j\Omega})} \right| > \overline{\delta P}(\omega), \ \forall \omega > 0, \tag{2.33}$$

where $\Omega = \omega T_s$.

2.6 Discussion

SP-based controllers are commonly used in control engineering to handle processes with dead-time. The choice of which controller to use will depend on characteristics such as the type of the process, performance and robustness requirements, and the simplicity of implementation and tuning. The classical SP is simple to tune and easy to implement, but may not be suitable for processes with significant model uncertainties and that are open-loop unstable or integrating. The

Figure 8 – SDTC implementation control structure.

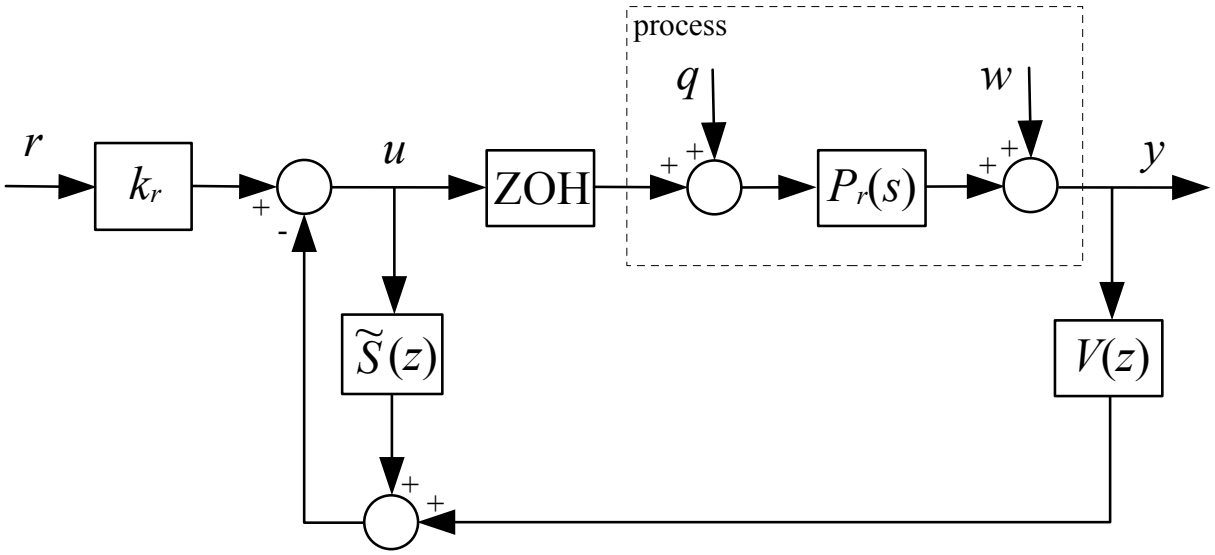

Source: The author.

FSP can be used for open-loop stable, unstable and integrating processes and is more robust than the SP. Nevertheless, for control systems where tuning and implementation simplicity are the choice, the SFSP can offer an excellent trade-off between robustness and performance. Another structure that also presents a solution to the issue at hand is the SDTC, which uses FIR filters in its feedback loop. Its tuning rules allow for the use of lower-order filters that are capable of simultaneously considering closed-loop robustness and noise attenuation.

3 SIMPLIFIED FILTERED SMITH PREDICTOR FOR HIGH-ORDER DEAD-TIME PROCESSES

In this chapter, a formulation of the SFSP for high-order dead-time processes is proposed. This formulation is based on state-space models, which allows its unified application to stable, unstable, and integrating linear processes of any order and with NMP zeros. The structure features a feedback gain as the primary controller and without explicit integrators, resulting in fewer tuning parameters and lower-order filters.

This chapter is organized as follows. Section 3.1 is dedicated to the reformulation of the SFSP. The proposed SFSP is extended to a state-space based approach in Section 3.2. Controller tuning is presented in Section 3.3. The stable implementation of the controller is presented in Section 3.4. Section 3.5 defines the closed-loop robust stability condition. In Section 3.6 a formulation to compute the maximum achievable robustness is presented. Controller tuning guidelines are explained in Section 3.7. Simulation examples were considered to evaluate the proposed structure in Section 3.8. Considerations and discussions of the results were performed in Section 3.9.

3.1 Reformulation of the Simplified FSP

The structure of the SFSP, proposed in (TORRICO et al., 2013), can be reformulated as illustrated in Fig. 9. The process can be represented by

$$P_r(z) = G_r(z)z^{-d_r}, \tag{3.1}$$

where $G_r(z)$ represents the undelayed dynamics and d_r the dead time.

The nominal process model is given by a FOPDT model

$$P(z) = G(z)z^{-d} = \frac{b}{z-a}z^{-d}. \tag{3.2}$$

where b is a constant, a and d are the pole and the dead time of the nominal process model, respectively. Parameters k and $F(z) = k_r$ are static gains and the robustness filter can be represented by

$$V(z) = \frac{N_v(z)}{D_v(z)}. \tag{3.3}$$

Furthermore, the conceptual reformulated SFSP structure can be reduced to a 2-degree-of-freedom (2DOF) conceptual equivalent structure, as presented in Fig. 10, where

$$F_{eq}(z) = \frac{k_r}{V(z)}, \tag{3.4}$$

Figure 9 – Reformulated SFSP structure.

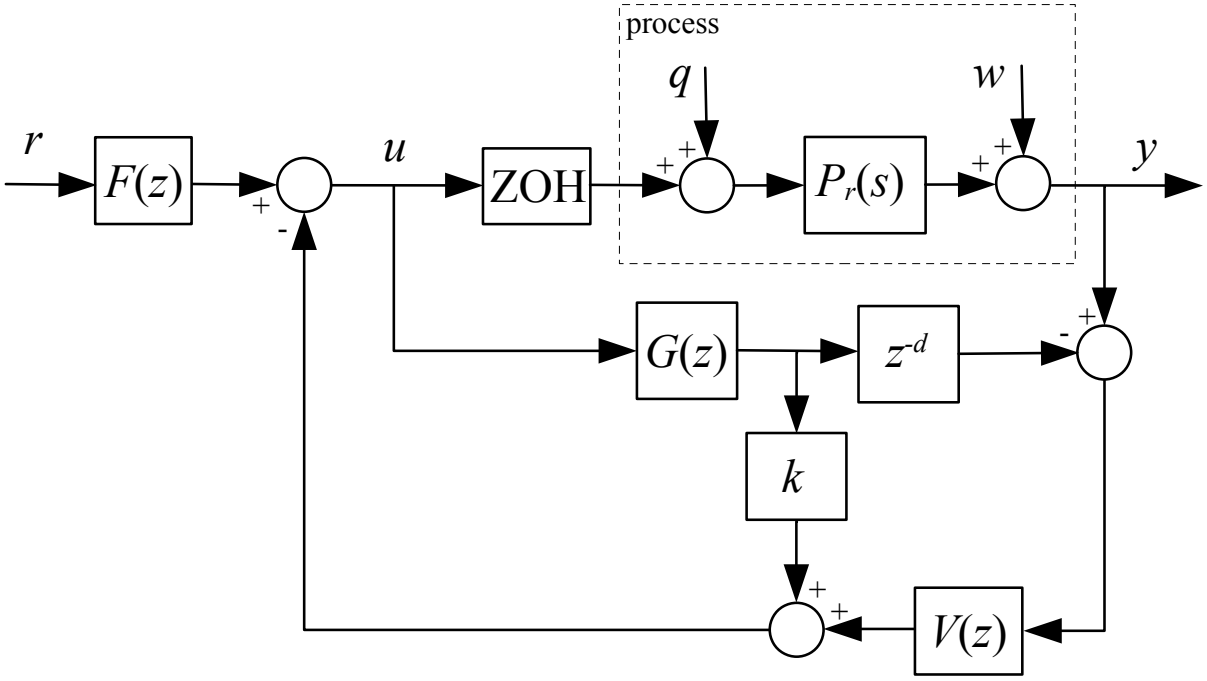

Source: The author.

Figure 10 – 2DOF conceptual equivalent structure.

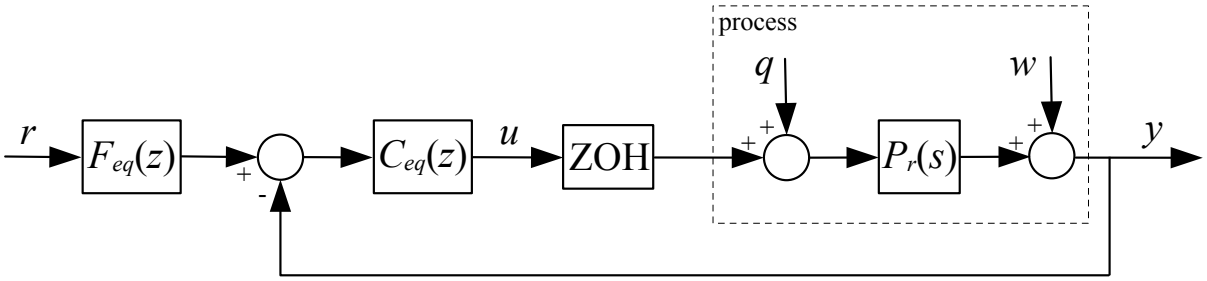

Source: The author.

$$C_{eq}(z) = \frac{V(z)}{1+S(z)}, \tag{3.5}$$

$$S(z) = G(z)(k - V(z)z^{-d}). \tag{3.6}$$

3.1.1 Closed-loop relations and robustness

Considering the nominal case ($P_r(z) = P(z)$), the closed-loop relations and the robustness index of the SFSP are given by (see Fig. 9)

$$H_{yr}(z) = \frac{Y(z)}{R(z)} = k_r \frac{bz^{-d}}{z - z_c}, \tag{3.7}$$

$$H_{yq}(z) = \frac{Y(z)}{Q(z)} = \frac{bz^{-d}}{z-a}\left[1 - \frac{bz^{-d}}{z - z_c}V(z)\right], \tag{3.8}$$

$$H_{un}(z) = \frac{U(z)}{N(z)} = \frac{-(z-a)V(z)}{z - z_c}, \tag{3.9}$$

$$I_r(\omega) = \left|\frac{z - z_c}{bV(z)}\right|_{z=e^{j\omega T_s}} > \overline{\delta P}(\omega), \tag{3.10}$$

$$z_c = a - bk, \tag{3.11}$$

where z_c is a specified closed-loop pole, $I_r(\omega)$ is defined as a robustness index and $\overline{\delta P}(e^{j\omega T_s})$ is the multiplicative uncertainty upper bound. Note that (3.10) condition guarantees closed-loop robust stability.

3.1.2 Controller tuning

The gain k is set for a desired closed-loop response, thus, it can be derived from (3.11)

$$k = \frac{a - z_c}{b}. \tag{3.12}$$

The reference gain k_r is chosen for set-point tracking with zero error at steady-state, it can be obtained from (3.7)

$$k_r = \frac{1 - z_c}{b}. \tag{3.13}$$

The filter $V(z)$ can be chosen as (TORRICO et al., 2013)

$$V(z) = \frac{v_0 + v_1 z^{-1}}{(1 - \beta z^{-1})^{n_v}}, \tag{3.14}$$

where β is a tuning parameter, n_v the filter order, v_0 and v_1 are derived from the conditions

$$V(1) = k_r, \tag{3.15}$$

and

$$k - V(a)a^{-d} = 0, \;\; a \neq 1, \tag{3.16}$$

to guarantee constant disturbance rejection and to eliminate the effect of the undesired poles from (3.8), respectively.

Note that, due to condition (3.15), $C_{eq}(z)$ has at least one integrator and $F_{eq}(1) = 1$, therefore, guaranteeing that any model mismatches does not results in steady-state error.

3.1.3 Implementation structure

The conceptual structure of the SFSP can be used only for open-loop stable models. In the case of unstable and integrating open-loop models, to avoid internal instability, the structure of Fig. 11 can be used (TORRICO et al., 2018), where

$$S(z) = \frac{b}{z-a}\left[k - \frac{N_v(z)}{D_v(z)}z^{-d}\right]. \tag{3.17}$$

Figure 11 – SFSP implementation structure.

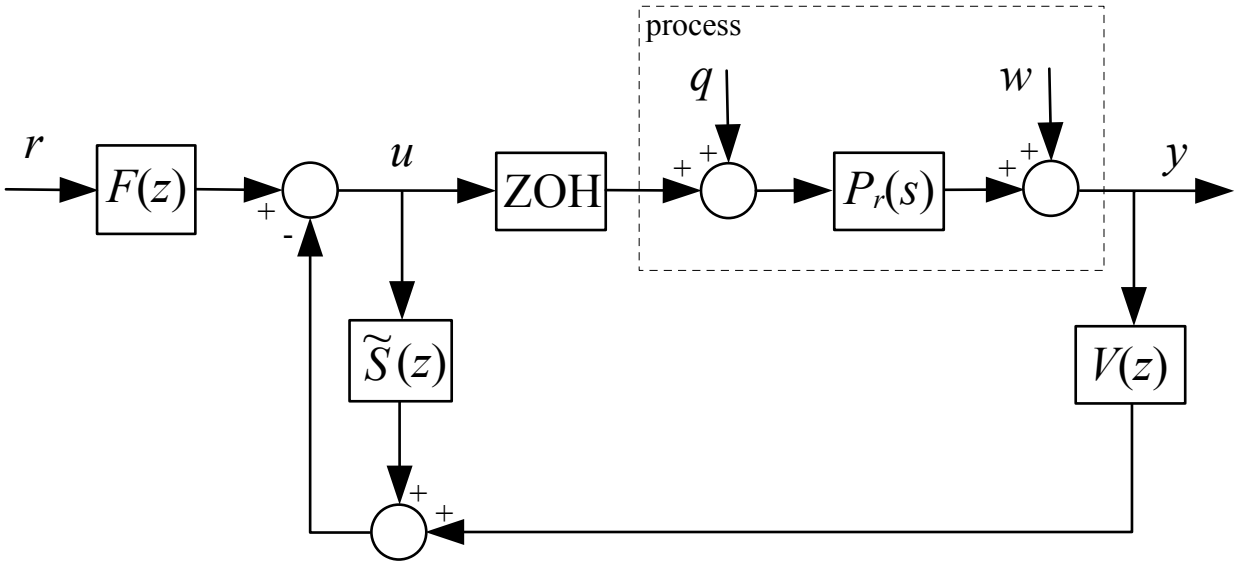

Source: The author.

Note that condition (3.16) allows to cancel the pole $z = a$ from $S(z)$, thus, using partial fraction decomposition for $\beta \neq a$, (3.17) can be written as

$$S(z) = \frac{bk}{z-a} - \frac{bka^d z^{-d}}{z-a} - \frac{N_v^*(z)z^{-d}}{D_v(z)}, \tag{3.18}$$

where $N_v^*(z)$ is a z^{-1} polynomial of order $n_v - 1$.

Consider the following Diophantine equation (SANZ; GARCÍA; ALBERTOS, 2018):

$$1 = P_Q(z)(z-a) + P_R(z), \tag{3.19}$$

where $P_Q(z)$ and $P_R(z)$ are, respectively, the quotient and the remainder of the polynomial long division $1/(z-a)$.

Solving the Diophantine equation up to d terms results

$$1 = \left(\sum_{i=1}^{d} a^{i-1}z^{-i}\right)(z-a) + a^d z^{-d}. \tag{3.20}$$

The above expression can be re-written as

$$\frac{1}{z-a} - \frac{a^d z^{-d}}{z-a} = \sum_{i=1}^{d} a^{i-1}z^{-i}. \tag{3.21}$$

By substituting (3.21) in (3.18), the expression for $S(z)$ results

$$\tilde{S}(z) = \sum_{i=1}^{d} ka^{i-1}bz^{-i} - \frac{N_v^*(z)}{D_v(z)}z^{-d}. \tag{3.22}$$

It is worth noting that function $S(z)$, from (3.22), has no longer the pole in $z = a$. Therefore, all its poles are within the unit circle, which guarantees internal stability.

3.2 Simplified FSP for high-order dead-time processes

The proposed structure is derived from the FSP and SFSP, as illustrated in Fig. 12. As can be seen, in this case, the nominal process model is represented using a space-state approach

$$P(z) = G(z)z^{-d} = C(zI - A)^{-1}Bz^{-d}, \tag{3.23}$$

where A, B, and C are in the canonical observable form, as defined in Appendix A. The pair (A,B) is controllable and (C,A) is observable.

Observe that, as in the SFSP, the proposed controller has feedback gain K, but its dimension is $1 \times n$ instead of being a scalar, and a robustness filter $V(z)$. Nevertheless, the

Figure 12 – Proposed structure.

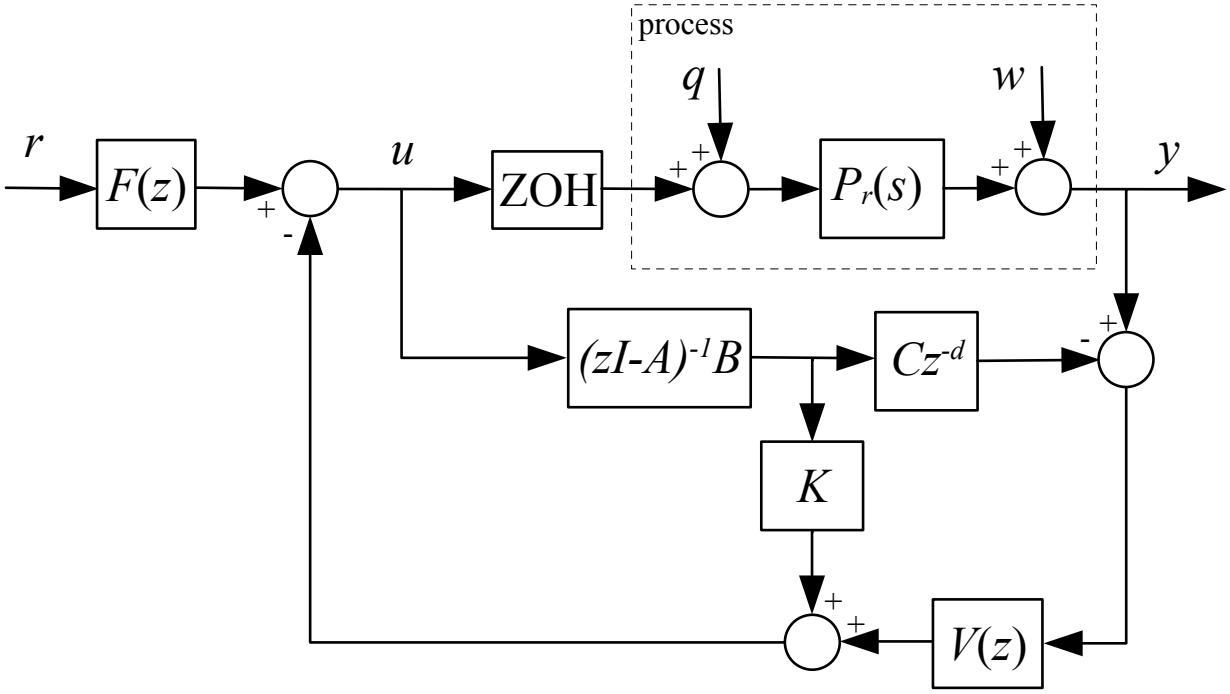

Source: The author.

proposed structure uses a reference filter $F(z)$ instead of a static gain to have more degrees of freedom.

Considering an equivalent 2DOF structure, as in Fig. 10, it is obtained

$$F_{eq}(z) = \frac{F(z)}{V(z)}, \tag{3.24}$$

$$C_{eq}(z) = \frac{V(z)}{1+S(z)}, \tag{3.25}$$

$$S(z) = \left(K - z^{-d}V(z)C\right)(zI-A)^{-1}B. \tag{3.26}$$

3.3 Controller tuning

3.3.1 Tuning of K and k_r

The primary controller is tuned to achieve a desired set-point response. For the nominal case, from Fig. 12, the set-point response is given by

$$H_{yr}(z) = F(z)C(zI-A+BK)^{-1}Bz^{-d}. \tag{3.27}$$

The feedback gain K can be set to obtain the desired characteristic polynomial

$$E_c(z) = \prod_{k=1}^{n}(z-p_k) = \det(zI-A+BK), \tag{3.28}$$

where p_k represents the desired closed-loop poles. The gain K can be obtained using the Ackermann formula (ACKERMANN, 1977)

$$K = [0\ 0\ ...\ 1]\left[B\ AB\ ...\ A^{n-1}B\right]^{-1} E_c(A). \tag{3.29}$$

The reference filter is proposed as

$$F(z) = k_r \cdot \frac{(1-\beta_f)^{n_p}}{(1-\beta_f z^{-1})^{n_p}} \cdot \frac{(1-\alpha_f z^{-1})^{n_z}}{(1-\alpha_f)^{n_z}}, \tag{3.30}$$

where n_p and n_z determine the filter order, while β_f and α_f are tuning parameters to obtain a desired dynamics of the set-point tracking response. To guarantee zero set-point tracking error at steady state, k_r is defined as

$$k_r = \left[C(I-A+BK)^{-1}B\right]^{-1}. \tag{3.31}$$

3.3.2 Tuning of V(z)

To establish the filter design conditions, initially, the equivalent 2DOF structure from Fig. 10 is considered. From (3.25) and (3.26), the filter $V(z)$ can be tuned to (i) cancel the undesired zeros of $S(z)$ originated by the poles of $P(z)$ and (ii) reject disturbances at steady state (constant, ramp, sinusoidal, etc.). Therefore, the following set of equations can be derived (TORRICO et al., 2018)

$$\begin{cases} 1+S(z)|_{z=p_i\neq 1} = 0, \\ \\ 1+S(z)|_{z=e^{\pm j\omega_k}} = 0, \\ \\ \dfrac{d^k}{dz^k}(1+S(z))\Big|_{z=1} = 0,\ k=0,...,m-1, \end{cases} \tag{3.32}$$

where p_i are simple poles of the plant, w_k are frequencies of sinusoidal disturbances, $m = m_1 + m_2$, m_1 is the number of model poles at $z = 1$, and m_2 is the disturbance order (1 for steps, 2 for ramps, etc.).

The predictor filter, also known as robustness filter, is defined in the following form

$$V(z) = \frac{v_0 + v_1 z^{-1} + ... + v_{n_s} z^{-n_s}}{(1-\beta_1 z^{-1})(1-\beta_2 z^{-1})...(1-\beta_{n_v} z^{-1})} \tag{3.33}$$

where $n_s + 1$ is equal to the number of equations in the set (3.32), the number of poles are $n_v \leq n_s + 1$, and poles β_i are free tuning parameters.

Using (3.32) and (3.33), a system with linear equations can be derived, whose solution let to determine the coefficients v_i of the filter $V(z)$. Considering $G(z) = N_g(z)/D_g(z)$, $G_k(z) = K(zI-A)^{-1}B = N_{gk}(z)/D_g(z)$, and $V(z) = N_v(z)/D_v(z)$, the set of equations from (3.32) results

$$\begin{cases} N_v(z) = \dfrac{N_{gk}(z)D_v(z)z^d}{N_g(z)}|_{z=p_i\neq 1}, \\ N_v(z) = \dfrac{(D_g(z)+N_{gk}(z))D_v(z)z^d}{N_g(z)}|_{z=e^{\pm jw_k}}, \\ \dfrac{d^k}{dz^k}[(D_g(z)+N_{gk}(z))D_v(z)-N_g(z)N_v(z)z^{-d}]|_{z=1}=0,\ k=0,...,m-1. \end{cases} \tag{3.34}$$

After defining the proper set of equations based on the process model and the type of disturbance to be rejected, the system of linear equations can be converted to matrix form and solved by matrix operations. Considering the system of linear equations $A_s v = B_s$, where A_s is the coefficients matrix, v is the variables vector and B_s is the vector of independent terms, the coefficients of the robustness filter numerator can be computed by $v = A_s^{-1}B_s$.

3.4 Stable implementation

In the case of both integrating and unstable open-loop processes, $S(z)$ defined in (3.26) presents internal instability problems due to some roots of polynomial $\det(zI-A)$ are not inside the unit circle. To avoid this problem, the implementation of $S(z)$ studied in Section 3.1.3 can be extended for higher-order models as follows.

The expression for $S(z)$ is given by

$$S(z) = \frac{N_{gk}(z)}{D_g(z)} - \frac{N_g(z)}{D_g(z)}\frac{N_v(z)}{D_v(z)}z^{-d}. \tag{3.35}$$

By using partial fraction decomposition in the term $G(z)V(z)$, when the poles of $V(z)$ are different from the poles of $G(z)$, it results

$$S(z) = K(zI-A)^{-1}B - KA^d(zI-A)^{-1}Bz^{-d} - \frac{N_v^*(z)}{D_v(z)}z^{-d}. \tag{3.36}$$

Consider the following Diophantine equation (SANZ; GARCÍA; ALBERTOS, 2018):

$$I = M_Q(z)(zI-A) + M_R(z), \tag{3.37}$$

where $M_Q(z)$, $M_R(z)$ are, respectively, the right quotient matrix and the right remainder matrix of the right division of polynomial matrices $I\cdot(zI-A)^{-1}$ (TZEKIS; KARAMPETAKIS; VARDULAKIS, 1999).

By solving the Diophantine equation up to d terms, it results in the expression

$$I = \left(\sum_{i=1}^{d} A^{i-1}z^{-i}\right)(zI-A) + A^d z^{-d}. \tag{3.38}$$

By right multiplying the above expression by $(zI-A)^{-1}$, one obtains

$$(zI-A)^{-1} = \sum_{i=1}^{d} A^{i-1}z^{-i} + A^d(zI-A)^{-1}z^{-d}. \tag{3.39}$$

By making $K(zI-A)^{-1}B$, the following expression can be obtained:

$$K(zI-A)^{-1}B - KA^d(zI-A)^{-1}Bz^{-d} = \sum_{i=1}^{d} KA^{i-1}Bz^{-i}. \tag{3.40}$$

By substituting (3.40) in (3.36), the expression for $S(z)$ results as

$$\tilde{S}(z) = \sum_{i=1}^{d} KA^{i-1}Bz^{-i} - \frac{N_v^*(z)}{D_v(z)}z^{-d}. \tag{3.41}$$

From (3.41), it can be noticed that the poles of $G(z)$ have been eliminated from $S(z)$, which guarantees internal stability for both integrating and unstable open-loop models.

3.5 Closed-loop robust stability

Following the robust stability condition from (2.5) in the z-domain, as presented in Section 2.1.3, for the proposed structure, robust stability in the case of modeling uncertainties can be established by

$$I_r(\omega) = \left|[V(e^{j\Omega})C(e^{j\Omega}I-A)^{-1}B]^{-1}[1+K(e^{j\Omega}I-A)^{-1}B]\right| > \overline{\delta P}(\omega). \tag{3.42}$$

3.6 Maximum achievable robustness

In this subsection is studied the bound of the maximum dead-time uncertainty, also called maximum achievable robustness, for stable, unstable, and integrating open-loop processes. For simplicity, to obtain an analytic solution, FOPDT models with dead-time uncertainty are considered. As studied in (NORMEY-RICO; CAMACHO, 2007), dead-time uncertainties represent the worst case scenario for DTCs. Besides, the analysis is performed in the continuous-time domain. For implementation issues, an equivalent discrete-time controller can be obtained by applying discretization methods.

A continuous-time first-order dead-time process model can be represented as

$$P(s) = G(s)e^{-Ls} = \frac{b}{s+a}e^{-Ls}, \tag{3.43}$$

where $a > 0$ for stable processes, $a < 0$ for unstable processes, and $a = 0$ for integrating processes.

Considering a desired closed-loop pole $-p_c$ as a tuning parameter ($-p_c$ is the root of $1+kG(s)=0$), the controller gains k and k_r are computed, respectively, by

$$k = \frac{p_c - a}{b}, \tag{3.44}$$

$$k_r = \frac{a}{b} + k. \tag{3.45}$$

The robustness filter can be represented as

$$V(s) = \frac{b_1 s + b_2}{s + \alpha}, \tag{3.46}$$

where

$$b_2 = k_r \alpha, \tag{3.47}$$

$$b_1 = \frac{k(a-\alpha)e^{-aL} + b_2}{a},\ a \neq 0, \tag{3.48}$$

for stable and unstable processes,

$$b_1 = \frac{p_c + \alpha + p_c \alpha L}{b},\ a = 0, \tag{3.49}$$

for integrating processes, and α is a tuning parameter.

The robustness index $I_r(\omega)$ is

$$I_r(\omega) = \frac{|1 + kG(\omega)|}{|V(\omega)G(\omega)|}. \tag{3.50}$$

Considering only dead-time uncertainties, the multiplicative uncertainty is given by

$$\delta P(\omega) = \frac{|P_r(j\omega) - P(j\omega)|}{|P(j\omega)|} = |e^{-j\omega\Delta L} - 1|,\ \omega > 0, \tag{3.51}$$

where $\Delta L = L_r - L$ and L_r represents the real process dead time. From (3.51) can be derived the following inequality:

$$\delta P(\omega) = |e^{-j\omega\Delta L} - 1| \leq \omega\Delta L. \tag{3.52}$$

3.6.1 Stable case

For stable processes with $a = p$ ($p > 0$), choosing by simplicity $\alpha = p$, the robustness index is obtained as

$$I_r(\omega) = \frac{|j\omega + p_c|}{p_c}. \tag{3.53}$$

From the above expression, the following inequality can also be obtained

$$I_r(\omega) = \frac{|j\omega + p_c|}{p_c} > \frac{\omega}{p_c}. \tag{3.54}$$

As the condition $I_r(\omega) > \delta P(\omega)$ must be satisfied to guarantee stability, then, from (3.51) and (3.54), it can be derived

$$\Delta L < \frac{1}{p_c},\ \ p_c > 0. \tag{3.55}$$

Note that (3.55) defines the robust achievable condition. High or low robustness can be obtained decreasing or increasing p_c, respectively.

3.6.2 Unstable and integrating cases

The maximum achievable robustness for unstable and integrating processes is obtained when $p_c \to 0$ and $\alpha \to 0$. Therefore, for unstable processes with $a = -p$ ($p > 0$), where p is the process pole, the maximum value of the robustness index results as

$$\lim_{\substack{p_c \to 0 \\ \alpha \to 0}} I_r(\omega) = \frac{\omega}{pe^{pL}} \tag{3.56}$$

By making $\delta P(\omega) < I_r(\omega)$, one can obtain the bound for the stabilizable dead-time uncertainty for unstable processes as

$$\Delta L < \frac{1}{pe^{pL}}. \tag{3.57}$$

It can be noticed from (3.57) that dominant dead-time lead to a lower bound for dead time uncertainty.

The particular case when $p \to 0$ represents integrating models. In this case, the maximum stabilizable dead-time is unbounded, because $\Delta L < \infty$.

3.7 Controller tuning guidelines

The tuning of the SFSP for high-order dead-time processes is mostly focused on disturbance rejection, while a desired set-point tracking performance can always be obtained by using a reference filter. Therefore, firstly the controller is tuned for disturbance rejection and, only after, for set-point tracking.

The disturbance rejection tuning is made trough two sets of parameters: the closed-loop poles p_k and the robustness filter poles β_i. The closed-loop poles have influence over both set-point tracking and disturbance rejection, while the poles of the robustness filter have influence only over disturbance rejection. The closed-loop poles and the robustness filter poles must be, respectively, $0 < p_k < 1$ and $0 \leq \beta_i < 1$. There is a trade-off between aggressiveness and robustness when choosing the values of p_k and β_i. When $p_k \to 0$ and $\beta_i \to 0$, a more aggressive response is obtained, while when $p_k \to 1$ and $\beta_i \to 1$ higher robustness is achieved.

For high-order processes, the values of p_k are often chosen, for simplicity, equally, but they can also be chosen differently depending on the desired closed-loop response.

The values of β_i can be chosen all equal, but sometimes, to tune both disturbance rejection and noise attenuation, these values can be split into two different ones. One or two poles to filter the measurement noise and the rest to obtain a desired trade-off between robustness and performance. It is suggested firstly to tune the poles associated with the robustness and then one or two poles for noise attenuation purposes. For improved robustness and noise attenuation, a pair of conjugated complex poles can also be used as $\beta_{1,2} = e^{-\sigma \pm j\rho}$, where $\rho/\sigma \leq tan(\pi/3)$ (TORRICO et al., 2018).

The set-point tracking is adjusted using the numerator and denominator poles of $F(z)$. To cancel the effect of some undesired slow dynamics, the numerator poles α_f can be used. However, if a slower response is desired, the denominator poles β_f can be used within the range $[0-1]$. Bigger values of β_f will have more influence over the set-point tracking dynamics.

3.8 Simulation examples

The proposed SFSP strategy is applied to several recent literature processes to evaluate the effectiveness of the design procedure. For comparison, disturbance rejection performance indices such as integrated absolute error (IAE) (da SILVA; FLESCH; NORMEY-RICO, 2020), control signal total variation (TV), and control variance (CV) are calculated and presented in Table 5. These indices are computed as follows:

$$IAE = \int_{t_q+2L}^{t_w} |r(t) - y(t)|dt, \tag{3.58}$$

$$TV = \sum_{i=1}^{N_q} |u_{i+1} - u_i|, \tag{3.59}$$

$$CV = \frac{1}{N_w - 1} \sum_{i=1}^{N_w} |u_i - \mu|^2, \tag{3.60}$$

where t_q is the time at which the disturbance is applied, L is the continuous-time input delay, N_q is the number of samples of the disturbance rejection response, t_w is the time at which the noise is applied, μ is the mean of the control signal, and N_w is the number of samples of the noise attenuation response.

The IAE and TV indices are computed for the disturbance rejection response only, that is, from the instant the disturbance is applied until it achieves a steady-state, while the CV index is computed for the range that noise is added to the output. For the three indices, the smaller they are, the better the controller performance.

The noise being used in the simulations is band-limited white noise. Theoretically, white noise has zero mean and a flat power spectral density (PSD). The PSD is dimensionless and its value is specified in each example.

3.8.1 Example 1: stable process

A stable dead-time process model with a NMP zero studied at (GENG et al., 2019; WANG; SU, 2015) is given by

$$P(s) = \frac{-s+1}{(3s+1)(2s+1)} e^{-s}. \tag{3.61}$$

The model uncertainty is described as in (GENG et al., 2019):

$$P_r(s) = \frac{(-s+1)e^{-s}}{(3s+1)(2s+1)} \cdot \frac{\omega_n^2 e^{-0.25s}}{s^2 + 2\xi\,\omega_n s + \omega_n^2}, \tag{3.62}$$

where $\omega_n = 20$ and $\xi = 0.25$. Note that there is a 25% dead-time uncertainty. The resulting multiplicative uncertainty is given by

$$\delta P(s) = \frac{\omega_n^2 e^{-0.25s}}{s^2 + 2\xi\,\omega_n s + \omega_n^2} - 1. \tag{3.63}$$

Choosing the sampling time $T_s = 0.1$ (s) a discrete-time model is obtained:

$$P(z) = \frac{-0.0152(z-1.1054)}{(z-0.9672)(z-0.9512)} z^{-10}. \tag{3.64}$$

The controller was designed according to the following sequence: (i) First, the feedback gain K was computed to place two closed-loop poles at $z = 0.77$; (ii) then, the robustness filter was tuned with two complex conjugate poles $\beta_{1,2} = e^{-0.05 \pm 0.0433j}$ to satisfy the robustness condition (3.42) and with a third real pole $\beta_3 = 0.91$ to attenuate measurement noise; (iii) finally, the reference filter was tuned with two poles $\beta_f = 0.945$ to attenuate the set-point tracking undershoot, with equivalent dynamics to that presented in (GENG et al., 2019). The computed feedback gain K, robustness filter $V(z)$, and reference filter $F(z)$ are shown in Table 1.

Table 1 – Example 1. Controllers parameters.

	(GENG et al., 2019)	SFSP
MESO	$L_0 = [12.5806 \quad 13.3414 \quad 0.0808]$	–
Feedback Controller	$\overline{K}_0 = [-0.9065 \quad 0.9530]$	$K = [286.9596 \;\; 282.1585]$
Predictor Filters	$F_1(z) = \Phi\Gamma(z)$ $F_2(z) = \dfrac{0.9893(z-0.9642)(z-0.9549)}{(z-0.96)^2}$	$V(z) = \dfrac{5.582z^3 - 10.65z^2 + 5.081z}{(z-0.91)(z^2 - 1.901z + 0.9048)}$
Reference Filter	$K_f(z) = \dfrac{0.2146(z-0.9512)^2 z}{(z-0.9047)(z-0.94)^2}$	$F(z) = \dfrac{0.10008z^2}{(z-0.945)^2}$

Source: The author.

In order to show the simplicity of the proposed controller filters and gains compared to those of the generalized predictor-based ADRC (GENG et al., 2019), they are defined in Table 1. The parameters of $F_1(z)$ are

$$\Gamma = \frac{(-0.0152z + 0.0168)(z-1)}{(z-0.96)^2}, \Phi = \sum_{i=1}^{d} c_p A_p^{i-1} b_p z^{-i},$$
$$A_p = \begin{bmatrix} 2.9184 & -2.8385 & 0.92 \\ 1 & 0 & 0 \\ 0 & 1 & 0 \end{bmatrix}, \; b_p = \begin{bmatrix} 1 \\ 0 \\ 0 \end{bmatrix}, \; c_p = \begin{bmatrix} 1 & -1.92 & 0.9216 \end{bmatrix}. \tag{3.65}$$

Fig. 13 shows the robustness of the proposed strategy and the one proposed in (GENG et al., 2019). As can be seen, the robustness index of the proposed controller is almost equivalent in comparison with the one from (GENG et al., 2019).

Figure 13 – Example 1. Robustness Index.

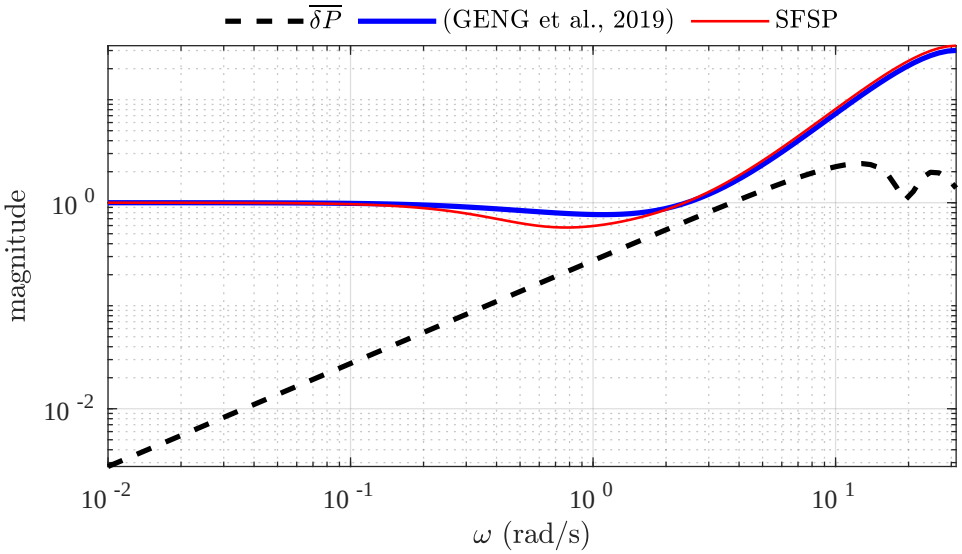

Source: The author.

The closed-loop response for the nominal case and the case with model uncertainties are shown respectively in Figs. 14 and 15 . A unit set-point change was applied at $t = 0$ (s), a unit constant disturbance at $t_q = 30$ (s), and band-limited white noise with PSD of 10^{-5} was added to the process output at $t_w = 60$ (s).

The disturbance rejection performance indices are listed in Table 5. Observe that, with respect to IAE and CV indices, the proposed controller has better performance than the ADRC from (GENG et al., 2019). The only exception is the TV index, given the more aggressive response.

3.8.2 Example 2: unstable process

The second-order process model with one unstable pole studied in (AJMERI; ALI, 2017; LIU; ZHANG; GU, 2005) is given by

$$P(s) = \frac{1}{(s-1)(0.5s+1)} e^{-1.2s}. \tag{3.66}$$

Using a sampling time of $T_s = 0.1$ (s), the discrete-time model is obtained as

$$P(z) = \frac{0.009691(z+0.9672)}{(z-1.105)(z-0.8187)} z^{-12}. \tag{3.67}$$

This example compares the proposed controller with the modified Smith predictor (MSP) presented in (AJMERI; ALI, 2017). The proposed controller was tuned for set-point tracking

Figure 14 – Example 1. Nominal case.

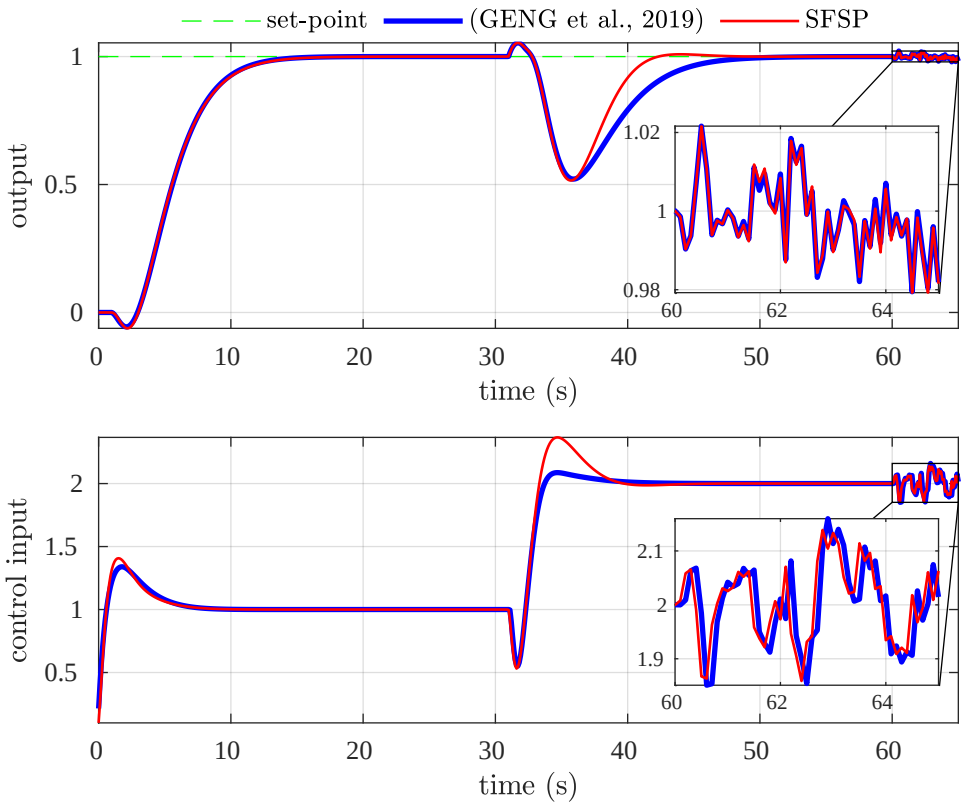

Source: The author.

computing the gain K for two closed-loop poles at $z = 0.96$ and $z = 0.92$. The set-point tracking was satisfactory with the reference filter $F(z) = k_r$. For disturbance rejection, the robustness filter was tuned with $\beta_{1,2} = 0$ and $\beta_3 = 0.9$. The controllers and filters of both strategies being compared are shown in Table 2.

Table 2 – Example 2. Controllers parameters.

	Ref. (AJMERI; ALI, 2017)	SFSP
Feedback Controller	–	$K = [2.8016 \;\; 1.7871]$
Tracking Controller	$G_{c1}(s) = \dfrac{0.4517(s+0.2288)}{s}$	–
Regulation Controller	$G_{c2}(s) = \dfrac{3556.2(s+1.856)(s+1.667)(s+0.01449)}{s(s+188.9)(s+52.91)}$	–
Stabilization Controller	$G_c(s) = \dfrac{1.4648(s+1.593)}{(s+2.333)}$	–
Predictor Filter	$G_f(s) = \dfrac{0.83333}{(s+0.8333)}$	$V(z) = \dfrac{32.47 - 58.94z^{-1} + 26.48z^{-2}}{1 - 0.9z^{-1}}$
Reference Filter	$F(s) = \dfrac{0.2288}{(s+0.2288)}$	$k_r = 0.1679$

Source: The author.

Figure 16 shows the responses for the nominal case. At $t = 0$, an unit set-point step

Figure 15 – Example 1. Case with model uncertainties.

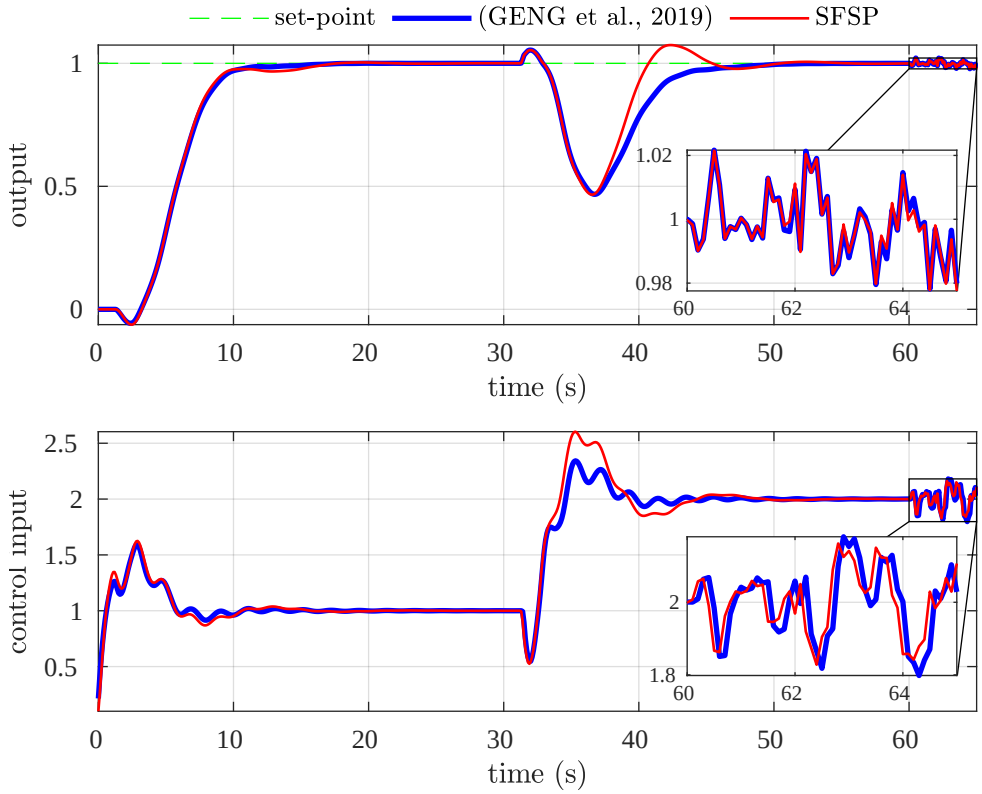

Source: The author.

change occurs, at $t_q = 50$ (s), a step disturbance of amplitude -0.05 is added to the process input, and, at $t_w = 100$ (s), band-limited white noise with PSD of 10^{-7} is added to the process output.

To show the proposed strategy robustness to uncertainties, a 12% dead-time uncertainty is assumed. The robustness index curves of both controllers are presented in Fig. 17. It can be seen that the robustness indices curves of both controllers cross the multiplicative uncertainty curve and, given the conservative characteristics of robustness curves, depending on how much they cross this curve, it means that the time responses are oscillatory or unstable.

In the case with model uncertainties, the responses of the MSP from (AJMERI; ALI, 2017) resulted unstable, therefore, only the responses of the proposed controller is seen in Fig. 18.

The performance indices of both controllers being compared are shown in Table 5. For the nominal case the proposed controller has better results than the MSP from (AJMERI; ALI, 2017) for all three indices. In the case with model uncertainties, as the MSP presented an unstable response, only the indices of the proposed controller are presented.

Figure 16 – Example 2. Nominal case.

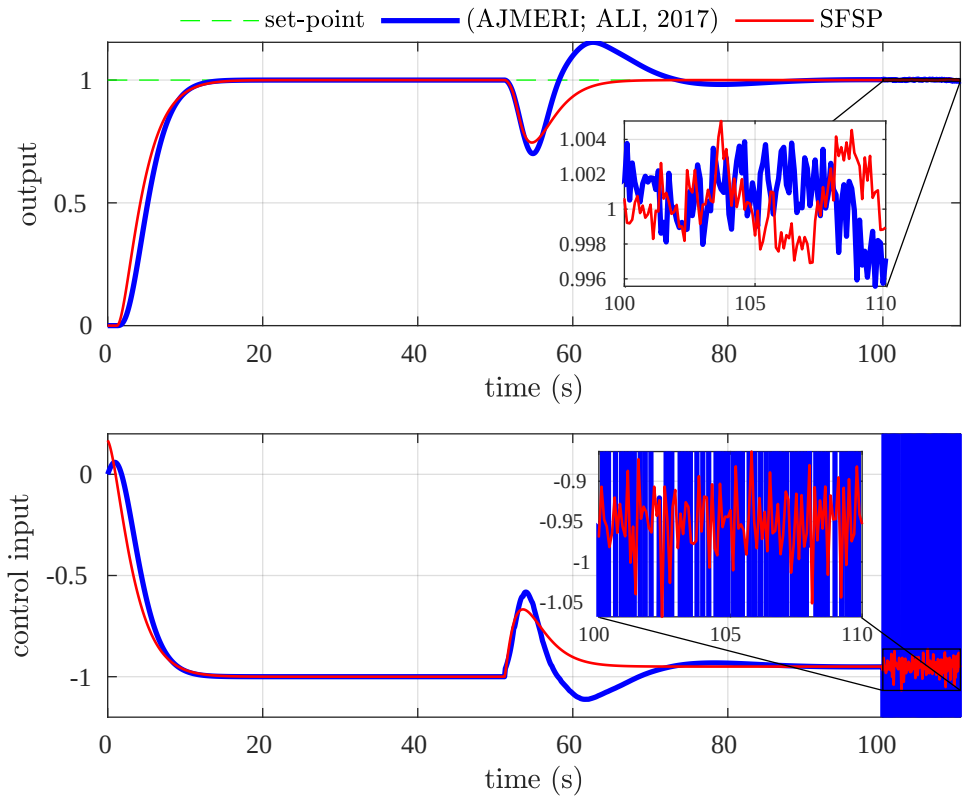

Source: The author.

Figure 17 – Example 2. Robustness Index.

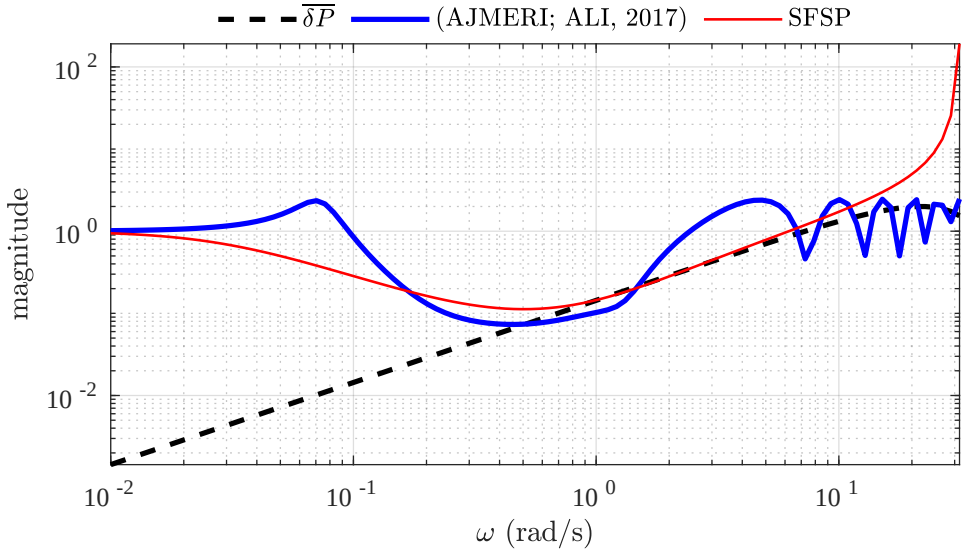

Source: The author.

Figure 18 – Example 2. Case with model uncertainties.

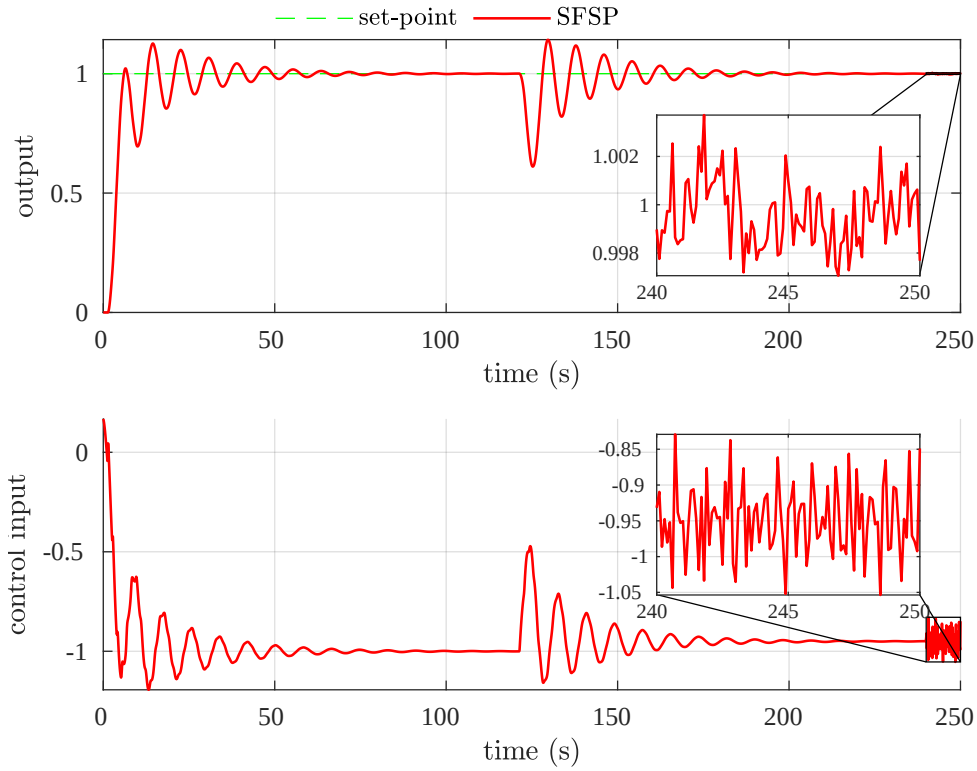

Source: The author.

3.8.3 *Example 3: integrating process*

Consider an integrating dead-time process with a NMP zero examined in the works (GENG et al., 2019; BEGUM; RAO; RADHAKRISHNAN, 2017):

$$P(s) = \frac{(1-0.2s)}{s(s-1)}e^{-0.2s}. \tag{3.68}$$

The obtained discrete model for a sampling time $T_s = 0.01$ (s) is given by

$$P(z) = \frac{-0.002(z-1.051)}{(z-1.01)(z-1)}z^{-20}. \tag{3.69}$$

The tuning procedure begins by setting the feedback gain K so as to obtain two closed-loop poles at $z = 0.93$ and $z = 0.92$. Then, the reference filter $F(z)$ was tuned to obtain a similar dynamics to that presented in (GENG et al., 2019), leading to $\beta_f = 0.994$ and $n_f = 2$. Lastly, the robustness filter $V(z)$ was tuned with one real pole $\beta_1 = 0.9925$ and two complex conjugate poles $\beta_{2,3} = e^{-0.006 \pm j0.0078}$ to obtain desired robustness characteristics as in (TORRICO et al., 2018). The obtained gains and filters for both proposed and reference (GENG et al., 2019) controllers are given by Table 3, aiming to highlight the simplicity of the proposed strategy.

To calculate the predictor filter $F_1(z)$ of reference (GENG et al., 2019), consider that

$$A_p = \begin{bmatrix} 3.0101 & -3.0201 & 1.0101 \\ 1 & 0 & 0 \\ 0 & 1 & 0 \end{bmatrix}, \; b_p = \begin{bmatrix} 1 \\ 0 \\ 0 \end{bmatrix} \text{ and } c_p = \begin{bmatrix} 1 & -1.866 & 0.8649 \end{bmatrix} \tag{3.70}$$

are the minimum-order state-space model, Φ can be calculated as

$$\Phi = \sum_{i=1}^{d} c_p A_p^{i-1} b_p z^{-i} \tag{3.71}$$

and $\Gamma(z)$ is defined as

$$\Gamma(z) = \frac{(-0.00196z + 0.00206)(z-1)}{(z-0.93)^2}. \tag{3.72}$$

In order to guarantee internal stability for the proposed strategy, $S(z)$ is obtained by (3.41). Notice that $S(z)$ is obtained from the feedback controller K, the robustness filter $V(z)$, and the nominal process model, which means that it does not require extra tuning parameters.

Table 3 – Example 3. Controllers parameters.

	(GENG et al., 2019)	SFSP
MESO	$L_0 = [2.2433 \quad 2.2894 \quad 0.0001]$	–
Feedback Controller	$\overline{K}_0 = [-14.5363 \quad 14.5849]$	$K = [3421.38 \;\; 3332.17]$
Predictor Filters	$F_1(z) = \Phi\Gamma(z)$ $F_2(z) = \dfrac{5.2952(z^2 - 1.955z + 0.956)}{(z-0.93)^2}$	$V(z) = \dfrac{4.269z^3 - 8.525z^2 + 4.256z}{(z-0.9925)(z^2 - 1.988z + 0.9881)}$
Reference Filter	$K_f(z) = \dfrac{0.0002(z-0.99)^2 z^2}{(z-0.9512)(z-0.992)^3}$	$F(z) = \dfrac{0.002006z^2}{(z-0.994)^2}$

Source: The author.

The closed-loop response for the nominal case and the case with model uncertainties are presented in Figs. 19 and 20, respectively. A set-point step change of magnitude 0.2 is applied at $t = 0$ (s) and a disturbance of magnitude -0.06 is applied to the control input at $t_q = 20$ (s). Band-limited white noise with PSD of 10^{-8} is applied to the process output at $t_w = 35$ (s). For the case with model uncertainties, the process dead time is 30% larger than the nominal value.

The disturbance rejection performance indices of both controllers are listed in Table 5. One can see that, with respect to IAE and CV, the proposed controller has better performance than the ADRC proposed in (GENG et al., 2019). As for the TV index, the proposed controller has bigger indices because it has faster responses.

Fig. 21 shows the robustness index for the proposed strategy and the one proposed in (GENG et al., 2019). For a fair comparison, the proposed strategy was tuned to have a similar robustness index to the one from (GENG et al., 2019).

Figure 19 – Example 3. Nominal case.

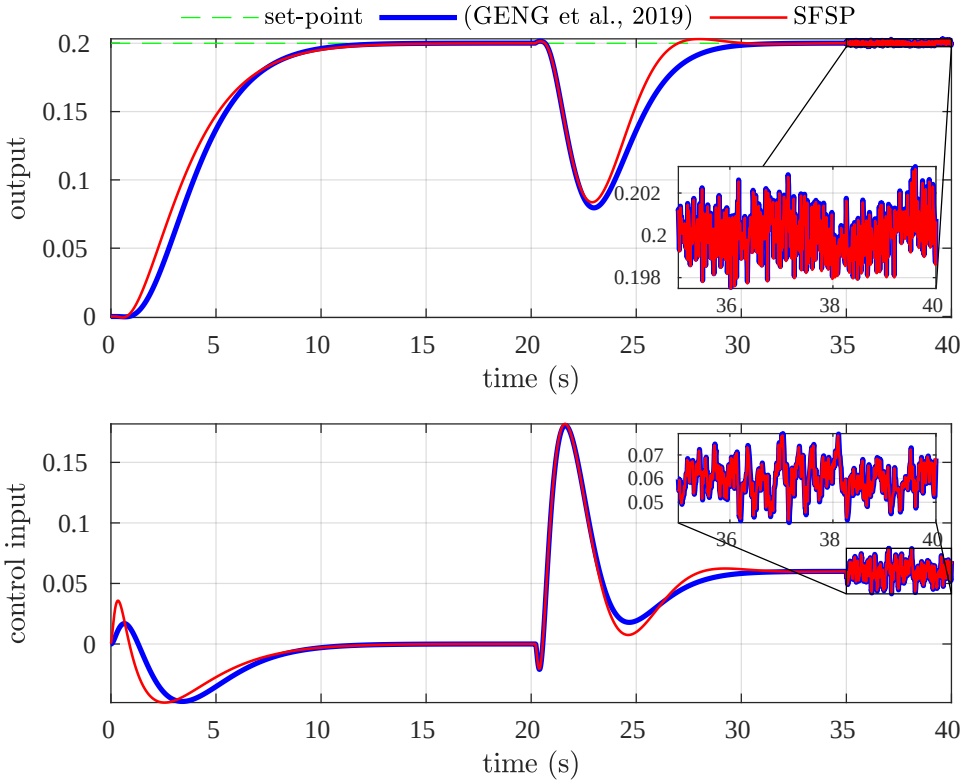

Source: The author.

3.8.4 Example 4: unstable process

Consider a second-order process model with one unstable pole, modified from (TORRICO et al., 2016; MATAUŠEK; RIBIĆ, 2012), and given by

$$P(s) = \frac{2}{(10s-1)(2s+1)} e^{-15s}. \tag{3.73}$$

Using a sampling time of $T_s = 1.5$ (s), it is obtained the discrete-time model

$$P(z) = \frac{0.09385(z+0.8198)}{(z-1.162)(z-0.4724)} z^{-10}. \tag{3.74}$$

In this example, the proposed controller is compared to a model predictive control (MPC) strategy based on the generalized predictive control (GPC), namely DTC-GPC (TORRICO et al., 2016). It is worth noting that the MPC theory has a much more advanced approach than the proposed strategy. Therefore, the objective of this comparison is not to show considerable improvements in performance, but to show that the proposed controller can have similar performance when compared to a more advanced control technique.

For set-point tracking, the proposed controller was tuned to have a similar response to the DTC-GPC response. The gain K was computed to place two closed-loop poles at $z = 0.97$ and $z = 0.46$. The set-point tracking response was satisfactory with only k_r, therefore, the reference

Figure 20 – Example 3. Case with model uncertainties.

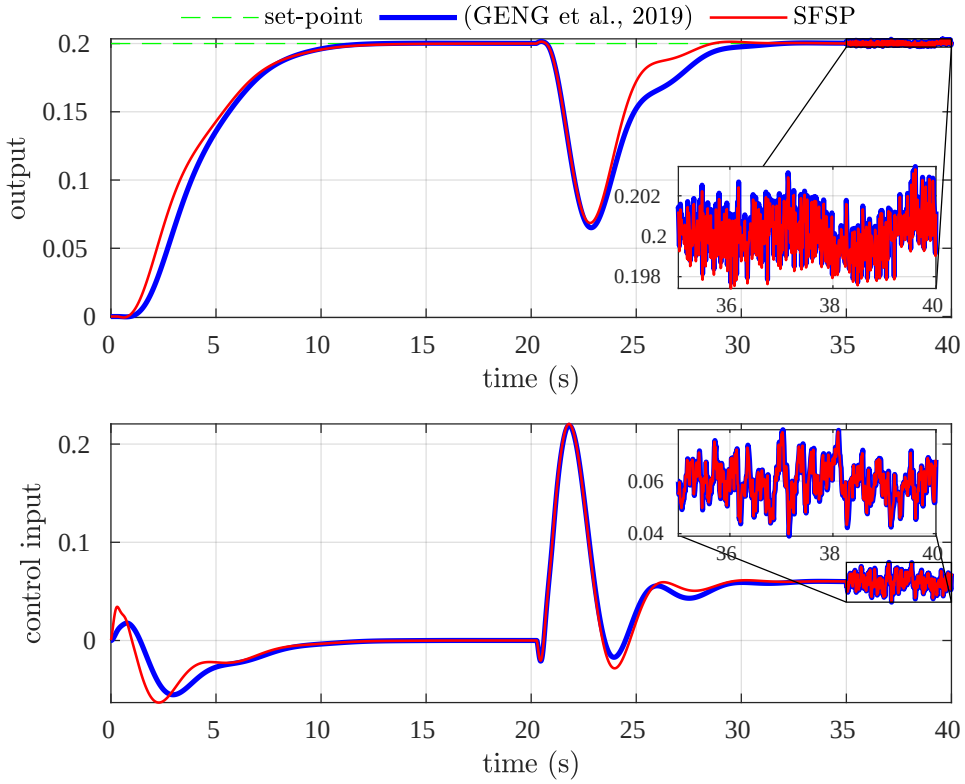

Source: The author.

Figure 21 – Example 3. Robustness Index.

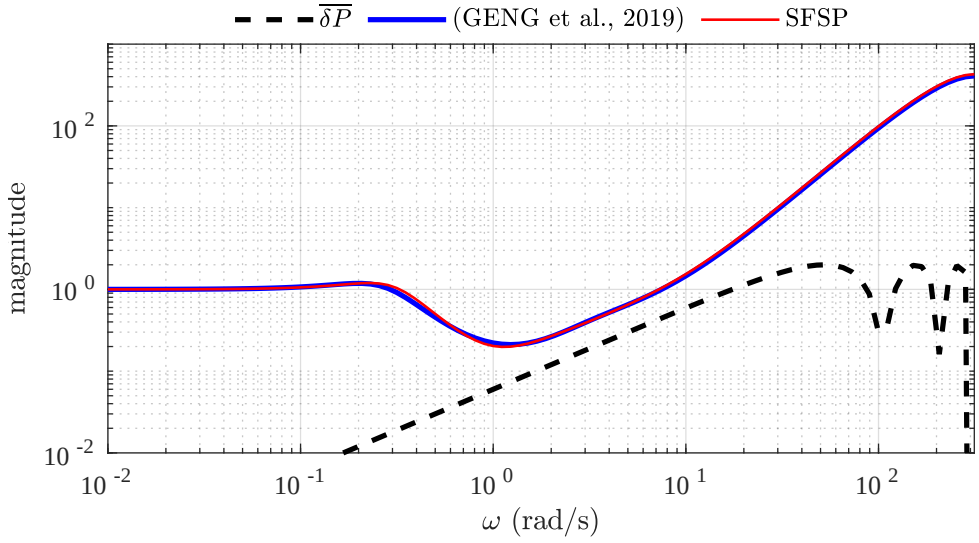

Source: The author.

filter resulted $F(z) = k_r = 0.0949$. For disturbance rejection, the robustness filter was tuned with $\beta_{1,2} = 0$ and $\beta_3 = 0.986$. The DTC-GPC was tuned for set-point tracking with the prediction horizon window equal to the control horizon window $N = N_u = 50$ and control weight $\lambda_j = 800$. For disturbance rejection, the filter $C(z)$ was tuned with $n_c = 1$ and $\alpha = 0.9866$. The components

of the two controllers are shown in Table 4.

Table 4 – Example 4. Controllers parameters.

	MPC	SFSP
Feedback Controller	$P_1(z) = 1.205 - 0.5687z^{-1}$	$K = [1.2548 \;\; 1.1237]$
Secondary Controller	$P_3(z) = 0.07971z^{-1}$	–
Predictor Filters	$T(z) = \dfrac{5.833 - 8.586z^{-1} + 2.754z^{-2}}{1 - 0.9866z^{-1}}$	$V(z) = \dfrac{5.925 - 8.721z^{-1} + 2.798z^{-2}}{1 - 0.986z^{-1}}$
Reference Filter	$k_r = 0.096$	$k_r = 0.0949$

Source: The author.

Figure 22 shows the responses for the nominal case. At $t = 0$, an unit set-point step change occurs, at $t_q = 501$ (s), a step disturbance of amplitude -0.01 is added to the process input, and, at $t_w = 1302$ (s), band-limited white noise with PSD of 10^{-5} is added to the process output.

Figure 22 – Example 4. Nominal case.

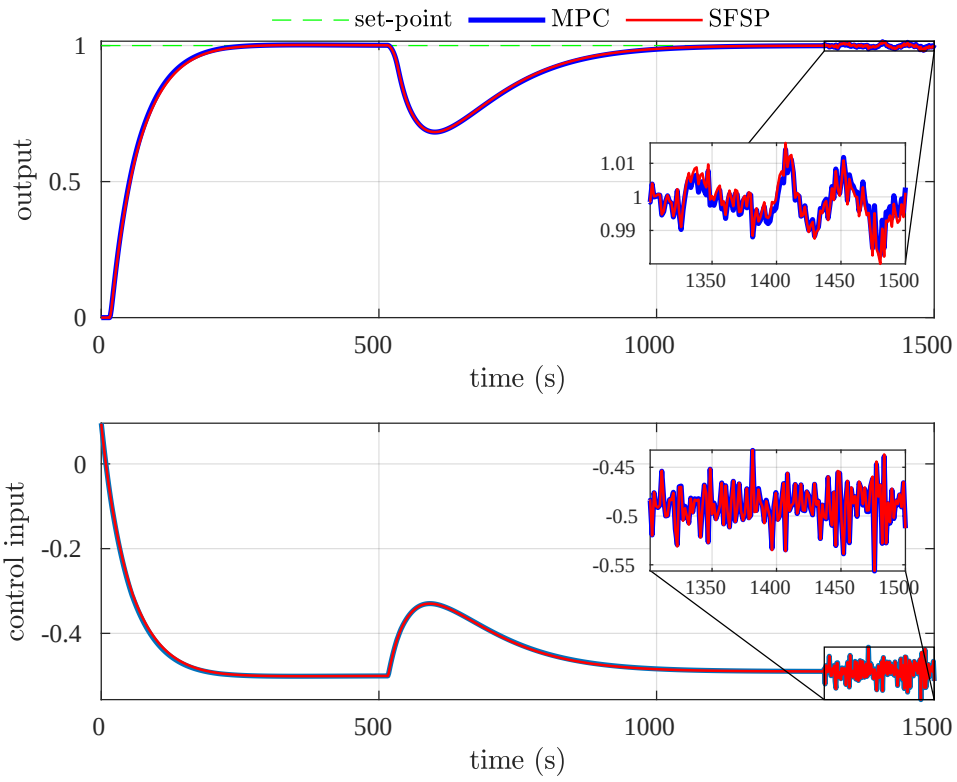

Source: The author.

To show the proposed strategy robustness to uncertainties, a 10% dead-time uncertainty is assumed. The robustness index curves of both controllers are presented in Fig. 23. As can be seen, both controllers have similar robustness index curves, but they touch the multiplicative

uncertainty curve. Given the conservative characteristics of robustness curves, that does not mean that the time responses are unstable, but that they can be oscillatory.

The responses for the case with model uncertainties are seen in Fig. 24, where, at $t = 0$ occurs the set-point step change, at $t_q = 1401$ (s) occurs the step disturbance, and at $t_w = 3303$ (s) noise is added to the process output. The time responses are oscillatory, but, even so, stable. It can be seen that the proposed strategy has similar control signal and output response to the DTC-GPC from (TORRICO et al., 2016).

Figure 23 – Example 4. Robustness Index.

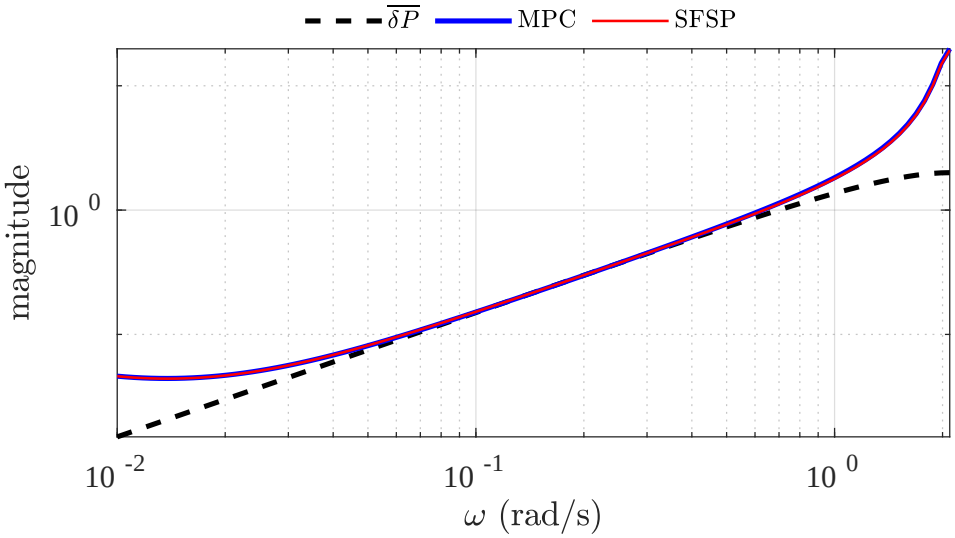

Source: The author.

Table 5 shows the performance indices of both controllers being compared. In the nominal case the proposed controller has better IAE than the DTC-GPC from (TORRICO et al., 2016) and similar TV index. In the case with model uncertainties the proposed strategy has better IAE and TV indices than the controller being compared with.

3.9 Discussion

In this chapter, a extension of the simplified filtered Smith predictor for high-order dead-time processes was presented. A state-space formulation of the proposed controller is presented in order to allow the use of process models of any order and with NMP zeros. The new formulation preserves the main characteristics of previous formulations of the SFSP, such as the simplicity in its tuning, good robustness characteristics, and the ability to satisfactory deal with measurement noise.

The proposed structure has a primary controller that is tuned to achieve a desired set-point tracking dynamics, while a robustness filter is tuned to ensure a good trade-off between robustness and performance. Furthermore, this structure has fewer tuning parameters and a lower-order filter compared to other structures in the literature.

Figure 24 – Example 4. Case with model uncertainties.

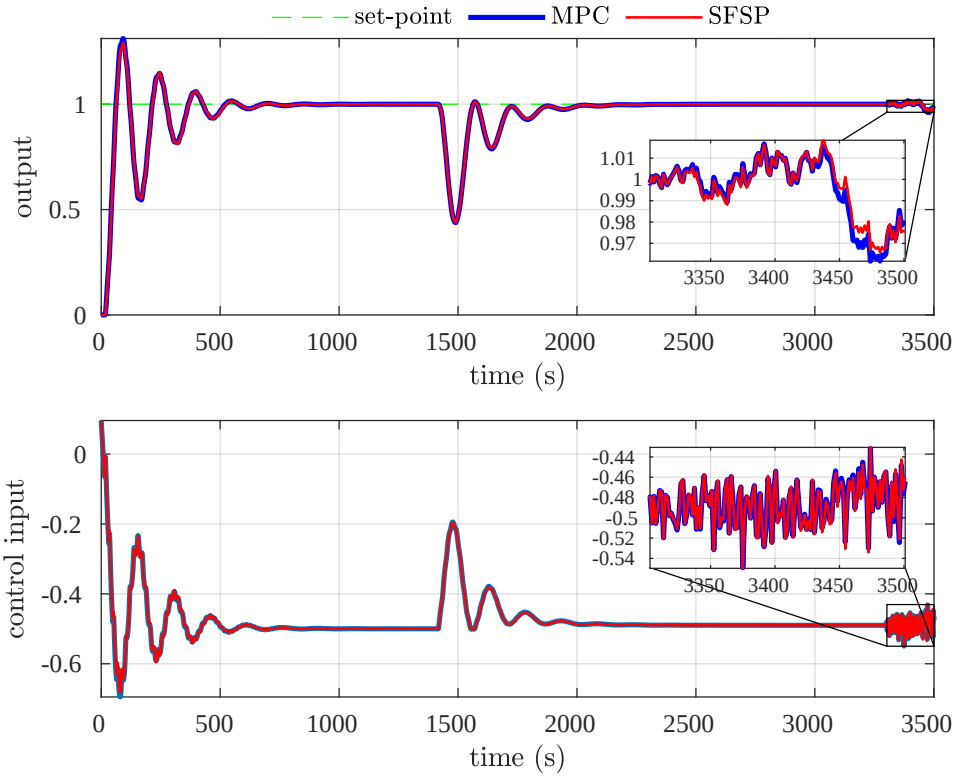

Source: The author.

Table 5 – Performance indices. The best performances are highlighted in bold text.

Example		Nominal			Robust		
		IAE	TV	CV	IAE	TV	CV
Example 1	SFSP	**2.22**	2.70	**0.005**	**2.63**	3.65	**0.0075**
	(GENG et al., 2019)	2.98	**2.07**	0.0057	2.99	**3.41**	0.0093
Example 2	SFSP	**1.47**	**0.63**	**0.0022**	**3.84**	**1.32**	**0.0027**
	(AJMERI; ALI, 2017)	2.54	1.15	26.26	–	–	–
Example 3	SFSP	**0.37**	0.46	**0.000045**	**0.37**	0.62	**0.000048**
	(GENG et al., 2019)	0.45	**0.43**	0.000049	0.46	**0.60**	0.000052
Example 4	SFSP	**66.83**	0.33	0.00044	**67.29**	**0.93**	0.00049
	MPC	67.82	0.33	**0.00042**	68.29	0.94	**0.00047**

Source: The author.

To evaluate the performance of the proposed controller, four simulation examples were presented, where comparisons with control structures from recent literature were made. To quantitatively measure the performance of the controllers in this comparisons, performance indices were calculated, as shown in Table 5. In all considered scenarios, the proposed SFSP obtained superior results in terms of the IAE index. As expected, due to the more aggressive

response of the control signal, the TV index showed similar results and was superior in 50% of the cases. Regarding the CV index, the proposed controller outperformed the other controllers in 75% of the evaluated cases.

It is important to emphasize that the proposed controller consists of a controller with a less complex structure and fewer tuning parameters when compared to other structures for high-order processes in the recent literature. Even so, the proposed SFSP still can achieve good performance and robustness levels.

4 FEEDFORWARD CONTROL OF DEAD-TIME PROCESSES WITH MEASURABLE DISTURBANCES

Feedforward control of processes with measurable disturbances is a control strategy devised with the objective of improve the disturbance rejection responses of control systems. By measuring the disturbance, this strategy can actuate earlier in time than feedback control strategies. As a result, the disturbances are more quickly rejected. Therefore, this chapter is dedicated to present the fundamentals of feedforward control for measurable disturbances and to introduce feedforward controllers for processes with dead time.

The organization of the chapter is as folows: Section 4.1 presents the basics of feedforward control for processes with measurable disturbances, Section 4.2 presents classical feedback plus feedforward control, and Section 4.3 introduces feedforward controllers for measurable disturbances based on the Smith predictor.

4.1 Classical feedforward control for measurable disturbances

The classical feedforward control for measurable disturbances is presented in Fig. 25, where $G_q(s)$ is the delay-free transfer function defined as $G_q(s) = Y(s)/Q(s)$ and $Cff(s)$ is the feedforward controller. $G(s)$ and $G_q(s)$ are stable transfer functions and the process variable is given by $Y(s) = G(s)U(s) + G_q(s)Q(s)$. Note that the process model depicted in Fig. 25 is internally unstable for open-loop unstable and integrating processes.

Figure 25 – Classical feedforward control structure.

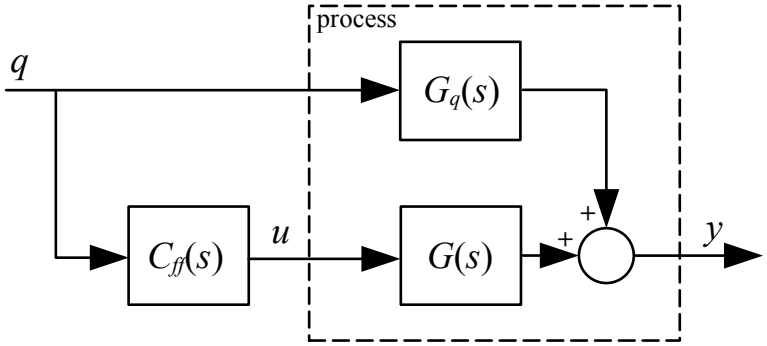

Source: The author.

The classical feedforward controller for measurable disturbances is then designed as

$$C_{ff}(s) = \frac{G_q(s)}{G(s)}. \tag{4.1}$$

As disadvantages of this classical method, implementation problems can arise depending on the poles and zeros of $G(s)$ and $G_q(s)$ (RODRÍGUEZ et al., 2016a). Furthermore, to design

$C_{ff}(s)$, firstly is necessary to identify the $G(s)$ and $G_q(s)$ and, aside from measuring the disturbance, the additional complexity in identifying $G_q(s)$ makes the feedforward controller less used in practice than feedback controllers (ÅSTRÖM; HÄGGLUND, 2006).

4.2 Classical feedback plus feedforward control for measurable disturbances

The control system from Fig. 25 only rejects disturbances. Therefore, to obtain a control system that can track the set point and reject faster measurable disturbances, the control structure of Fig. 26, with feedback and feedforward controllers, was devised. As $G_q(s)$ is not in the feedback path, note that the process model presented in Fig. 26 is internally unstable for open-loop unstable and integrating processes.

Figure 26 – Classical feedback plus feedforward control structure.

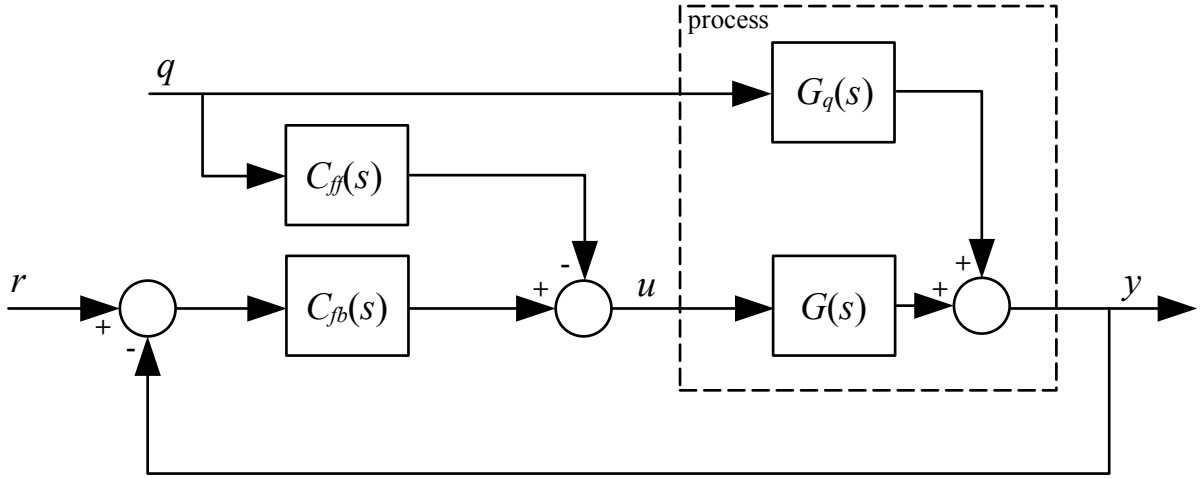

Source: The author.

As seen in Fig. 26, the control signal u is composed by components due to the feedback and feedforward controllers.

Several works have proposed tuning rules for feedback plus feedforward controllers for measurable disturbances. Among them are (VERONESI et al., 2017; RODRÍGUEZ et al., 2020).

4.3 Feedforward controllers for measurable disturbances based on the Smith predictor

When the process have dead times, the problem of feedforward control for measurable disturbances turns even more complex. This Section briefly presents different strategies to better deal with the presence of dead time in the process.

4.3.1 Important definitions and concepts

4.3.1.1 Process model

In this Section, the transfer functions used by the controllers are represented in the continuous-time domain by

$$P(s) = \frac{Y(s)}{U(s)} = G(s)e^{-Ls}, \tag{4.2}$$

$$P_q(s) = \frac{Y(s)}{Q(s)} = G_q(s)e^{-L_q s}, \tag{4.3}$$

where L_q is a time delay.

Therefore, by discretizing each of these transfer functions with a ZOH, it results

$$P(z) = \frac{Y(z)}{U(z)} = G(z)z^{-d}, \tag{4.4}$$

$$P_q(z) = \frac{Y(z)}{Q(z)} = G_q(z)z^{-d_q}, \tag{4.5}$$

where d_q is a discrete-time delay.

4.3.1.2 Equivalent feedback plus feedforward control structure

The control structure of Fig. 27 is used to turn easier the control analysis. A discrete-time domain counter part of this Figure is easily obtained by discretizing each controller parameter with a ZOH.

Figure 27 – Equivalent feedback plus feedforward structure.

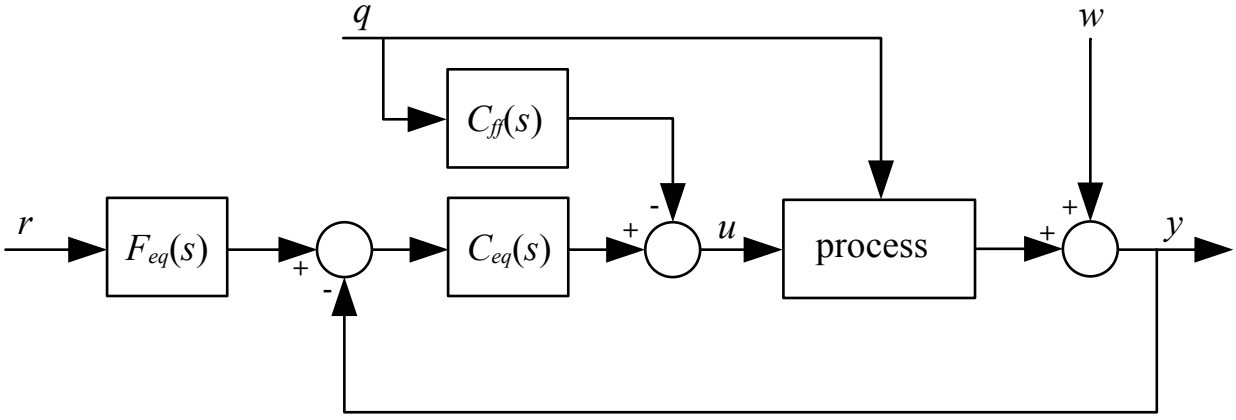

Source: The author.

4.3.1.3 Closed-loop robust stability analysis

The feedforward controller does not affect the closed-loop robust stability of a feedback plus feedforward control system. Therefore, for such control systems, the closed-loop robust stability analysis takes into account only the feedback controller.

4.3.2 FSP with feedforward action for measurable disturbances

The FSP with feedforward action for measurable disturbances (FSP-FF) is presented in (RODRÍGUEZ et al., 2016a) and can use in its design and tuning stable, unstable and integrating models of any order. Its conceptual control structure is shown in Fig. 28, where $F_{ff}(s)$ is the feedforward filter. Note that its feedback controller has the same conceptual control structure of the FSP.

Figure 28 – Conceptual structure of the FSP with feedforward action.

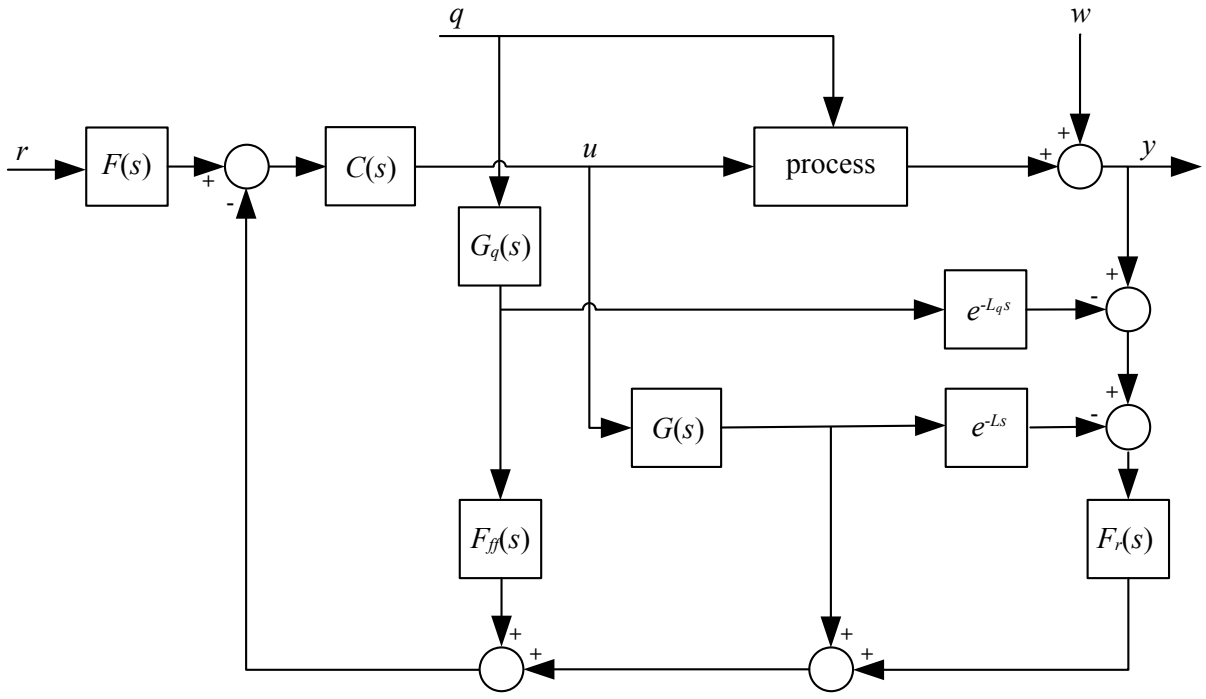

Source: The author.

By reducing the conceptual structure of the FSP-FF to the structure of Fig. 27, one gets

$$F_{eq}(s) = \frac{F(s)}{F_r(s)}, \tag{4.6}$$

$$C_{eq}(s) = \frac{C(s)F_r(s)}{1+C(s)S(s)}, \tag{4.7}$$

$$C_{ff}(s) = \frac{C(s)S_q(s)}{1+C(s)S(s)}, \tag{4.8}$$

where

$$S(s) = G(s)(1 - F_r(s)e^{-Ls}), \tag{4.9}$$

$$S_q(s) = G_q(s)(F_{ff}(s) - F_r(s)e^{-L_q s}). \tag{4.10}$$

In the nominal case, by considering that the process can be represented by $Y(s) = P(s)U(s) + P_q(s)Q(s)$, the following transfer functions are obtained:

$$H_{yr}(s) = \frac{Y(s)}{R(s)} = \frac{F(s)C(s)P(s)}{1 + C(s)G(s)}, \tag{4.11}$$

$$H_{yq}(s) = \frac{Y(s)}{Q(s)} = P_q(s) - \frac{F_{ff}(s)G_q(s)C(s)P(s)}{1 + C(s)G(s)}. \tag{4.12}$$

4.3.2.1 Stable implementation

The conceptual control structure of Fig. 28 is internally unstable for open-loop unstable and integrating processes. Furthermore, after the discretization of each controller parameter and after the proper cancellation of poles and zeros of $G(z)$ from $C_{eq}(z)$ and of $G_q(z)$ from $C_{ff}(z)$, the FSP-FF must be always implemented in practice in the control structure of Fig. 29.

Figure 29 – Implementation structure of the FSP with feedforward action.

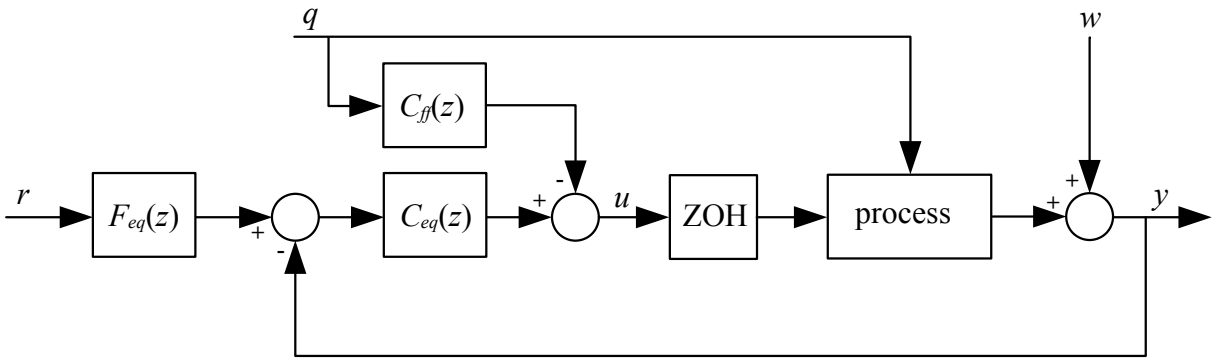

Source: The author.

4.3.2.2 Closed-loop robust stability

As explained in Section 4.3.1.3, only the feedback controller is took in account in the closed-loop robust stability analysis. Therefore, the closed-loop robust stability condition for the FSP-FF is the same as the FSP, resulting

$$I_r(\omega) = \left| \frac{1 + C(j\omega)G(j\omega)}{F_r(j\omega)C(j\omega)G(j\omega)} \right| > \overline{\delta P}(\omega), \ \forall \omega > 0. \tag{4.13}$$

4.3.3 SDTC with feedforward action for measurable disturbances

The SDTC with feedforward action for measurable disturbances (SDTC-FF) presented in (ALVES LIMA et al., 2019) is a controller that uses only first-order transfer functions in its design and tuning. These transfer functions can be stable, unstable or integrating. The conceptual control structure of the SDTC-FF is shown in Fig. 30, where $V_{ff}(z)$ is the feedforward filter. Note that the feedback controller from the conceptual structure of the SDTC-FF is the same as the SDTC.

Figure 30 – Conceptual structure of the SDTC with feedforward action.

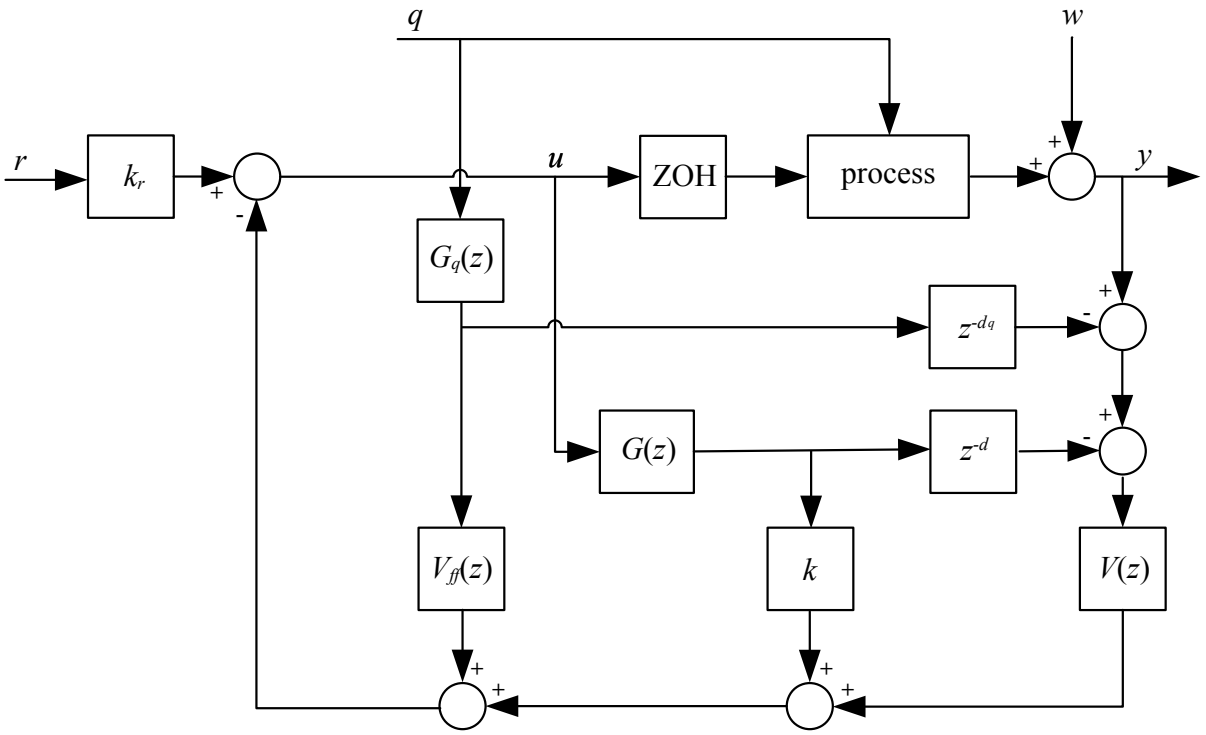

Source: The author.

After reducing the conceptual control structure of Fig. 30 to the equivalent control structure of Fig. 27, it results

$$F_{eq}(z) = \frac{k_r}{V(z)}, \tag{4.14}$$

$$C_{eq}(z) = \frac{V(z)}{1+S(z)}, \tag{4.15}$$

$$C_{ff}(z) = \frac{S_q(z)}{1+S(z)}, \tag{4.16}$$

where

$$S(z) = G(z)(k - V(z)z^{-d}), \tag{4.17}$$

$$S_q(s) = G_q(z)(V_{ff}(z) - V(z)z^{-d_q}). \tag{4.18}$$

By considering that the process can be represented by $Y(s) = P(s)U(s) + P_q(s)Q(s)$, the following transfer functions are obtained for the nominal case:

$$H_{yr}(z) = \frac{Y(z)}{R(z)} = \frac{k_r P(z)}{1 + kG(z)}, \tag{4.19}$$

$$H_{yq}(z) = \frac{Y(z)}{Q(z)} = P_q(z) - \frac{V_{ff}(z)G_q(z)P(z)}{1 + kG(z)}. \tag{4.20}$$

$$H_{uw}(z) = \frac{U(z)}{W(z)} = \frac{-V(z)}{1 + kG(z)}. \tag{4.21}$$

4.3.3.1 Stable implementation

For stable processes, the conceptual control structure from Fig. 30 can be used for practical implementation. However, this structure is internally unstable for open-loop unstable and integrating process. Therefore, for such cases, the implementation structure from Fig. 31 must be used in practice. To obtain $\tilde{S}(z)$ and $\tilde{S}_q(z)$, one needs to make pole-zero cancellations in $S(z)$ and $S_q(z)$. More specifically, one needs to eliminate the poles of $G(z)$ from $S(z)$ and the poles of $G_q(z)$ from $S_q(z)$, following the tuning procedure of $V(z)$ and $V_ff(z)$ (ALVES LIMA et al., 2019), respectively.

Figure 31 – Implementation structure of the SDTC with feedforward action.

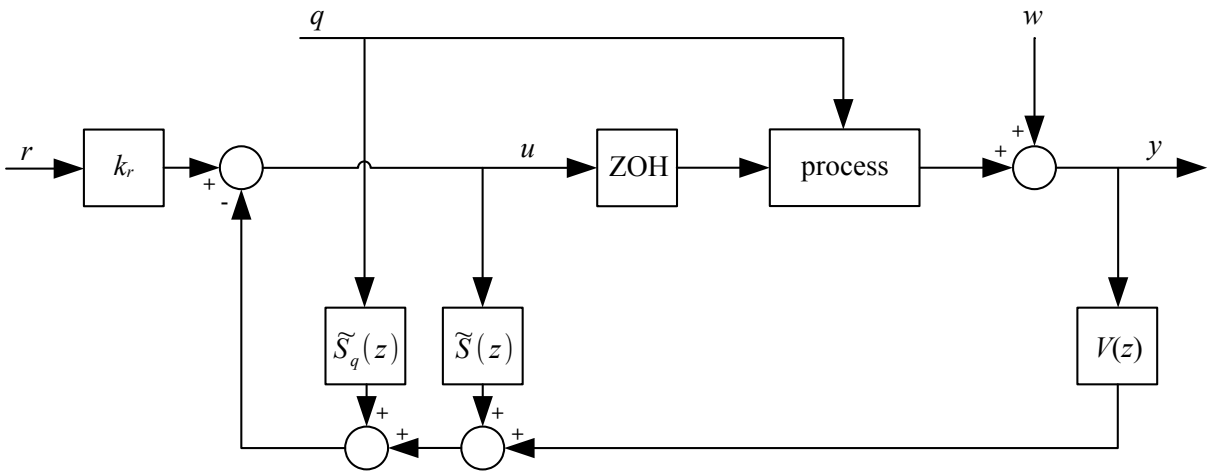

Source: The author.

4.3.4 Closed-loop robust stability

As mentioned previously, the feedback controller of the SDTC-FF has the same control structure of the SDTC for first-order models. Therefore, as the feedforward controller does not influence the closed-loop robust stability analysis, the robust stability condition of the SDTC-FF results the same as in the SDTC for first-order models:

$$I_r(\omega) = \left| \frac{1 + kG(e^{j\Omega})}{V(e^{j\Omega})G(e^{j\Omega})} \right| > \overline{\delta P}(\omega), \ \forall \omega > 0, \tag{4.22}$$

where $\Omega = \omega T_s$.

4.4 Discussion

When it is possible to measure the disturbance acting on the process, using feedforward control structures combined with feedback controllers is a good strategy for obtaining faster rejection responses. When dealing with processes with time delays, the synthesis of controllers becomes increasingly challenging, due to obstacles that arise from this phenomenon so recurrent in process control. The two SP-based controllers previously studied in this chapter were proposed envisioning a solution to this problem, which is the use of feedforward structures for processes with dead time.

Both structures use the addition of a filter in the feedforward loop that is designed to attenuate the influence of the disturbance on the process output. The difference between the structures lies in their syntheses and the feedback predictor structures they are based on. While one is based on the FSP, which is basically composed of a reference filter, a robustness filter and a primary controller with an explicit integrator, the other is based on the SDTC for first-order models, which is composed of gains and a robustness filter.

5 SMITH PREDICTOR-BASED FEEDFORWARD CONTROLLER FOR MEASURABLE DISTURBANCES

In this chapter, a feedforward extension for the SFSP to deal with measurable disturbances in high-order dead-time processes is proposed. Even by achieving faster disturbance rejection responses, the proposed structure maintains the good robustness and noise attenuation properties characteristic of SFSP.

When compared to other structures in the literature, the proposed approach has the advantage of being based on gains and having only one robustness filter, unlike most others in the literature. Additionally, the proposed structure has a feedforward gain, which accelerates even more the rejection of disturbances.

This chapter is organized as follows: Section 5.1 defines the process model; Section 5.2 describes the formulation of the SFSP with feedforward action; a guide on how the controller is designed is presented in Section 5.3; Section 5.4 presents the stable implementation of the controller; in Section 5.5 the closed-loop robust stability is analyzed; guidelines for tuning the proposed controller are given in Section 5.6; the simulation examples are presented in Section 5.7; Section 5.8 presents experimental results obtained with internal temperature control of a NICU; the considerations and discussions of the results are shown in Section 5.9.

5.1 The process model

Consider a dead-time process where the control input, the measurable disturbance, the output, and the measurement noise are represented, respectively, by u, q, y, $w \in \mathbb{R}$. The Laplace transforms of these signals are, respectively, $U(s)$, $Q(s)$, $Y(s)$, $W(s)$, and their z-transforms are, respectively, $U(z)$, $Q(z)$, $Y(z)$, $W(z)$. Thus, this open-loop process is represented in state space as:

$$\begin{cases} \tilde{x}(t+1) = \tilde{A}\tilde{x}(t) + \tilde{B}\begin{bmatrix} u(t-d) \\ q(t-d_q) \end{bmatrix}, \\ y(t) = \tilde{C}\tilde{x}(t) + w(t), \end{cases} \tag{5.1}$$

where t is the discrete-time, d and d_q are dead times, $\tilde{x} \in \mathbb{R}^{\tilde{n}}$ are the states, the pair $(\tilde{A}, \tilde{B})$ is controllable, the pair $(\tilde{C}, \tilde{A})$ is observable and ($\tilde{A}$, $\tilde{B}$, $\tilde{C}$) are matrices of appropriate dimensions.

For control design, the input-output transfer functions from (5.1) are computed, whose minimal realizations are given by

$$P(z) = \frac{Y(z)}{U(z)} = G(z)z^{-d} = C(zI - A)^{-1}Bz^{-d} = \mathbb{M}\left[\tilde{C}(zI - \tilde{A})^{-1}\tilde{B}_1\right] z^{-d}, \tag{5.2}$$

$$P_q(z) = \frac{Y(z)}{Q(z)} = G_q(z)z^{-d_q} = C_q(zI - A_q)^{-1}B_q z^{-d_q} = \mathbb{M}\left[\tilde{C}(zI - \tilde{A})^{-1}\tilde{B}_2\right] z^{-d_q}, \tag{5.3}$$

where the operator $\mathbb{M}[\cdot]$ is the minimal realization of $[\cdot]$, $\tilde{B} = [\tilde{B}_1\ \tilde{B}_2]$, the pairs (A,B) and (A_q,B_q) are controllable, (A,C) and (A_q,C_q) are observable, and the matrices (A, B, C) and (A_q, B_q, C_q) are in the observable canonical form, as shown in Appendix A. In addition, to avoid unstable modes outside the feedback path, it is assumed that the set of eigenvalues λ_i of A_q satisfying the condition $|\lambda_i| \geq 1$ also belongs to the set of eigenvalues of A.

For simulation purposes, the following transfer functions in the s-domain represent the input-output relationships of the open-loop process:

$$P(s) = \frac{Y(s)}{U(s)} = G(s)e^{-Ls} = C^*(sI - A^*)^{-1}B^*e^{-Ls}, \tag{5.4}$$

$$P_q(s) = \frac{Y(s)}{Q(s)} = G_q(s)e^{-L_q s} = C_q^*(sI - A_q^*)^{-1}B_q^*e^{-L_q s}, \tag{5.5}$$

where the order of $G(s)$ is n, the order of $G_q(s)$ is n_q, L and L_q are dead times. The pairs (A^*,B^*) and (A_q^*,B_q^*) are controllable, (A^*,C^*) and (A_q^*,C_q^*) are observable, therefore, the state-space representations $(A^*,B^*,C^*,0)$ and $(A_q^*,B_q^*,C_q^*,0)$ are, respectively, minimal realizations of $G(s)$ and $G_q(s)$ (CHEN, 1984).

By using transfer functions (5.4) and (5.5), an augmented state-space process model is given by

$$\begin{cases} \dot{\bar{x}}(t) = \bar{A}\bar{x}(t) + \bar{B}\begin{bmatrix} u(t-L) \\ q(t-L_q) \end{bmatrix}, \\ y(t) = \bar{C}\bar{x}(t) + w(t), \end{cases} \tag{5.6}$$

where t is the discrete-time, $\bar{x} \in \mathbb{R}^{(n+n_q)}$ are the states,

$$\bar{A} = \begin{bmatrix} A^* & \mathbf{0} \\ \mathbf{0} & A_q^* \end{bmatrix}, \bar{B} = \begin{bmatrix} B^* & \mathbf{0} \\ \mathbf{0} & B_q^* \end{bmatrix}, \bar{C} = \begin{bmatrix} C^* & C_q^* \end{bmatrix}.$$

Note that this realization is not necessarily minimal and can present unstable unobservable modes. Therefore, to simulate the process model and avoid these modes, the process is represented by the minimal realization of (5.6):

$$\begin{cases} \dot{\check{x}}(t) = \check{A}\check{x}(t) + \check{B}\begin{bmatrix} u(t-L) \\ q(t-L_q) \end{bmatrix}, \\ y(t) = \check{C}\check{x}(t) + w(t), \end{cases} \tag{5.7}$$

where $\check{x} \in \mathbb{R}^{\check{n}}$, $\check{n}$ is the the McMillian degree of (5.6), the pair $(\check{A},\check{B})$ is controllable, the pair $(\check{C},\check{A})$ is observable and ($\check{A}$, $\check{B}$, $\check{C}$) are matrices of appropriate dimensions.

In practice, to obtain a state-space minimal realization from a not minimal realization, one can apply, for example, the Kalman decomposition (KALMAN, 1965). Alternatively, by using MATLAB®, one can also apply the function `minreal`.

5.2 Simplified FSP with feedforward action

The proposed control structure is illustrated in Fig. 32. This structure combines both the SFSP to compensate dead times and a proposed feedforward structure (highlighted in blue) to enhance the rejection of measurable disturbances. In this proposed structure, the process is represented in the upper box, $r \in \mathbb{R}$ is the set-point, whose z-transform is $R(z)$, k_r is a reference gain, K is the state feedback gain of the SFSP predictor, K_q is the state feedforward gain, k_f is the feedforward gain, $V(z)$ is the robustness filter, the signals r_s and y_s, whose z-transforms are, respectively, $R_s(z)$ and $Y_s(z)$, compose the control signal such that $u = r_s - y_s$.

Figure 32 – Conceptual proposed structure.

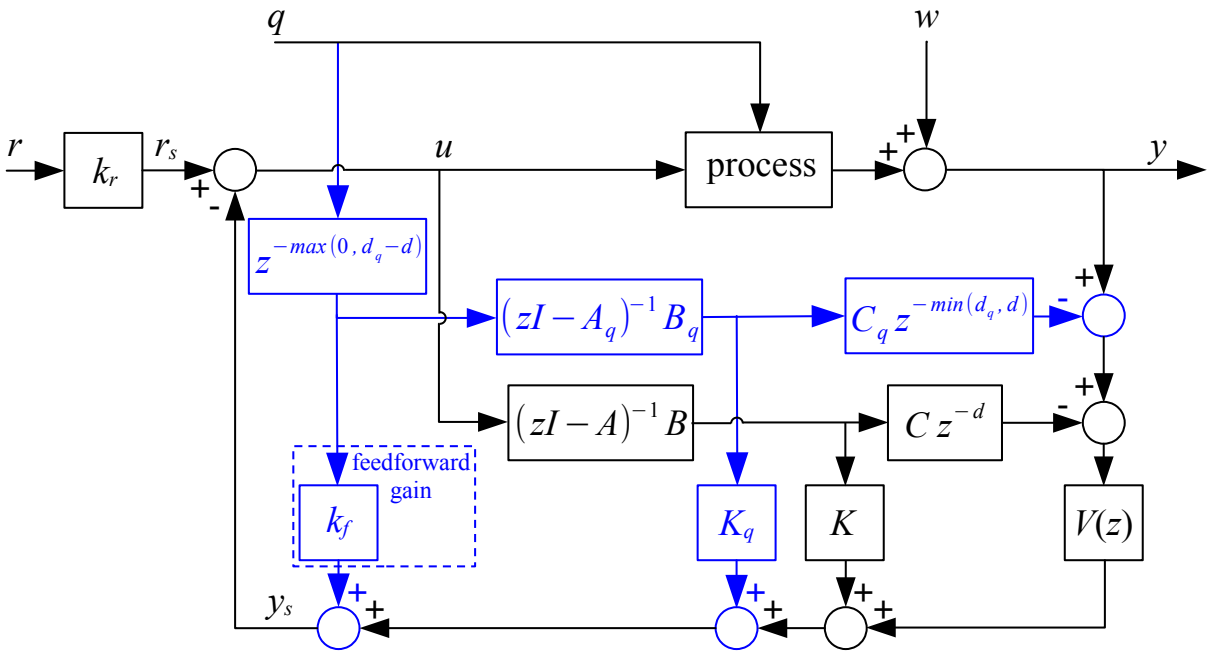

Source: The author.

It is important to highlight that the proposed feedforward controller added a proportional gain k_f in the direct path, analogously to the proportional-integral (PI), to improve the transient responses of disturbance attenuation.

To better understand its design, the conceptual proposed structure can be reduced to another conceptual equivalent structure, as presented in Fig. 33, where

Figure 33 – Conceptual equivalent structure.

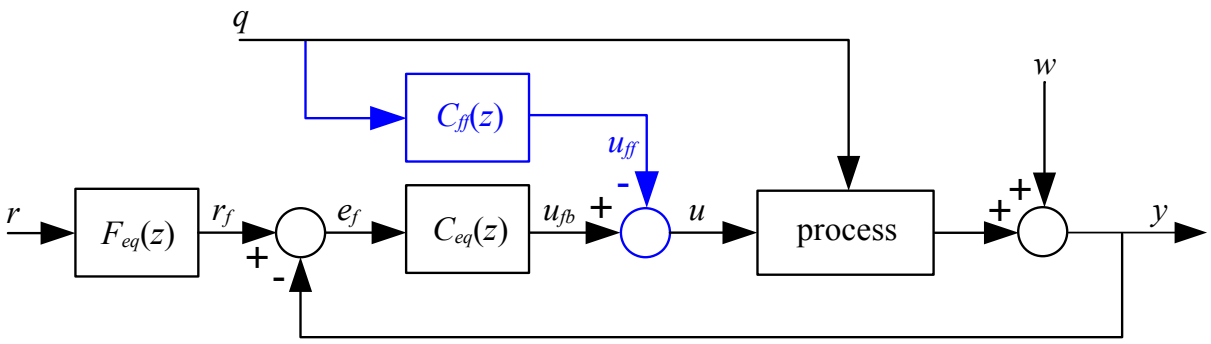

Source: The author.

$$F_{eq}(z) = \frac{R_f(z)}{R(z)} = \frac{k_r}{V(z)}, \tag{5.8}$$

$$C_{eq}(z) = \frac{U_{fb}(z)}{E_f(z)} = \frac{V(z)}{1+S(z)}, \tag{5.9}$$

$$C_{ff}(z) = \frac{U_{ff}(z)}{Q(z)} = \frac{S_q(z)}{1+S(z)}, \tag{5.10}$$

$$S(z) = \frac{\Phi(z)}{U(z)} = (K - V(z)Cz^{-d})(zI - A)^{-1}B, \tag{5.11}$$

$$S_q(z) = \frac{\Phi_q(z)}{Q(z)} = [k_f + (K_q - V(z)C_q z^{-\min(d_q,d)})(zI - A_q)^{-1}B_q]z^{-\max(0,d_q-d)}, \tag{5.12}$$

the signals r_f, e_f, u_{fb}, and u_{ff}, whose z-transforms are, respectively, $R_f(z)$, $E_f(z)$, $U_{fb}(z)$, and $U_{ff}(z)$, are defined by the relations $e_f = r_f - y$ and $u = u_{fb} - u_{ff}$.

It is important to note that, if $d \geq d_q$, (5.12) results

$$S_q(z) = \frac{\Phi_q(z)}{Q(z)} = k_f + (K_q - V(z)C_q z^{-d_q})(zI - A_q)^{-1}B_q \tag{5.13}$$

and, if $d_q > d$, it results

$$S_q(z) = \frac{\Phi_q(z)}{Q(z)} = [k_f + (K_q - V(z)C_q z^{-d})(zI - A_q)^{-1}B_q]z^{-(d_q-d)}. \tag{5.14}$$

As shown in Fig. 34, the signals ϕ, ϕ_q, and y_f, whose z-transforms are $\Phi(z)$, $\Phi_q(z)$ and $Y_f(z)$, compose the signal $y_s = \phi_q + \phi + y_f$. Although the conceptual structures from Figs. 32

and 33 are helpful for analysis purposes, in practice, the structure presented in Fig. 34 is used for implementation. For integrating and unstable open-loop processes, the conceptual control structure from Fig. 32 is internally unstable and cannot be implemented (TORRICO et al., 2021). The transfer functions $\tilde{S}(z)$ and $\tilde{S}_q(z)$, from the implementation structure, are the minimal realizations from (5.11) and (5.12), respectively.

Figure 34 – Implementation structure.

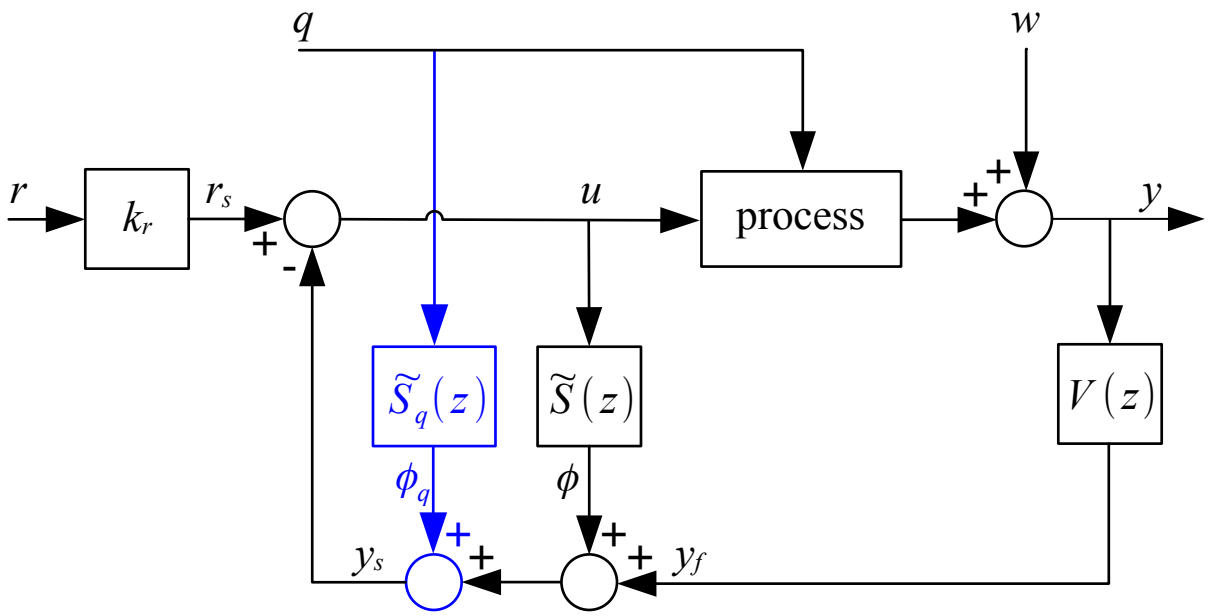

Source: The author.

Following the previously presented analysis, the input-output relationships of the proposed structure are given by

$$H_{yr}(z) = \frac{Y(z)}{R(z)} = k_r M(z), \tag{5.15}$$

$$H_{yq}(z) = \frac{Y(z)}{Q(z)} = P_q(z) - M(z)\left[k_f + K_q(zI - A_q)^{-1}B_q\right], \tag{5.16}$$

$$H_{uw}(z) = \frac{U(z)}{W(z)} = -V(z)\left[I - K(zI - A + BK)^{-1}B\right], \tag{5.17}$$

where

$$M(z) = C(zI - A + BK)^{-1}Bz^{-d}. \tag{5.18}$$

It is suggested to tune the proposed controller following the steps: (i) using (5.15) design the constant gains K and k_r for the desired closed-loop reference tracking response; (ii) design

the robustness filter $V(z)$ to guarantee null steady-state error for disturbance rejection and to satisfy the robust stability condition; (iii) using (5.16), design the constant gains K_q and k_f of the feedforward controller to eliminate the effects of the process model open-loop poles over the disturbance rejection response.

Alternatively, the proposed controller can be simultaneously tuned using, for example, an optimization method as in (SÁ RODRIGUES et al., 2021). In the next section, the controller tuning is analyzed in detail.

5.3 Controller tuning

5.3.1 Tuning of K and k_r

The feedback controller K is a gain vector with dimension $1 \times n$, where n is the order of the process model. It is tuned to obtain a desired characteristic polynomial

$$E_c(z) = (z-\alpha)^n = \det(zI - A + BK), \tag{5.19}$$

where α are the desired closed-loop poles. The pole allocation problem can be solved employing the Ackermann's formula (ACKERMANN, 1977):

$$K = \begin{bmatrix} 0 & 0 & \cdots & 1 \end{bmatrix} \begin{bmatrix} B & AB & \cdots & A^{n-1}B \end{bmatrix}^{-1} E_c(A). \tag{5.20}$$

To guarantee that (5.8) has unit static gain at the steady state ($z = 1$), a scalar constant gain k_r is used. Its value is computed as

$$k_r = [C(I - A + BK)^{-1}B]^{-1}, \tag{5.21}$$

or, alternatively,

$$k_r = \frac{1}{M(1)}, \tag{5.22}$$

where M is defined in (5.18).

5.3.2 Tuning of V(z)

The robustness filter $V(z)$ is designed following two objectives: (i) reject disturbances (step-like, ramp-like, sinusoidal, etc) at the steady state and (ii) cancel slow or unstable poles from the process and disturbance models. Based on these two objectives, a set of equations is defined:

$$\begin{cases} \frac{d^k}{dz^k}(1+S(z))\Big|_{z=1} = 0, \; k = 0, \cdots, m-1, \\ 1+S(z)\Big|_{z=p_i \neq 1} = 0, \\ 1+S(z)\Big|_{z=e^{\pm j\omega_k}} = 0, \end{cases} \tag{5.23}$$

where the operator $\frac{d^k}{dz^k}(\cdot)$ is the k-th derivative of $(\cdot)$ with relation to z, $m = m_1 + m_2$, m_1 is the number of poles in the model at $z = 1$, m_2 is the order of disturbance (1 for step-like, 2 for ramp-like, etc), p_i are the non-integrating undesired poles of the process and disturbance models, and ω_k are the frequencies of the sinusoidal disturbances.

The robustness filter is then defined as follows

$$V(z) = \frac{v_1 + v_2 z^{-1} + \cdots + v_{n_s} z^{-(n_s-1)}}{(1-\beta z^{-1})^{n_v}}, \tag{5.24}$$

where n_s is equal to the number of equations from the set (5.23), the number of poles are $n_v = n_s$, and β are tuning parameters which must be different from the poles of $G(z)$.

After the choice of β, using (5.23) and (5.24), a system of linear equations involving the variables v_i can be readily solved (TORRICO et al., 2021).

Furthermore, from the first set of equations of (5.23), it can be obtained that the equivalent feedback controller $C_{eq}(z)$ has at least one pole at $z = 1$ and that $V(1) = k_r$. Therefore, the equivalent reference filter in (5.8) has unity static gain, that is, $F_{eq}(1) = 1$. Due to that and the integral action in $C_{eq}(z)$, any model mismatch does not result in steady-state error.

5.3.3 Tuning of K_q and k_f

The gains K_q and k_f must be computed following two objectives: (i) to cancel the effects of the disturbance model open-loop dynamics, improving the transient response of the disturbance rejection and (ii) to obtain an internally stable feedforward controller. Therefore, considering $S_q(z) = N_{Sq}(z)/D_{Sq}(z)$, the following conditions must be obeyed:

$$\begin{cases} \frac{d^k}{dz^k} N_{Sq}(z)\Big|_{z=1} = 0, \; k = 0, \cdots, \; m_q, \\ N_{Sq}(z)\Big|_{z=p_{qi}\neq 1} = 0, \end{cases} \tag{5.25}$$

where $m_q = m_{q1} + m_{q2}$, m_{q1} is the number of poles of $G_q(z)$ at $z = 1$, m_{q2} is the order of disturbance (1 for step-like, 2 for ramp-like, etc), and p_{qi} are the non-integrating poles of $G_q(z)$.

5.4 Stable implementation

Satisfying conditions (5.23) and (5.25), the proposed controller is designed to cancel the open-loop poles of the model, given by $\det(zI - A)$ and $\det(zI - A_q)$, from $S(z)$ and $S_q(z)$, respectively. Then, the canceled modes are unobservable and can lead to internal stability problems in the case of open-loop unstable or integrating processes. For practical implementation, the unobservable modes of $S(z)$ and $S_q(z)$ can be eliminated by using the minimal realizations of these transfer functions. Following the formulation from (TORRICO et al., 2021), expression (5.11) for $S(z)$ has the minimal realization

$$\tilde{S}(z) = \sum_{i=1}^{d} KA^{i-1}Bz^{-i} - \frac{N_V^*(z)}{D_V(z)} z^{-d}, \tag{5.26}$$

where $D_V(z)$ is the denominator of $V(z)$ and the numerator $N_V^*(z)$ is obtained by partial fraction decomposition of $G(z)V(z)$, resulting

$$G(z)V(z) = \frac{N_G^*(z)}{D_G(z)} + \frac{N_V^*(z)}{D_V(z)}. \tag{5.27}$$

Note that, as explained in Section 5.3.2, the tuning parameters β of $V(z)$ must be different from the poles of $G(z)$, guaranteeing that the partial fraction decomposition (5.27) is unique.

Following the formulation to obtain $\tilde{S}(z)$ from (TORRICO et al., 2021), the minimal realization of $S_q(z)$ is obtained, for $d \geq d_q$, as

$$\tilde{S}_q(z) = k_f + \sum_{i=1}^{d_q} K_q A_q^{i-1} B_q z^{-i} - \frac{N_{Vq}^*(z)}{D_V(z)} z^{-d_q} \tag{5.28}$$

and, for $d_q > d$, as

$$\tilde{S}_q(z) = \left(k_f + \sum_{i=1}^{d} K_q A_q^{i-1} B_q z^{-i} - \frac{N_{Vq}^*(z)}{D_V(z)} z^{-d} \right) z^{-(d_q - d)}, \tag{5.29}$$

where the partial fraction decomposition of $G_q(z)V(z)$ results as

$$G_q(z)V(z) = \frac{N_{Gq}^*(z)}{D_{Gq}(z)} + \frac{N_{Vq}^*(z)}{D_V(z)}. \tag{5.30}$$

It is important to note that, as explained in Section 5.1, the unstable poles of $G_q(z)$ are also poles of $G(z)$, guaranteeing that the partial fraction decomposition (5.30) is also unique.

5.5 Closed-loop robust stability analysis

A sufficient condition of robust stability widely used for feedback control is (MORARI; ZAFIRIOU, 1989)

$$I_r(\omega) = \frac{|1 + C_{eq}(e^{j\Omega}) P(e^{j\Omega})|}{|C_{eq}(e^{j\Omega}) P(e^{j\Omega})|} > \overline{\delta P}(\omega), \tag{5.31}$$

where $\overline{\delta P}$ is the norm-bound multiplicative uncertainty of the process, I_r is a robustness index, $\Omega = T_s \omega$, and Ω is within the range $[0,\ \pi]$.

For the proposed control strategy, using (5.9), (5.11), and (5.31), the following robust stability condition (the same as in (3.42)) is obtained

$$I_r(\omega) = \left| [V(e^{j\Omega}) C(e^{j\Omega} I - A)^{-1} B]^{-1} [1 + K(e^{j\Omega} I - A)^{-1} B] \right| > \overline{\delta P}(\omega). \tag{5.32}$$

From (5.32) it can be seen that the robustness filter plays an essential role in improving robustness. A detailed study of the filter tuning that at once includes performance, robustness, and noise attenuation is presented in (TORRICO et al., 2018).

5.6 Controller tuning guidelines

The main objective of tuning the SFSP with feedforward action is disturbance rejection. Although the disturbance rejection is influenced by both feedback and feedforward loops, the feedforward loop does not have free tuning parameters, and the proposed controller is tuned in the same way as the original SFSP.

The free tuning parameters of the SFSP are the closed-loop poles α, which influence both reference tracking and disturbance rejection, and the poles of the robustness filter β, which only influence the disturbance rejection. The poles α and β can be chosen between the interval $[0,\ 1)$. Their choice is made in order to meet the performance and robustness criteria of the closed-loop system. Thus, when they tend to 0, a more aggressive response will be obtained, and when they tend to 1, more robustness will be obtained.

As an illustration example, Fig. 35 shows the influence of the tuning of the poles of the robustness filter, given by β, over the robust stability condition (5.32). From this Figure, to satisfy condition (5.32) and maintain the same minimum distance between the robustness and uncertainties curves, it is easy to note that the values of β must be chosen considering the value of the dead-time uncertainty.

More information on how to properly choose the poles β of the robustness filter $V(z)$ can be found in (TORRICO et al., 2018; SÁ RODRIGUES et al., 2021).

5.7 Simulation examples

In this section, three simulation examples for stable, unstable, and integrating processes, where $d > d_q$, are presented. The proposed controller is compared with other control structures from the recent literature. Only second-order or lower models are used for comparative reasons with the proposed ones found in the literature. However, the proposed controller can be applied to high-order dead-time processes by using the simple tuning strategy presented in the paper. This comparison was made taking into account the disturbance rejection performance indices, such as integrated absolute error (IAE), total variation (TV) of the control signal, and control variance (CV). The expressions for these indices are

$$IAE = \int_{t_q+L}^{\infty} |r(t) - y(t)| dt, \tag{5.33}$$

$$TV = \sum_{i=1}^{N_q} |u_{i+1} - u_i|, \tag{5.34}$$

$$CV = \frac{1}{N_w - 1} \sum_{i=1}^{N_w} |u_i - \mu|^2, \tag{5.35}$$

Figure 35 – Robust stability for different values of dead-time uncertainties and β.

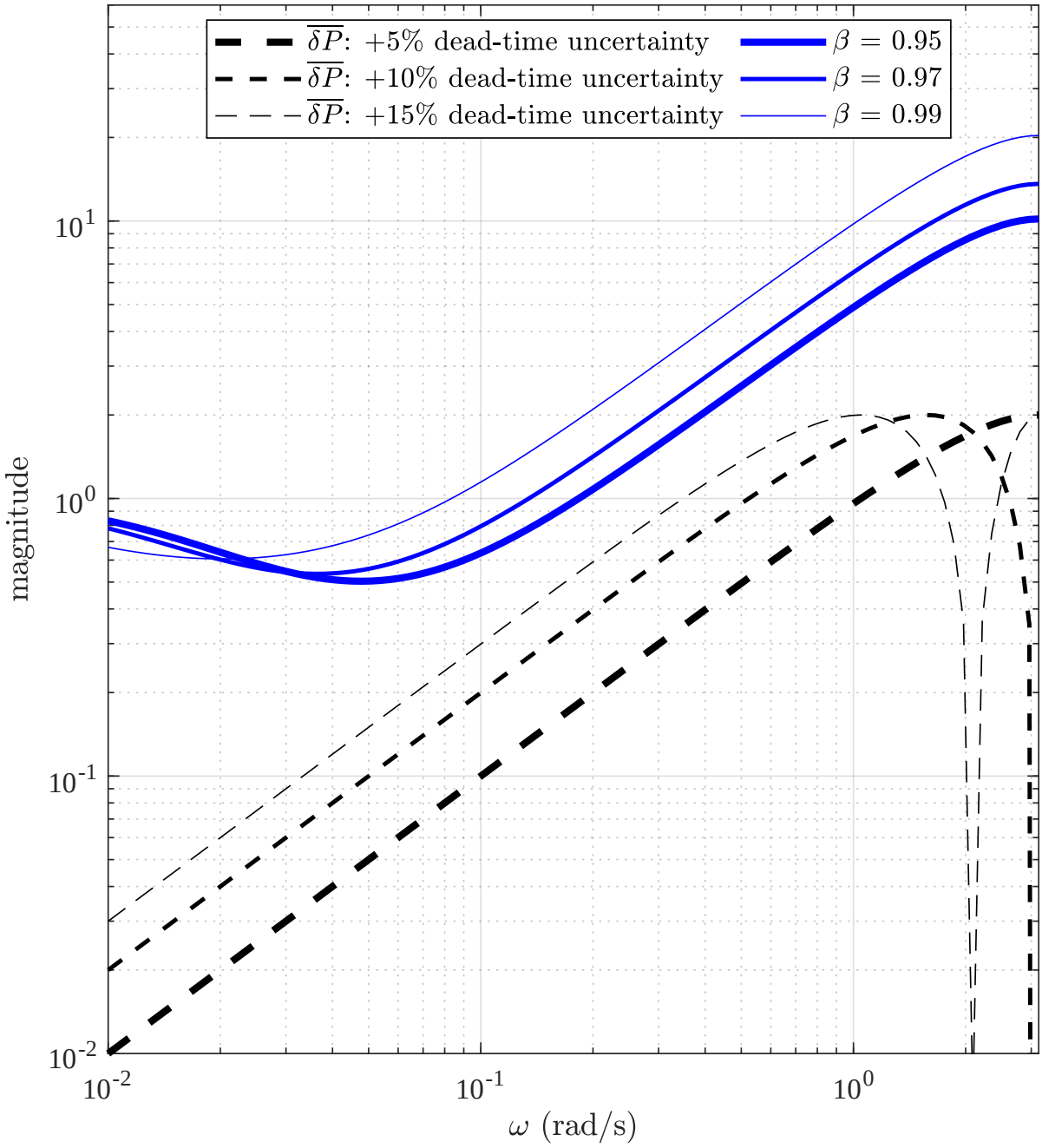

Source: The author.

where t_q is the time at which the disturbance is applied, L is the continuous-time input delay, N_q is the number of samples of the disturbance rejection response, μ is the mean of the control signal, and N_w is the number of samples of the noise attenuation response.

The CV index is computed at the beginning of the simulations when the closed-loop system is at the steady state and at the time interval when band-limited white noise is added to the output. The IAE and the TV indices are then computed only after the noise stops affecting the output. Band-limited white noise is used in the simulations and its PSD value is specified in each example.

All three simulation examples were performed using linearized models of the described processes. By using the input-output transfer functions $P(s)$ and $P_q(s)$ presented in each example and following the ideas from Section 5.1, the transfer functions (5.2) and (5.3), $P(z)$ and $P_q(z)$, respectively, and the state-space minimal realization process (5.7) were obtained. Note that (5.2) and (5.3) were obtained by considering a zero-order hold (ZOH), while (5.7) was obtained using the command `minreal` from MATLAB®.

5.7.1 Example 1: stable process

The model of a boiler is used to assess the performance of the proposed strategy. The process is from the Abbott Power Plant in Champaign, IL, which is powered by oil and gas and used for heating and power generation (PELLEGRINETTI; BENTSMAN, 1996). It is desired to control the steam pressure $y_1(t)$, while the fuel rate $u_1(t)$ is the manipulated variable and the steam demand $d_1(t)$ is the measurable disturbance. Other inputs, outputs, and disturbances are considered constant, as in (PELLEGRINETTI; BENTSMAN, 1996). Hence, one can find the linearized process and disturbance transfer functions of the boiler, respectively, as

$$P(s) = \frac{0.355}{24.75s+1}e^{-6.75s}, \tag{5.36}$$

$$P_q(s) = \frac{-0.712}{195.8s+1}. \tag{5.37}$$

The equivalent discrete-time transfer functions with sampling period $T_s = 0.25\ (s)$ are

$$P(z) = \frac{0.003568}{z-0.9899}z^{-27}, \tag{5.38}$$

$$P_q(z) = \frac{-0.0009085}{z-0.9987}. \tag{5.39}$$

The controller was designed to compute the feedback gain K in order to obtain a closed-loop pole $\alpha = 0.75$ and the robustness filter was designed with poles $\beta = 0.988$ with multiplicity

$n_v = 3$, to satisfy the robustness condition (5.32) for a dead-time uncertainty of 10% in the process model and to attenuate the measurement noise.

A comparison of the proposed controller (SFSP-FF) is made with those presented in (ALVES LIMA et al., 2019) and (RODRÍGUEZ et al., 2016a). All these controllers have feedforward action for measurable disturbances. The controller from (RODRÍGUEZ et al., 2016a) was tuned in the continuous-time domain, for set-point tracking, with $\tau_{rt} = 6.75$ and, for disturbance rejection, with $\tau_{sp} = 20$ and $\tau_{dr} = 1.5$. The controller from (ALVES LIMA et al., 2019) was tuned in the discrete-time domain, for set-point tracking, with $p_c = 0.5724$, for disturbance rejection, with $\beta_{SDTC-FF} = 0.9752$ and $\alpha_{SDTC-FF} = 0.8796$. As the SFSP-FF, these two controllers were implemented in the discrete-time domain with sampling period $T_s = 0.25\ (s)$. The components of the controllers being compared are shown in Table 6.

Table 6 – Example 1. Controllers parameters.

	(RODRÍGUEZ et al., 2016a)	(ALVES LIMA et al., 2019)	SFSP-FF
Reference filter	$\frac{0.01815}{z-0.9818}$	119.8401	67.2541
Feedback controller	$\frac{10.33z-10.22}{z-1}$	117.0232	70.0710
Robustness filter	$\frac{0.7308z^2-1.431z+0.6999}{(z-0.9876)^2}$	$\frac{2.974z}{z-0.9752}$	$\frac{2.018z^3-4.003z^2+1.985z}{(z-0.988)^3}$
k_f	-	-	-1.9366
K_q	-	-	67.3510
Feedforward filter	$\frac{28.57z^2-55.24z+26.69}{(z-0.8465)^2}$	$\frac{531.1z-516.6}{z-0.8796}$	-

Source: The author.

Figure 36 shows the robustness condition from (5.32) considering the given process model uncertainty. For a fair comparison, all controllers have similar robustness. Figures 37 and 38 show the output and control signals for the simulations of the nominal case and of the case with model uncertainties, respectively. In the simulation, band-limited white noise with PSD of $5 \cdot 10^{-4}$ was added to the process output at the first 10 (s), a step disturbance of $d_1(t) = 30\%$ in the steam demand occurs at $t_q = 20\ (s)$. Even though all the compared controllers have been designed with similar levels of robustness, the proposed controller rejects the disturbance much faster, as confirmed by the IAE indices shown in Table 4. Because of the more aggressive response, as expected, the TV index of the proposed controller is higher.

5.7.2 Example 2: unstable process

In this example, the control of a chemical reactor with a non-ideal mixture is studied. Its nonlinear model is described by

$$\frac{\mathrm{dC(t)}}{\mathrm{d}t} = \frac{F(t)}{V}[C_i(t) - C(t)] - \frac{k_1 C(t)}{[k_2 C(t) + 1]^2} \tag{5.40}$$

where $C_i(t)$ and $C(t)$ are the input and output concentrations, respectively, $F(t)$ is the inflow and V is the reactor volume. The values of the constant parameters of the model are $k_1 = 10\ (l/s)$, $k_2 = 10\ (l/mol)$, and $V = 1\ (l)$.

Figure 36 – Example 1. Robustness index.

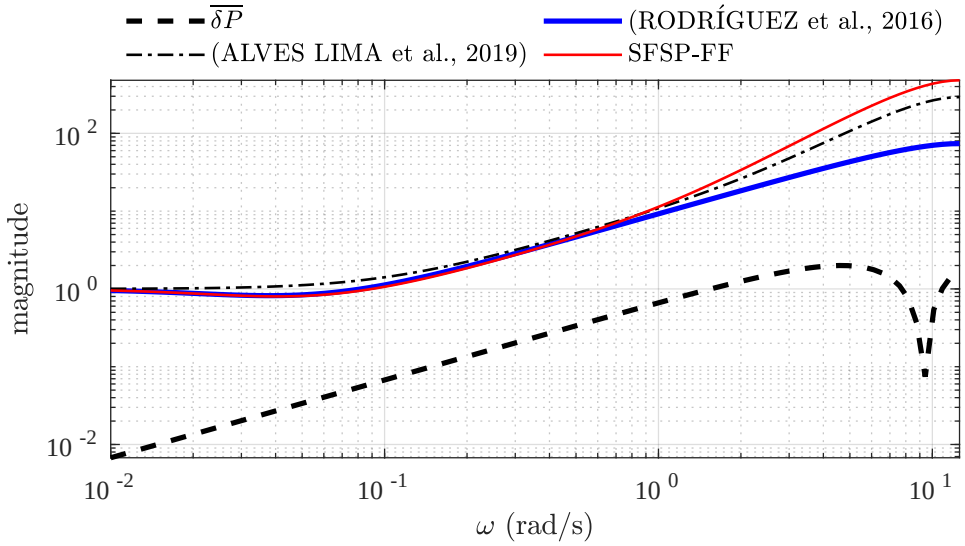

Source: The author.

Figure 37 – Example 1. Nominal case.

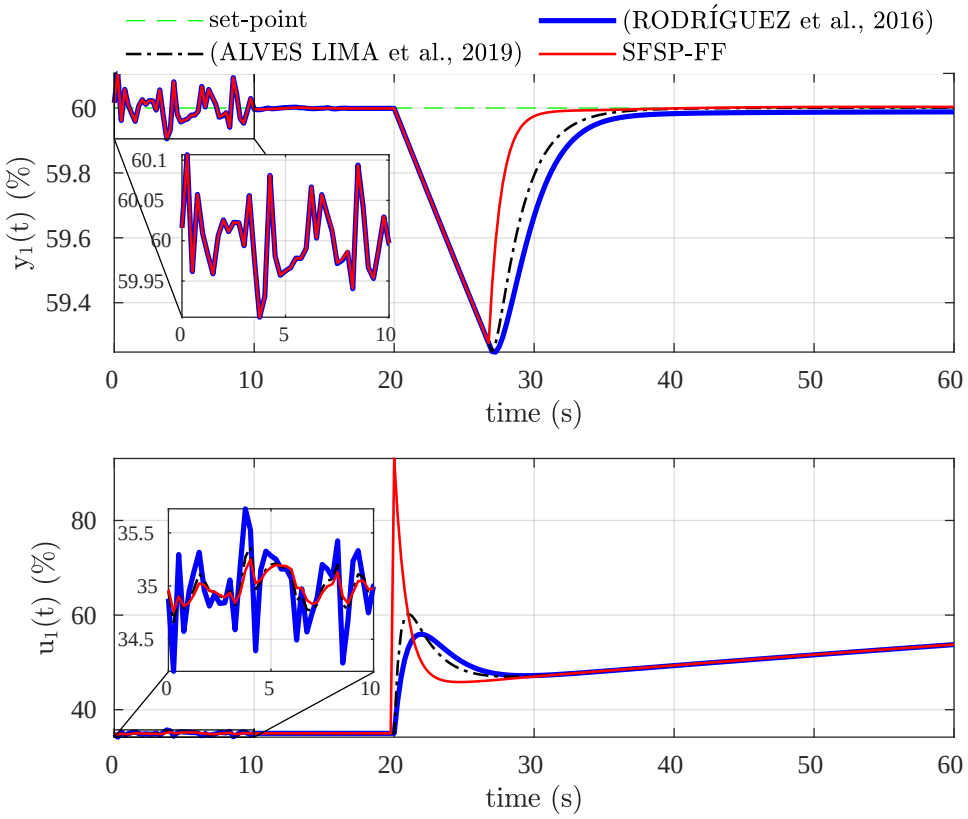

Source: The author.

For control purposes, as studied in (CHIDAMBARAM; REDDY, 1996), $C(t)$ is the variable to be controlled, $C_i(t)$ is the manipulated variable, and $F(t)$ is the disturbance variable. The linearized model at its operation point has the following transfer functions (RODRÍGUEZ et

Figure 38 – Example 1. Case with model uncertainties.

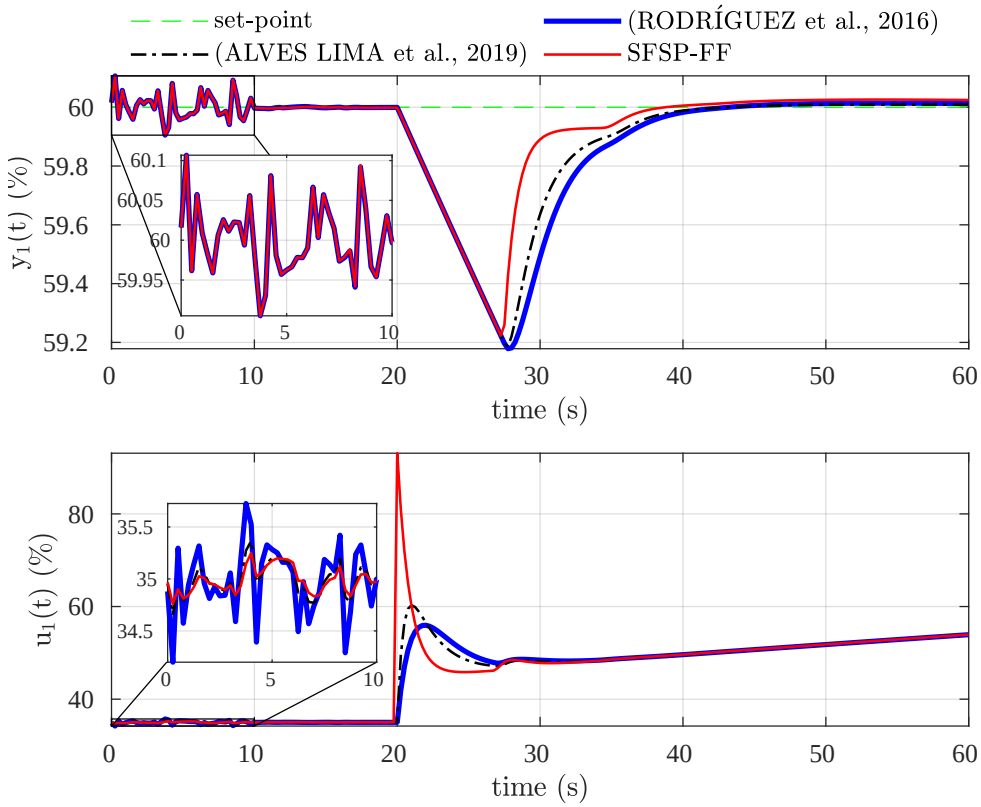

Source: The author.

al., 2016a):

$$P(s) = \frac{3.433}{103.1s - 1} e^{-20s}, \tag{5.41}$$

$$P_q(s) = \frac{-206.9346}{103.1s - 1} e^{-10s}. \tag{5.42}$$

Discretization of the transfer functions with sampling period $T_s = 1\ (s)$, leads to:

$$P(z) = \frac{0.03364}{z - 1.01} z^{-20}, \tag{5.43}$$

$$P_q(z) = \frac{-2.017}{z - 1.01} z^{-10}. \tag{5.44}$$

In this example, two different tunings of the SFSP-FF are considered, namely SFSP-FF1 and SFSP-FF2. For the SFSP-FF1, the feedback controller was tuned with $\alpha = 0.2$, while for the SFSP-FF2, it was chosen $\alpha = 0.7$. As $P(z)$ is a first-order transfer function, for both tunings,

$n = 1$. To satisfy the robustness condition (5.32) for a dead-time uncertainty of 10% in the process model and to attenuate measurement noise, for both controllers, the robustness filter was tuned with $\beta = 0.98$ with multiplicity $n_v = 2$. Both controllers are compared with the one presented in (RODRÍGUEZ et al., 2016a), that was tuned, for set-point tracking, with $\tau_{rt} = 20$, for disturbance rejection, with $\tau_{sp} = 26$ and $\tau_{dr} = 2.5$. As the proposed controllers, the one from (RODRÍGUEZ et al., 2016a) was implemented in the discrete-time with sampling period $T_s = 1\ (s)$. The components of the three controllers are presented in Table 7.

Table 7 – Example 2. Controllers parameters.

	(RODRÍGUEZ et al., 2016a)	SFSP-FF1	SFSP-FF2
Reference filter	$\frac{0.4558z-0.4333}{(z-0.9775)}$	23.9093	8.9660
Feedback controller	$\frac{3.294z-3.219}{z-1}$	24.2006	9.2573
Robustness filter	$\frac{1.256z^3-3.632z^2+3.5z-1.124}{(z-0.9623)^2}$	$\frac{1.66z^2-1.651z}{(z-0.98)^2}$	$\frac{0.6425z^2-0.639z}{(z-0.98)^2}$
k_f	-	-570.3513	-255.3927
K_q	-	26.6655	10.2002
Feedforward filter	$\frac{23.45z^3-66.13z^2+62.09z-19.41}{(z-0.6703)^2}$	-	-

Source: The author.

Figure 39 shows the robustness indices of the controllers being compared considering the dead-time uncertainty. As can be seen, the robustness of the two tunings of the SFSP-FF is better at medium and high frequencies, where the robust stability condition is critical when considering dead-time uncertainties (NORMEY-RICO; CAMACHO, 2007).

Figure 39 – Example 2. Robustness Index.

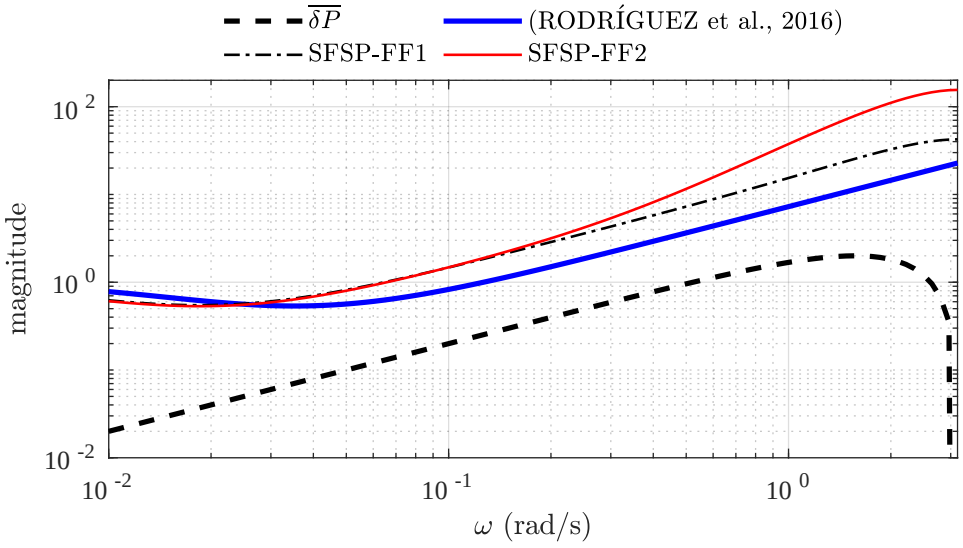

Source: The author.

For simulation, band-limited white noise with PSD of 10^{-3} is added to the output at the

first 50 (s) and a disturbance of $F(t) = 0.015$ (l/s) is applied to the input flow at $t = 100$ (s). The time responses of the controllers for the nominal case and the case with model uncertainties are shown in Figs. 40 and 41, respectively. From these figures, it is evident that the two tunings of the proposed controllers provide faster disturbance rejection, as confirmed by the performance indices presented in Table 4. The FSFP-FF1 tuning presented the best IAE index and the highest TV index, due to the aggressiveness of the tuning. The SFSP-FF2, with a more robust tuning, presented the best TV and CV indices and a better IAE than the controller from (RODRÍGUEZ et al., 2016a).

Figure 40 – Example 2. Nominal case.

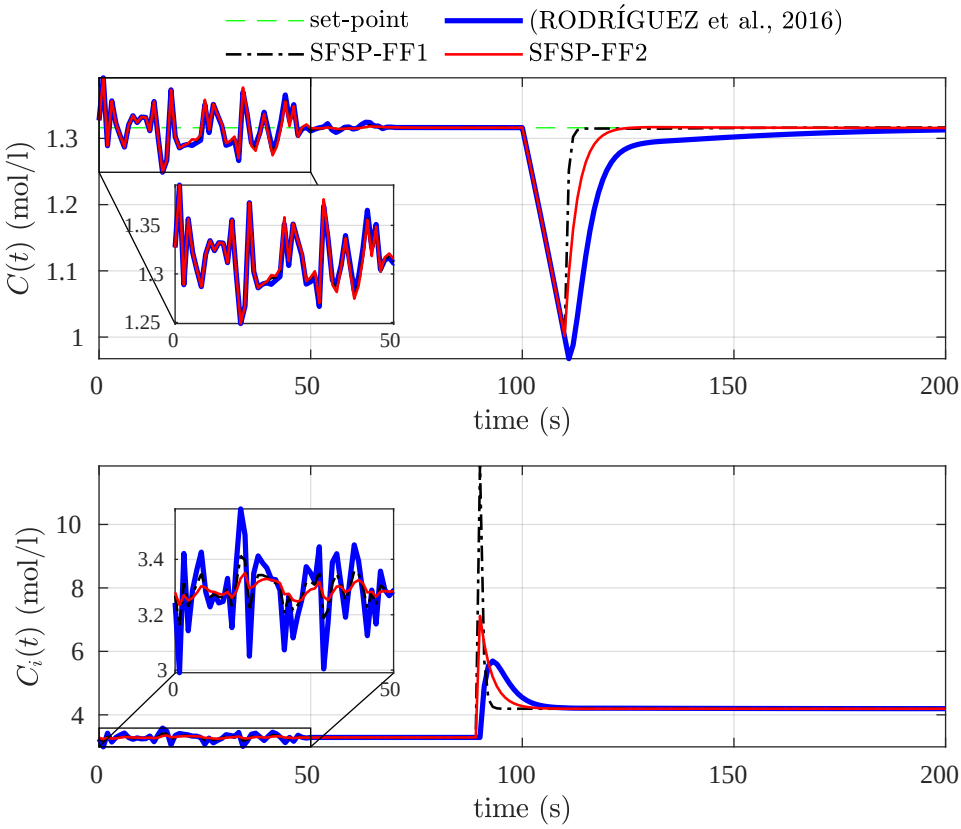

Source: The author.

5.7.3 Example 3: integrating disturbance

In this case, a continuous stirred-tank reactor (CSTR) model is studied (HENSON; SEBORG, 1997). The CSTR performs an irreversible reaction where its temperature $T(t)$ is controlled with external cooling with temperature $T_c(t)$ and the disturbance is $V_0(t) = \int_0^t F_0(\tau)d\tau$, where $F_0(t)$ is the measurable inlet flow rate.

As defined in (RODRÍGUEZ et al., 2016a), the transfer functions for a certain operating point are given by

$$P(s) = \frac{1.7316(s+1.178)}{(s^2+1.757s+1.207)}e^{-s}, \tag{5.45}$$

Figure 41 – Example 2. Case with model uncertainties.

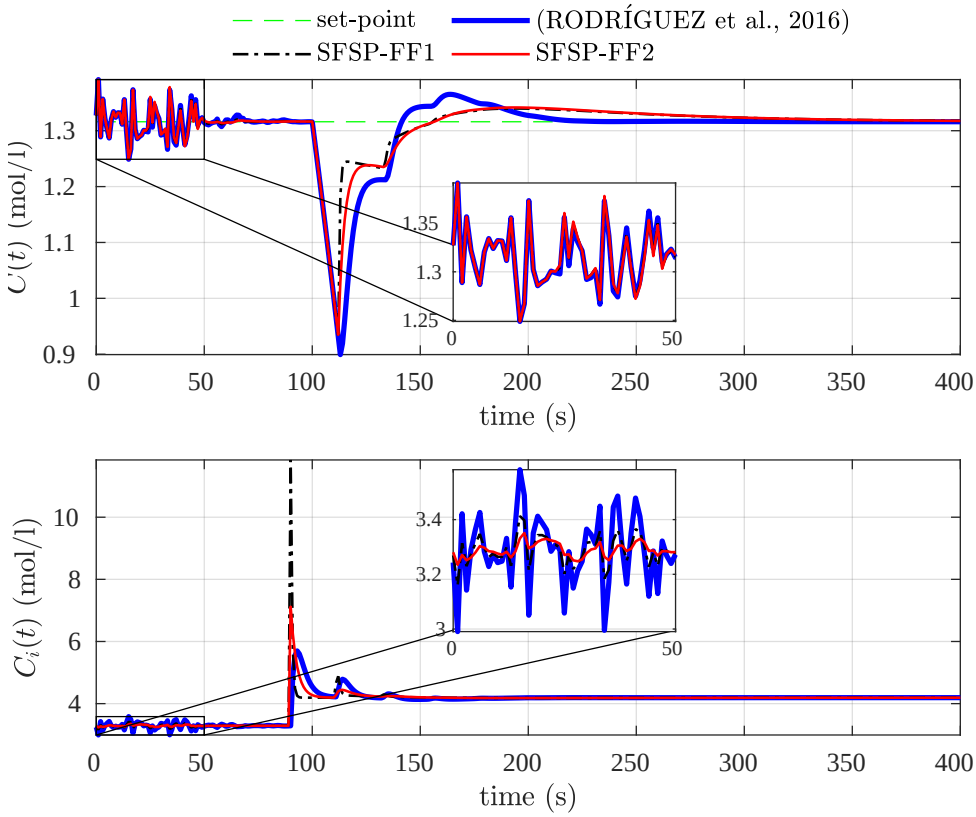

Source: The author.

$$P_q(s) = \frac{0.048615(s-4.275)(s+1.358)}{(s^2+1.757s+1.207)} e^{-0.25s}. \tag{5.46}$$

Discretization of the transfer functions with sampling period $T_s = 0.05\ (s)$ leads to

$$P(z) = \frac{0.085321(z-0.9428)}{(z^2-1.913z+0.9159)} z^{-20}, \tag{5.47}$$

$$P_q(z) = \frac{0.002148(z-1.239)(z-0.9343)}{(z^2-1.913z+0.9159)} z^{-5}. \tag{5.48}$$

The SFSP-FF was tuned with desired closed-loop poles $\alpha = 0.95$ with multiplicity $n = 2$ and, for the robustness filter, with poles $\beta = 0.97$ with multiplicity $n_v = 4$.

The proposed controller is compared with the control strategy presented by (RODRÍGUEZ et al., 2016a). This strategy was tuned in the continuous-time domain, for set-point tracking, with $\tau_{rt} = 10$, for disturbance rejection, with $\tau_{sp} = 1$ and $\tau_{dr} = 0.5$. It was implemented in the discrete-time domain with sampling period $T_s = 0.05\ (s)$. Table 8 shows the components of both controllers.

Table 8 – Example 3. Controllers parameters.

	(RODRÍGUEZ et al., 2016a)	SFSP-FF
Reference filter	$\frac{0.05719}{(z-0.9428)}$	0.5123
Feedback controller	$\frac{1.208z^2-2.528z+1.322)}{(z-1)(z-0.946)}$	[10.7204 11.2087]
Robustness filter	$\frac{1.649z^2-3.263z+1.614}{(z-0.9512)^2}$	$\frac{0.01861z^4-0.05394z^3+0.05213z^2-0.0168z}{(z-0.97)^4}$
k_f	-	-0.0699
K_q	-	[140.8091 136.0207 130.9232]
Feedforward filter	$\frac{3.682z^2-7.242z+3.56}{(z-0.9048)^2}$	-

Source: The author.

A dead-time uncertainty of 10% is considered in the case with model uncertainties. The robustness indices of both controllers are shown in Fig. 42. The proposed controller presents a better index at medium and high frequencies.

Figure 42 – Example 3. Robustness Index.

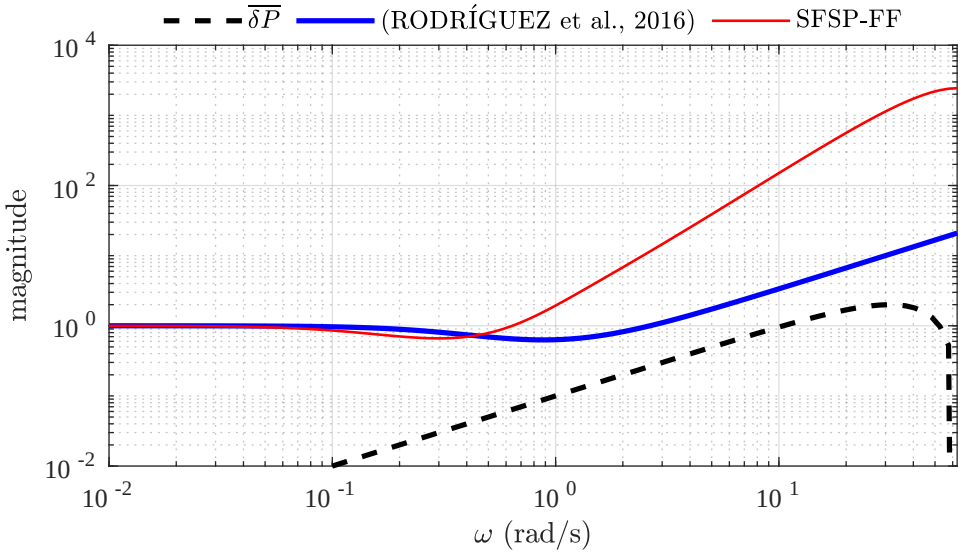

Source: The author.

In the simulation, white noise with PSD of $5 \cdot 10^{-4}$ is added to the output for the first $t = 5$ (s) and a disturbance of $F_0(t) = 20$ (l/min) in the inlet flow rate is applied at $t = 10$ (s), which is equivalent to apply a ramp-like disturbance $V_0(t) = 20(t-10)$ (l) to the process. Figures 43 and 44 show the time responses for the nominal case and the case with model uncertainties, respectively. The proposed controller presents faster disturbance rejection with a smaller undershoot. Table 4 shows that the SFSP-FF presented better indices in all compared scenarios. It is worth noting that the IAE and CV are much smaller than those of the controller from (RODRÍGUEZ et al., 2016a).

Figure 43 – Example 3. Nominal case.

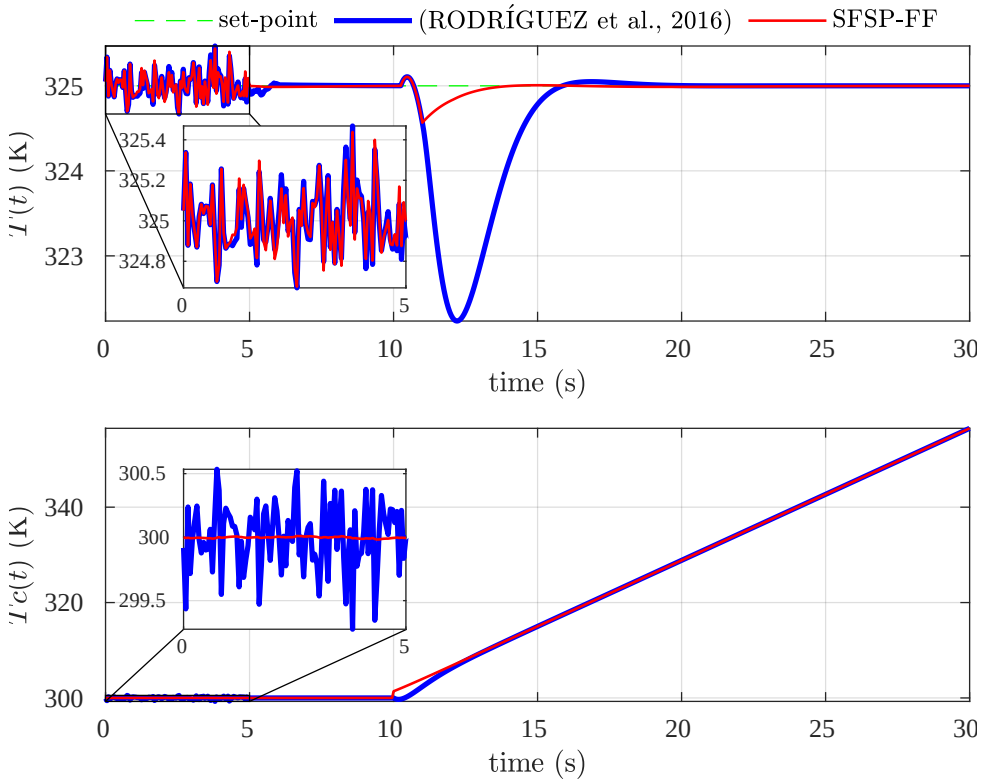

Source: The author.

Table 9 – Performance indices. The best performances are highlighted in bold text.

Example		Nominal			Robust		
		IAE	TV	CV	IAE	TV	CV
Example 1	SFSP-FF	**0.76**	55.20	**0.015**	**2.21**	56.67	**0.015**
	(ALVES LIMA et al., 2019)	2.00	45.34	0.025	3.57	46.00	0.025
	(RODRÍGUEZ et al., 2016a)	2.96	**36.28**	0.11	4.13	**36.03**	0.11
Example 2	SFSP-FF1	**0.29**	7.66	0.0027	**5.70**	9.19	0.0028
	SFSP-FF2	0.89	**2.93**	**0.0006**	6.58	**3.48**	**0.0006**
	(RODRÍGUEZ et al., 2016a)	3.11	3.91	0.015	7.09	5.50	0.016
Example 3	SFSP-FF	**0.50**	**55.14**	**0.00003**	**2.95**	**55.41**	**0.00003**
	(RODRÍGUEZ et al., 2016a)	6.48	57.14	0.065	7.28	57.42	0.07

Source: The author.

Figure 44 – Example 3. Case with model uncertainties.

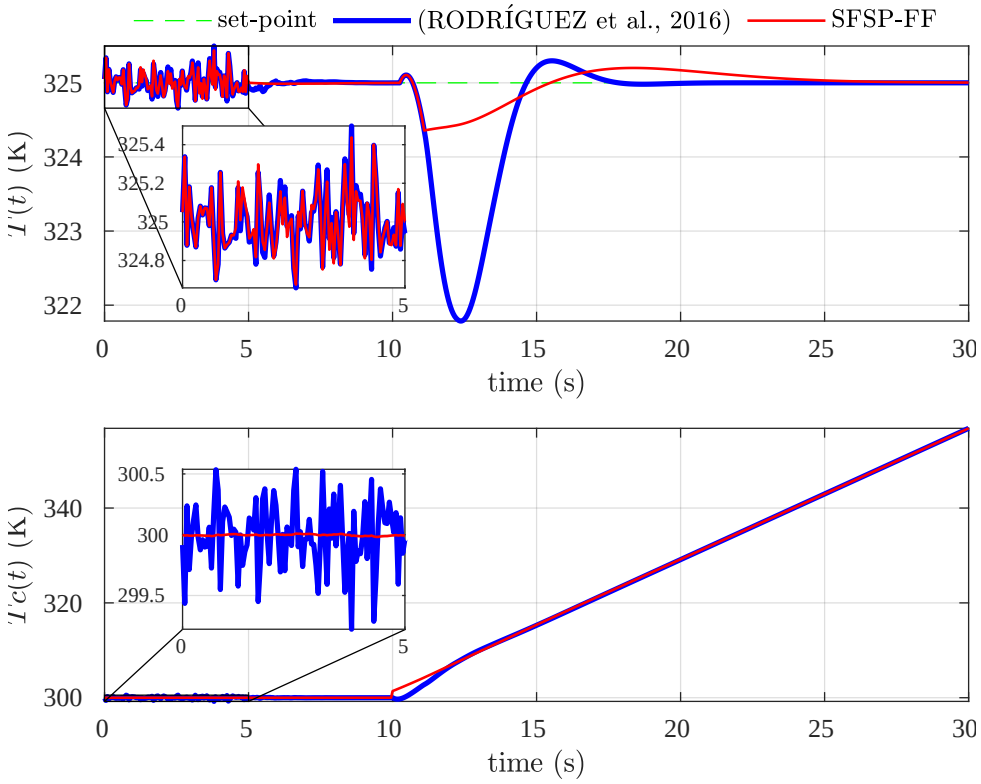

Source: The author.

5.8 Temperature control in a NICU

Experiments in a NICU were performed to evaluate the proposed strategy in a practical application. Figure 45 shows a picture of the NICU connected to a desktop computer. This computer can communicate with the NICU's hardware to receive the internal temperature and relative humidity measurements and send the pulse width modulation (PWM) duty cycles of the voltages at the heater and humidifier. Therefore, the complete system of the NICU is a two-inputs-two-outputs process. However, only the temperature loop is of interest in the performed experiments.

The process variable is the temperature in the NICU and the control variable is the PWM duty cycle of the voltage at the heater. Disturbances occur when the ports of the NICU are opened and the external cooler air goes into the NICU's dome. Therefore, in these experiments, a unit step change in the measurable disturbance input is considered when one port is opened.

By performing an identification experiment, the following discrete-time transfer functions, with sampling period $T_s = 0.4$ (min), were obtained

$$P(z) = \frac{0.002718}{z - 0.9621} z^{-6}, \tag{5.49}$$

Figure 45 – Temperature control in a NICU connected to a desktop computer.

Source: The author.

$$P_q(z) = \frac{-0.06204}{z-0.9445} z^{-30}. \tag{5.50}$$

Note in (5.49) and (5.50) that $d_q > d$. Therefore, the tuning of the proposed controller is based on the appropriate formulation for this case.

The SFSP-FF is compared to the SFSP presented in (TORRICO et al., 2021). The two controllers were tuned for set-point tracking with $\alpha = 0.85$ with multiplicity $n = 1$. The robustness filters of both controllers were tuned to satisfy condition (5.32), considering the uncertainties of $P(z)$ as $+10\%$ in the static gain and time constant, and $+0.4$ (min) in the dead time. After a considerable number of model identification procedures, at different operation points, it was observed that each of the model parameters varied up to a certain range. Therefore, the considered uncertainty for each parameter follow this range. The upper bound of the norm of multiplicative uncertainty, computed by (2.4), results

$$\overline{\delta P}(\omega) = \left| \frac{1-0.962e^{-j\omega T_s}}{e^{j\omega T_s}-0.9654} - 1 \right|. \tag{5.51}$$

The SFSP was tuned with $\beta = 0.85$ with multiplicity $n_v = 2$, while the SFSP-FF was tuned with $\beta = 0.9$ with multiplicity $n_v = 3$. The parameters of both controllers are presented in Table 10.

The robustness indices of both controllers are presented in Fig. 46, where it can be seen that the proposed strategy presents better index at mid and high frequencies.

Figure 47 shows the temperature responses from the NICU for both controllers. A set-point step change from 24^oC to 28^oC was applied at $t = 10$ (min) and one port of the NICU was opened at $t_q = 58$ (min). For the SFSP-FF, the unit step change in the measurable disturbance

Table 10 – Temperature control in a NICU. Controllers parameters.

	SFSP	SFSP-FF
Reference gain	55.1861	55.1861
Feedback controller	41.2255	41.2255
Robustness filter	$\frac{21.48z^2-20.24z}{(z-0.85)^2}$	$\frac{16.37z^3-30.89z^2+14.57z}{(z-0.9)^3}$
k_f	-	-22.8247
K_q	-	34.7522

Source: The author.

Figure 46 – Temperature control in a NICU. Robustness index.

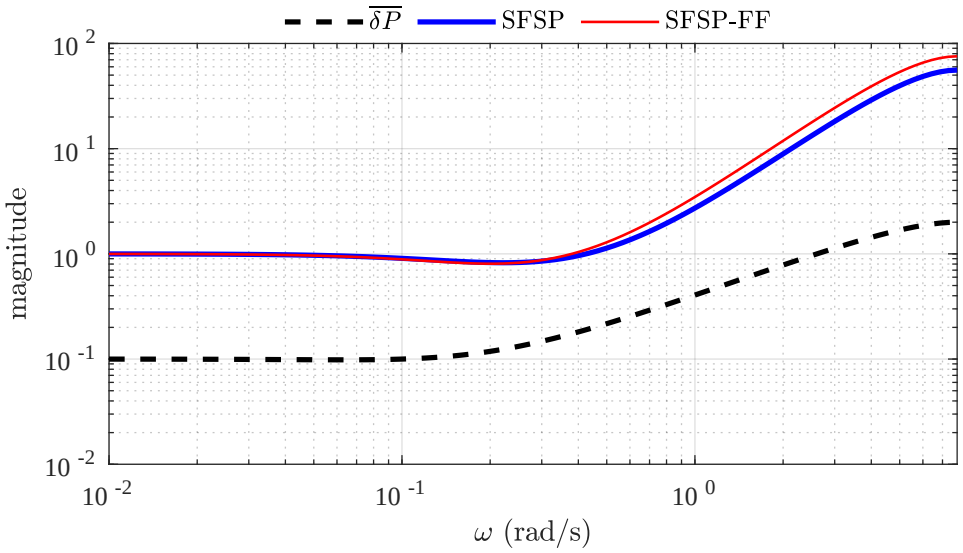

Source: The author.

input was also applied at $t_q = 58$ (min). From Fig. 47, it can be seen that the control input of the SFSP-FF begins to actuate sooner than the control input of the SFSP to reject the disturbance. This results in a much faster disturbance rejection by the SFSP-FF than by the SFSP.

Table 11 shows the IAE index for both controllers, computed in the time interval while the port of the NICU is open. The IAE was calculated by

$$IAE = \int_{t_q}^{\infty} |r(t) - y(t)| dt. \tag{5.52}$$

Note that the IAE of the SFSP-FF is 40.23% smaller than the IAE of the SFSP.

5.9 Discussion

In this chapter, a feedforward control structure for the simplified filtered Smith predictor for high-order dead-time process was presented. The purpose was to obtain better disturbance rejection results for processes with time delay, when it is possible to measure the disturbances.

Figure 47 – Temperature control in a NICU. Temperature responses from the NICU.

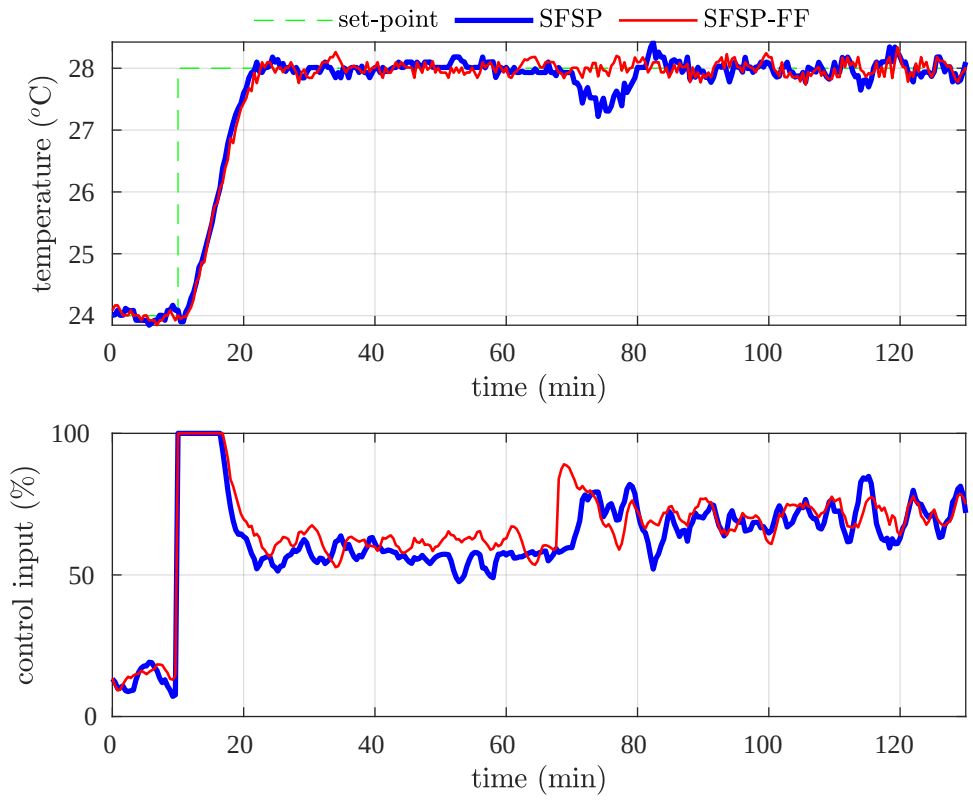

Source: The author.

Table 11 – IAE index for disturbance rejection. The best index is highlighted in bold text.

Temperature control in a NICU	IAE
SFSP-FF	**5.78**
SFSP	9.67

Source: The author.

The main characteristic of the proposed controller, when compared to others in the literature, is the addition of a proportional gain in the feedforward loop. This gain is responsible for a faster actuation, reducing the effect of the disturbance in the process output.

As can be seen in the simulation examples, the proposed controller is able to reject measurable disturbances more quickly than other control structures based on the Smith predictor. This is achieved by preserving a simple control structure based only on two tuning parameters, the feedback gain K and the robustness filter $V(z)$, while the controllers being compared with use additional tuning parameters and another filter for the feedforward controller.

Better simulation results were obtained in terms of IAE and CV indices for all six

scenarios. The IAE index of the proposed controller, for example, was up to 1196% better in the nominal case when compared with the other structures. Regarding the trade-off between performance and robustness, it was obtained better TV results in four out of the six presented scenarios.

Looking ahead to the use of the controller in real processes, the strategy was applied to the temperature control of a NICU, where the measurable disturbance is considered in the opening of a port. As expected, the proposed strategy showed better results than the conventional SFSP for high-order dead-time process, with faster disturbance attenuation response and improving the IAE index by 40.23%.

6 CONCLUSION

This work presented control strategies based on the Smith predictor focusing on high-order dead-time processes and on enhanced disturbance rejection performance.

Relevant and popular Smith predictor-based controllers were presented and their main characteristics were highlighted. These controllers were presented such that the reader could better understand the contributions and control problems that led to the formulation of the SFSP for high-order dead-time processes.

The SFSP, intended initially for FOPDT models, was generalized for any order NMP processes. The main properties, such as simplicity, robustness, and good performance of the original SFSP were preserved by using a state-space formulation of the predictor. The primary controller is tuned to obtain a desired set-point dynamics, while the robustness filter considering a desired trade-off between robustness and performance.

Three literature examples were used to validate the properties of the proposed strategy. For a fair comparison, the performance indices IAE, TV, and CV were calculated. The proposed SFSP showed better results of IAE for all scenarios. As expected, because of the aggressiveness of the control input, the TV index presented similar results, being better in 50% of all cases. As for the CV, the proposed controller was better in 75% of all cases. Another significant merit is that the good results were achieved with a controller with less complexity and fewer tuning parameters compared to very recent works.

The basic fundamentals of feedforward control for measurable disturbances were presented and its advantages and drawbacks were explained. For dead-time processes, by measuring the disturbance and feedforwarding it, it was shown how the feedforward controller can actuate before the effects of the disturbance reach the process output and how a faster disturbance rejection is obtained.

This work also presented a feedforward controller for a strategy based on the Smith predictor. When dealing with measurable disturbances, the proposed controller has faster disturbance rejection when compared to other controllers from the recent literature. Furthermore, this is accomplished by maintaining a simple control structure based on just two free tuning parameters, the feedback gain K and the robustness filter $V(z)$, while the controllers being compared with present one more free tuning parameter, the feedforward filter.

From simulation results, the proposed controller showed better IAE and CV indices for all six scenarios. The improvement in the IAE index was between $61,5\%$ to 1196%, even with similar or better robustness. Even though enhanced performance for disturbance rejection was achieved, the TV index was better in four out of six scenarios, thus showing a good compromise between performance and robustness.

In the temperature control in a NICU, a real application, the proposed strategy showed better results than the conventional SFSP, with faster disturbance rejection response and improving in 40.23% the IAE index. Furthermore, this application is a versatile example of how the proposed feedforward control system can be implemented in practice.

Therefore, given their effectiveness and promising results, the controllers proposed in this work show great potential for real industrial applications.

REFERENCES

ACKERMANN, J. E. On the synthesis of linear control systems with specified characteristics. *Automatica*, v. 13, n. 1, p. 89 – 94, 1977. ISSN 0005-1098. Cited 2 times in pages 45 and 77.

AJMERI, M.; ALI, A. Analytical design of modified Smith predictor for unstable second-order processes with time delay. *International Journal of Systems Science*, Taylor & Francis, v. 48, n. 8, p. 1671–1681, 2017. Cited 4 times in pages 52, 53, 54, and 62.

ALBERTOS, P.; GARCÍA, P. Robust control design for long time-delay systems. *Journal of Process Control*, v. 19, n. 10, p. 1640–1648, 2009. Cited in page 25.

ALBERTOS, P.; SANZ, R.; GARCIA, P. Disturbance rejection: A central issue in process control. In: *2015 4th International Conference on Systems and Control (ICSC)*. [S.l.: s.n.], 2015. p. 1–8. Cited 2 times in pages 24 and 26.

ALVES LIMA, T.; TORRICO, B. C.; de ALMEIDA FILHO, M. P.; FORTE, M. D. N.; PEREIRA, R. D. O.; NOGUEIRA, F. G. First-order dead-time compensation with feedforward action. In: *2019 18th European Control Conference (ECC)*. [S.l.: s.n.], 2019. p. 3638–3643. Cited 5 times in pages 26, 69, 70, 83, and 90.

ARTSTEIN, Z. Linear systems with delayed controls: a reduction. *IEEE Transactions on Automatic Control*, v. 27, n. 4, p. 869–879, 1982. Cited in page 24.

ÅSTRÖM, K.; HÄGGLUND, T. *Advanced PID Control*. [S.l.]: ISA - The Instrumentation, Systems and Automation Society, 2006. Cited in page 65.

BEGUM, K. G.; RAO, A. S.; RADHAKRISHNAN, T. Enhanced IMC based PID controller design for non-minimum phase (NMP) integrating processes with time delays. *ISA Transactions*, v. 68, p. 223–234, 2017. Cited in page 56.

CASTILLO, A.; GARCÍA, P. Predicting the future state of disturbed LTI systems: A solution based on high-order observers. *Automatica*, v. 124, p. 109365, 2021. Cited in page 25.

CASTILLO, A.; GARCÍA, P.; FRIDMAN, E.; ALBERTOS, P. Extended state observer-based control for systems with locally Lipschitz uncertainties: LMI-based stability conditions. *Systems & Control Letters*, v. 134, p. 104526, 2019. Cited in page 25.

CHEN, C.-T. *Linear system theory and design*. [S.l.]: Saunders college publishing, 1984. Cited in page 73.

CHIDAMBARAM, M.; REDDY, G. P. Nonlinear control of systems with input and output multiplicities. *Computers & Chemical Engineering*, Pergamon, v. 20, n. 3, p. 295–299, mar 1996. Cited in page 84.

da SILVA, L. R.; FLESCH, R. C. C.; NORMEY-RICO, J. E. Controlling industrial dead-time systems: When to use a PID or an advanced controller. *ISA Transactions*, v. 99, p. 339–350, 2020. Cited in page 50.

DAVISON, E. J. The feedforward control of linear multivariable time-invariant systems. *Automatica*, Elsevier, v. 9, n. 5, p. 561–573, 1973. Cited in page 26.

FU, C.; TAN, W. Control of unstable processes with time delays via ADRC. *ISA Transactions*, v. 71, p. 530 – 541, 2017. ISSN 0019-0578. Cited in page 25.

GARCÍA-MAÑAS, F.; GUZMÁN, J. L.; RODRÍGUEZ, F.; BERENGUEL, M.; HÄGGLUND, T. Experimental evaluation of feedforward tuning rules. *Control Engineering Practice*, Elsevier Ltd, v. 114, n. January, p. 104877, 2021. Cited in page 26.

GARCÍA, P.; ALBERTOS, P. A new dead-time compensator to control stable and integrating processes with long dead-time. *Automatica*, v. 44, n. 4, p. 1062–1071, 2008. Cited in page 25.

GARCÍA, P.; ALBERTOS, P. Robust tuning of a generalized predictor-based controller for integrating and unstable systems with long time-delay. *Journal of Process Control*, v. 23, n. 8, p. 1205–1216, 2013. Cited in page 25.

GENG, X.; HAO, S.; LIU, T.; ZHONG, C. Generalized predictor based active disturbance rejection control for non-minimum phase systems. *ISA Transactions*, v. 87, p. 34 – 45, 2019. ISSN 0019-0578. Cited 7 times in pages 25, 50, 51, 52, 56, 57, and 62.

GUZMÁN, J. L.; HÄGGLUND, T. Simple tuning rules for feedforward compensators. *Journal of Process Control*, Elsevier, v. 21, n. 1, p. 92–102, 2011. Cited in page 26.

HAST, M.; HÄGGLUND, T. Low-order feedforward controllers: Optimal performance and practical considerations. *Journal of Process Control*, Elsevier, v. 24, n. 9, p. 1462–1471, 2014. Cited in page 26.

HENSON, M. A.; SEBORG, D. E. *Nonlinear process control*. [S.l.]: Prentice Hall PTR Upper Saddle River, New Jersey, 1997. Cited in page 87.

KALMAN, R. E. Irreducible realizations and the degree of a rational matrix. *Journal of the Society for Industrial and Applied Mathematics*, SIAM, v. 13, n. 2, p. 520–544, 1965. Cited in page 73.

LIU, T.; GARCÍA, P.; CHEN, Y.; REN, X.; ALBERTOS, P.; SANZ, R. New predictor and 2DOF control scheme for industrial processes with long time delay. *IEEE Transactions on Industrial Electronics*, v. 65, n. 5, p. 4247–4256, May 2018. ISSN 0278-0046. Cited in page 25.

LIU, T.; HAO, S.; LI, D.; CHEN, W.-H.; WANG, Q.-G. Predictor-based disturbance rejection control for sampled systems with input delay. *IEEE Transactions on Control Systems Technology*, v. 27, p. 772–780, 2019. Cited in page 25.

LIU, T.; TIAN, H.; RONG, S.; ZHONG, C. Heating-up control with delay-free output prediction for industrial jacketed reactors based on step response identification. *ISA Transactions*, v. 83, p. 227 – 238, 2018. ISSN 0019-0578. Cited in page 25.

LIU, T.; ZHANG, W.; GU, D. Analytical design of two-degree-of-freedom control scheme for open-loop unstable processes with time delay. *Journal of Process Control*, v. 15, n. 5, p. 559–572, 2005. Cited in page 52.

MATAUšEK, M. R.; RIBIć, A. I. Control of stable, integrating and unstable processes by the modified smith predictor. *Journal of Process Control*, v. 22, n. 1, p. 338–343, 2012. Cited in page 58.

MICHIELS, W.; NICULESCU, S.-I. On the delay sensitivity of Smith predictors. *International Journal of Systems Science*, Taylor & Francis, v. 34, n. 8-9, p. 543–551, 2003. Cited in page 24.

MORARI, M.; ZAFIRIOU, E. *Robust Process Control*. Englewood Cliffs, NJ: Prentice Hall, 1989. Cited 4 times in pages 24, 29, 30, and 79.

NORMEY-RICO, J. E.; CAMACHO, E. F. *Control of dead-time processes*. [S.l.]: Springer, 2007. Cited 3 times in pages 24, 47, and 86.

NORMEY-RICO, J. E.; CAMACHO, E. F. Unified approach for robust dead-time compensator design. *Journal of Process Control*, v. 19, n. 1, p. 38–47, 2009. Cited 3 times in pages 24, 32, and 33.

PELLEGRINETTI, G.; BENTSMAN, J. Nonlinear control oriented boiler modeling – a benchmark problem for controller design. *IEEE Transactions on Control Systems Technology*, v. 4, n. 1, p. 57–64, 1996. Cited in page 82.

RODRÍGUEZ, C.; ARANDA-ESCOLÁSTICO, E.; GUZMÁN, J. L.; BERENGUEL, M.; HÄGGLUND, T. Revisiting the simplified internal model control tuning rules for low-order controllers: Feedforward controller. *IET Control Theory and Applications*, v. 14, n. 12, p. 1612–1618, 2020. Cited 2 times in pages 26 and 65.

RODRÍGUEZ, C.; NORMEY-RICO, J.; GUZMáN, J.; BERENGUEL, M. On the filtered Smith predictor with feedforward compensation. *Journal of Process Control*, v. 41, p. 35 – 46, 2016. Cited 10 times in pages 26, 64, 67, 83, 85, 86, 87, 88, 89, and 90.

RODRÍGUEZ, C.; NORMEY-RICO, J. E.; GUZMÁN, J. L.; BERENGUEL, M.; DORMIDO, S. Low-order feedback-feedforward controller for dead-time processes with measurable disturbances. *IFAC-PapersOnLine*, Elsevier, v. 49, n. 7, p. 591–596, 2016. Cited in page 26.

SANTOS, T. L. M.; BOTURA, P. E. A.; N.-R., J. E. Dealing with noise in unstable dead-time process control. *Journal of Process Control*, Elsevier, v. 20, n. 7, p. 840–847, 2010. Cited in page 24.

SANZ, R.; GARCÍA, P.; ALBERTOS, P. A generalized Smith predictor for unstable time-delay SISO systems. *ISA Transactions*, v. 72, p. 197 – 204, 2018. ISSN 0019-0578. Cited 3 times in pages 25, 43, and 46.

SANZ, R.; GARCÍA, P.; DíEZ, J. L.; BONDIA, J. Artificial pancreas system with unannounced meals based on a disturbance observer and feedforward compensation. *IEEE Transactions on Control Systems Technology*, v. 29, n. 1, p. 454–460, 2021. Cited in page 26.

SANZ, R.; GARCÍA, P.; FRIDMAN, E.; ALBERTOS, P. Robust predictive extended state observer for a class of nonlinear systems with time-varying input delay. *International Journal of Control*, Taylor & Francis, v. 93, n. 2, p. 217–225, 2020. Cited in page 25.

SILVA, W. A.; TORRICO, B. C.; CORREIA, W. B.; REIS, L. L. dos. Adaptive feedforward control applied in switched reluctance machines drive speed control in fault situations. *Journal of Dynamic Systems, Measurement, and Control*, American Society of Mechanical Engineers Digital Collection, v. 140, n. 5, 2018. Cited in page 26.

SKOGESTAD, S. Simple analytic rules for model reduction and pid controller tuning. *Journal of Process Control*, v. 13, n. 4, p. 291–309, 2003. Cited in page 31.

SMITH, O. J. M. Closer control of loops with dead time. *Chemical Engineering Progress*, v. 53, n. 5, p. 217–219, 1957. Cited 2 times in pages 24 and 29.

SÁ RODRIGUES, R. C.; SOMBRA, A. K. R.; TORRICO, B. C.; PEREIRA, R. D. O.; FORTE, M. D. do N.; FILHO, M. P. de A.; NOGUEIRA, F. G. Tuning rules for unstable dead-time processes. *European Journal of Control*, v. 59, p. 250–263, 2021. Cited 3 times in pages 25, 77, and 80.

TORRICO, B. C.; ANDRADE, F. V.; PEREIRA, R. D. O.; NOGUEIRA, F. G. Anti-windup dead-time compensation based on generalized predictive control. In: *2016 American Control Conference (ACC)*. [S.l.: s.n.], 2016. p. 5449–5454. Cited 2 times in pages 58 and 61.

TORRICO, B. C.; CAVALCANTE, M. U.; BRAGA, A. P. S.; NORMEY-RICO, J. E.; ALBUQUERQUE, A. A. M. Simple tuning rules for dead-time compensation of stable, integrative, and unstable first-order dead-time processes. *Industrial & Engineering Chemistry Research*, ACS Publications, v. 52, n. 33, p. 11646–11654, 2013. Cited 6 times in pages 25, 27, 34, 35, 39, and 41.

TORRICO, B. C.; CORREIA, W. B.; NOGUEIRA, F. G. Simplified dead-time compensator for multiple delay siso systems. *ISA Trans.*, v. 60, p. 254–261, 2016. Cited 3 times in pages 25, 36, and 37.

TORRICO, B. C.; FILHO, M. P. de A.; LIMA, T. A.; FORTE, M. D. do N.; Sá, R. C.; NOGUEIRA, F. G. Tuning of a dead-time compensator focusing on industrial processes. *ISA Transactions*, v. 83, p. 189 – 198, 2018. ISSN 0019-0578. Cited 8 times in pages 25, 37, 42, 45, 49, 56, 79, and 80.

TORRICO, B. C.; PEREIRA, R. D. O.; SOMBRA, A. K. R.; NOGUEIRA, F. G. Simplified filtered Smith predictor for high-order dead-time processes. *ISA Transactions*, v. 109, p. 11–21, 2021. Cited 5 times in pages 25, 76, 78, 79, and 92.

TZEKIS, P.; KARAMPETAKIS, N. P.; VARDULAKIS, A. I. On the division of polynomial matrices. *IMA Journal of Mathematical Control and Information*, v. 16, n. 4, p. 391–401, 12 1999. Cited in page 46.

VERONESI, M.; GUZMáN, J.; VISIOLI, A.; HäGGLUND, T. Closed-loop tuning rules for feedforward compensator gains**this work has been partially funded by the following project dpi2014-55932-c2-1-r financed by the spanish ministry of economy and competitiveness and eu-erdf funds. *IFAC-PapersOnLine*, v. 50, n. 1, p. 7523–7528, 2017. 20th IFAC World Congress. Cited in page 65.

WANG, L.; SU, J. Disturbance rejection control for non-minimum phase systems with optimal disturbance observer. *ISA Transactions*, v. 57, p. 1 – 9, 2015. ISSN 0019-0578. Cited 3 times in pages 24, 25, and 50.

WATANABE, K.; ITO, M. A process-model control for linear systems with delay. *IEEE Transactions on Automatic Control*, v. 26, n. 6, p. 1261–1269, December 1981. Cited in page 24.

ZHANG, B.; TAN, W.; LI, J. Tuning of Smith predictor based generalized ADRC for time-delayed processes via IMC. *ISA Transactions*, v. 99, p. 159 – 166, 2020. Cited in page 25.

ZHAO, S.; GAO, Z. Modified active disturbance rejection control for time-delay systems. *ISA Transactions*, v. 53, n. 4, p. 882 – 888, 2014. ISSN 0019-0578. Disturbance Estimation and Mitigation. Cited in page 25.

APPENDIX

APPENDIX A – OBSERVABLE CANONICAL FORM

A process model with dead time $T(z) = X(z)z^{-h}$ can be represented as

$$T(z) = \frac{b_n z^{n-1} + b_{n-1} z^{n-2} + \cdots + b_2 z + b_1}{z^n + a_n z^{n-1} + \cdots + a_2 z + a_1} z^{-h} = C(zI - A)^{-1} B z^{-h}, \tag{A.1}$$

where, in the canonical observable form,

$$A = \begin{bmatrix} -a_n & 1 & 0 & \cdots & 0 \\ -a_{n-1} & 0 & 1 & \cdots & 0 \\ \vdots & \vdots & \vdots & \ddots & 0 \\ -a_2 & 0 & 0 & \cdots & 1 \\ -a_1 & 0 & 0 & \cdots & 0 \end{bmatrix}_{n \times n}, \; B = \begin{bmatrix} b_n \\ b_{n-1} \\ \vdots \\ b_2 \\ b_1 \end{bmatrix}_{n \times 1}, \; C = \begin{bmatrix} 1 & 0 & \cdots & 0 \end{bmatrix}_{1 \times n}. \tag{A.2}$$